

Newcastle
University

A Marine Waste Biorefinery

**A thesis submitted for the degree of Doctor of Philosophy
(PhD) at Newcastle University**

by

Ahmed Said Hamed Al Hatrooshi

November 2019

Abstract

Biodiesel is a renewable alternative to 'petro-diesel'. There is already an established, conventional production technology based on refined vegetable oils. However, this is always more expensive than producing petroleum-based diesel, mainly due to the feedstock cost. Use of a cheap, non-edible feedstock, such as waste shark liver oil (WSLO), would reduce the biodiesel production cost and make the process economically viable.

WSLO is obtained by exposing sharks' livers to the sun until they melt and collecting the oil produced. Sharks' livers comprise 25-30% of their body weight. Historically, the discarded WSLO was used for waterproofing wooden boats. However, this application is no longer required, as modern boats are made of fibreglass. The excess WSLO derived from these discarded sharks' livers has great potential for being further processed into valuable products, including biodiesel, squalene and omega-3 polyunsaturated fatty acids (PUFA), such as eicosapentaenoic (EPA) and docosahexaenoic (DHA). The glyceride components of the WSLO can be converted into biodiesel using existing biodiesel processing technologies, while the squalene, EPA and DHA may be extracted and sold as value-added products through biorefinery processes.

This study investigated the production of fatty acid methyl ester (FAME) from WSLO using both acid (sulfuric acid, H_2SO_4) and base (sodium hydroxide, NaOH) catalysts. Due to the high levels of free fatty acids (FFA) in WSLO, homogeneous alkali-catalysed transesterification was less effective than the acid-catalysed process, resulting in a maximum WSLO to FAME conversion of only 40% after 15 min at a 60°C temperature, a 1.5 wt.% of NaOH catalyst and a 6:1 molar ratio of methanol to WSLO. The acid-catalysed transesterification of the WSLO was investigated, using Design of Experiments (DoE), by a response surface method. The acid-catalysed process achieved 99% FAME conversion during a 6.5 h reaction time at a 60°C temperature, a 5.9 wt. % of H_2SO_4 catalyst and a 10:3 molar ratio of methanol to WSLO.

Saponification of WSLO for extracting squalene was also investigated using a DoE methodology to obtain the operating conditions for highest squalene extraction. The results showed 101.6 ± 1.3 % squalene recovery at the following operating conditions: a 5 min reaction time, a 9.9 wt. % of water loading and a 20:1 molar ratio of ethanol to oil. Aqueous silver nitrate (AgNO_3) was employed for extracting EPA and DHA from fatty acid ethyl esters produced from the WSLO. The highest EPA and DHA recoveries achieved were 66.2% EPA and 83.4% DHA. These came from extractions using a 2 h reaction time, a mixing speed of 300 rpm, a 20°C reaction temperature, and a 50 wt. % of silver nitrate concentration.

Techno-economic analysis was performed to assess the commercial feasibilities of acid-catalysed biodiesel production using WSLO and alkali-catalysed biodiesel production using refined vegetable oil (rapeseed oil). Aspen HYSYS-V9 was used to simulate both production types at plant capacity of 12,000 te/y and lifespan of 20 years. Net present values (NPVs) of US \$34.8 and US \$4.9 million were obtained for the acid-catalysed WSLO process and the alkali-catalysed vegetable oil process, respectively. The internal rate of return (IRR) was calculated to be 260% for the acid-catalysed process and 56% for the alkali-catalysed process. Therefore, the acid-catalysed process is more profitable than the alkali-catalysed process due to its higher IRR percentage. Sensitivity analysis was also conducted to show the effect of certain variables on the NPV of both biodiesel production types. It was concluded that the biodiesel selling price has more effect on the NPV than the glycerol variation price, whereas the triglyceride feedstock purchase prices have the largest influence on the NPV of the two processes.

Dedication

This Ph.D. thesis is dedicated to Mariam, Said and Mohammed and my parents for their love, encouragement, support and prayers.

Acknowledgment

All grace is due to Allah (God) for giving me this opportunity to embark on my PhD program. My sincere gratitude and acknowledgement to my supervision team Prof. Adam Harvey and Dr. Valentine Eze for their guidance and valuable contributions. Also, I would like to express my gratitude to my parents, wife and family for their patient, support and prayers. My sincere thanks to all members of the Process Intensification Group (PIG), administrative staff and office colleagues for their usual support and co-operation. I also express my appreciations to Diwan Royal Court of Oman Government for funding this research.

Table of Contents

Abstract.....	i
Dedication.....	iii
Acknowledgment.....	iv
Nomenclature and Abbreviations	xii
Chapter 1 Introduction.....	16
1.1 Biodiesel.....	18
1.2 Waste Shark Liver Oil as a Feedstock for Biodiesel.....	18
1.3 Recovery of Squalene and Omega-3 PUFAs from Waste Shark Liver Oil	20
1.3.1 Omega-3 PUFAs Recovery	20
1.3.2 Squalene Recovery and Novelty	21
1.4 A General Overview of a Proposed WSLO-based Biorefinery.....	22
1.5 Research Aim and Objectives:	24
1.6 Thesis Layout	25
Chapter 2 Literature Review	27
2.1 Biofuel Feedstock and Global Biofuel Production.....	27
2.2 Biodiesel Production Technologies.....	29
2.3 Factors that Affect Biodiesel Production Reactions.....	30
2.3.1 Type of Catalyst	30
2.3.2 Alkali Catalyst.....	31
2.3.3 Acid Catalyst.....	33
2.3.4 Enzyme Catalyst.....	33
2.3.5 Alcohol Quantity	34
2.3.6 Reaction Temperature and Catalyst Concentration.....	34
2.3.7 Moisture Content and Free Fatty Acid Content	35
2.4 Types of Reactors for Biodiesel Production.....	36
2.4.1 Static mixers reactor	37
2.4.2 Micro-reactors	38

2.4.3 Oscillatory flow reactors	39
2.4.4 Spinning reactors.....	41
2.4.5 Acoustic reactors	42
2.5 Bio-refining of Waste Shark Liver Oil.....	43
2.5.1 Biodiesel Production from Waste Shark Liver Oil	43
2.5.2 Extraction Process of Omega-3 Polyunsaturated Fatty Acids (PUFAs).....	44
2.5.3 Squalene Extraction Process	55
2.6 Summary	59
Chapter 3 Materials and Methods	62
3.1 Introduction.....	62
3.2 Materials.....	62
3.3 Experimental Methods	63
3.3.1 Determinations of the Density of the Waste Shark Liver Oil	63
3.3.2 Water Content by Karl Fischer Titration	63
3.3.3 Determination of Lipid Classes, Squalene and Free Fatty Acids	64
3.3.4 Alkali-Catalysed Transesterification.....	65
3.3.5 Acid-Catalysed Transesterification.....	66
3.3.6 Squalene Extraction by Saponification	66
3.3.7 EPA and DHA Extraction Using Aqueous Silver Nitrate.....	68
3.3.8 Analysis of FAME, EPA, DHA and Squalene Contents Using Gas Chromatography.....	71
3.3.9 Fourier Transform Infrared Spectroscopy.....	74
3.3.10 Nuclear Magnetic Resonance.....	79
3.3.11 Error Analysis	82
Chapter 4 Results and Discussion	84
4.1 Waste Shark Liver Oil Characterisation	84
4.2 NMR Analysis for FAME Produced from Acid Catalysed Transesterification	87
4.3 Monitoring Waste Shark liver Oil Transesterification Using FTIR.....	89
4.4 Waste Shark Liver Oil Transesterification and FAME Conversions with the Catalysts ...	90

4.5 Parametric Study and Optimisation of Acid-catalysis of WSLO Transesterification	92
4.6 Squalene Recovery from Waste Shark Liver Oil	94
4.6.1 Effect of the Extraction Parameters on Squalene Recovery.....	97
4.6.2 Optimal Conditions for Squalene Recovery.....	99
4.7 EPA and DHA Extraction	100
4.7.1 Effect of Process Parameters on EPA and DHA Extraction	101
Chapter 5 Techno-economic Analysis.....	105
5.1 Process Description	105
5.1.1 Acid-Catalysed Transesterification of WSLO to Biodiesel	109
5.1.2 Alkali-Catalysed Transesterification of Refined Vegetable Oil.....	110
5.2 Economic Analysis.....	111
5.3 Sensitivity Analysis	117
5.4 Summary.....	119
Chapter 6 Conclusions and Further Work	120
6.1 Conclusions	120
6.2 Further Work	122
References	123
Appendices	I
Appendix A: WSLO Fatty Acid Profile	I
Appendix B: Analysis of Waste Shark Liver Oil by Iatroscan MK-6.....	II
Appendix C: GC Chromatogram showing squalene in the WSLO FAME Sample.....	III
Appendix C 1: Squalene peak after 5 min reaction time of WSLO saponification	IV
Appendix C 2: Squalene peak after 30 min reaction time of WSLO saponification	V
Appendix C 3 :Squalene peak after 60 min reaction time of WSLO saponification	VI
Appendix C 4 : Squalene peak after washing.....	VII
Appendix D: European Biodiesel Specification EN 14214	VIII
Appendix E: ASTM Biodiesel Standard D 6751	IX

List of Figures

Figure 1.1: Worldwide energy consumption (Urban, 2015).....	16
Figure 1.2: Projection regarding biofuel consumption in the transport sector in Million Tonnes of Oil Equivalent (Mtoe)(IEA, 2017).....	17
Figure 1.3: Structure of EPA (a) and DHA (b) (Holub and Holub, 2004).....	20
Figure 1.4: Squalene (Fox, 2009).....	21
Figure 1.5: Flow diagram of WSLO Biorefinery.....	23
Figure 2.1: Biofuels production by region (PikeResearch, 2012).....	27
Figure 2.2: Bioethanol yield of different feedstocks (Halder et al., 2019).....	28
Figure 2.3: Alkali-catalysed biodiesel production (Leung et al., 2010).....	32
Figure 2.4: CSTR diagrammatic sketch (Zhao et al., 2015).....	36
Figure 2.5: Batch reactor (Dimian et al., 2014).....	37
Figure 2.6: Experimental setup: (a) static mixer closed-loop system ,and (b)internal structure of static mixer (Qiu et al., 2010).....	38
Figure 2.7: The configuration of oscillatory flow reactor (Harvey and Lee, 2012).....	40
Figure 2.8: Schematic of oscillatory flow reactor for biodiesel production (Harvey and Lee, 2012).....	41
Figure 2.9: A schematic view of a spinning disk reactor (Pask et al., 2012).....	41
Figure 2.10: Ether lipids (Fernández et al., 2013).....	43
Figure 2.11: Structure of EPA (a) and DHA (b) (Holub and Holub, 2004).....	44
Figure 2.12: General overview of common omega-3 extraction methods (Lembke, 2013a).....	46
Figure 2.13: Formation of urea crystals in the absence and presence of long chain fatty acids (Shahidi and Wanasundara, 1998).....	47
Figure 2.14: Enrichment of total ω 3-fatty acids of seal blubber oil upon low temperature crystallization. A, triacylglycerol form; B, free fatty acid form (Wanasundara, 2001).....	48
Figure 2.15: Molecular distillation for production of omega 3 ester (Flavourtech, 2009; Atadashi et al., 2013).....	50
Figure 2.16: Pressure-temperature phase diagram for CO ₂ (Grandison and Lewis, 1996; King, 2003).....	51
Figure 2.17: Flow scheme of the SFF process (Fiori et al., 2014)Streams: F=FAEE feed, M=CO ₂ make up, S=CO ₂ to column, E=extract, E1=extract CO ₂ free, L0=reflux, R= raffinate, R1=raffinate CO ₂ free. Equipment: COL=fractionation column, SP=separator, HE=heat exchanger, CV=control valve.....	52
Figure 2.18: Squalene chemical structure (Popa et al., 2015a).....	55

Figure 2.19: Short path distillation (Flavourtech, 2009)	56
Figure 2.20: Supercritical carbon dioxide extraction (FluidsScience, 2015)	58
Figure 3.1: C30 Karl Fischer Titrator (Mettler Toledo, UK)	63
Figure 3.2: Iatroskan MK-6 (Scientifique, 2014)	64
Figure 3.3: Experimental set up.....	65
Figure 3.4: WSLO saponification.....	68
Figure 3.5: General overview of EPA and DHA extraction (Shanmugam and Donaldson, 2015)	69
Figure 3.6: process for recovery of EPA and DHA from aqueous and emulsion phases.....	70
Figure 3.7: Experimental steps for the EPA and DHA extractions. Arrow in Figure 3.7 (a) refers to the residual oil layer, arrow in Figure 3.7 (b) refers to the de-emulsification layer and the arrow in Figure 3.7(c) refers to the de-complexation layer.	70
Figure 3.8: Gas chromatography (Chaintreau, 2007).....	71
Figure 3.9: Squalene calibration curve.....	73
Figure 3.10: The relationship of the vibrational infrared region to others types of energy transition (Pavia <i>et al.</i> , 2008).....	75
Figure 3.11: Different types of bond with the infrared absorption range (Pavia <i>et al.</i> , 2008).	76
Figure 3.12: Stretching and bending modes (Pavia <i>et al.</i> , 2008).	76
Figure 3.13: Stretching and bending vibration of methyl group (Pavia <i>et al.</i> , 2008).....	77
Figure 3.14: A schematic diagram of an FTIR (Pavia <i>et al.</i> , 2008).	78
Figure 3.15: Diamagnetic shielding or diamagnetic anisotropy (Pavia <i>et al.</i> , 2008)	79
Figure 3.16: A typical chemical shift scale on NMR spectrum chart (Pavia <i>et al.</i> , 2008).....	80
Figure 4.1: NMR spectra of the FAME from WSLO.....	87
Figure 4.2: Proton NMR Chart.....	88
Figure 4.3: NMR spectra for pure squalene	88
Figure 4.4: FTIR 4 hrs transesterification reaction using acid catalyst.....	89
Figure 4.5: 3-D FTIR transesterification reaction using acid catalyst.....	89
Figure 4.6: Effect of mixing intensity on WSLO transesterification at 60°C, with a 6h reaction time, a 30:1 methanol to oil molar ratio and using a 3wt.% of the H ₂ SO ₄ catalyst.....	90
Figure 4.7: FAME conversions for transesterification of WSLO at 720rpm mixing speed using, (a) 1.5 wt.% NaOH at 6:1 methanol to oil molar ratio, 60°C temperature and 60min reaction time, (b) 1.5 wt.% H ₂ SO ₄ at 30:1 methanol to oil molar ratio, 60°C temperature and 6h reaction time.	91
Figure 4.8: effect of the reaction parameters (reaction time (h), methanol molar ratio and catalyst concentration (wt.%)) on conversions of WSLO to FAME.	93

Figure 4.9: Effects plot for squalene recovery	96
Figure 4.10: Effect of process parameters on squalene recovery; (a) ethanol molar ratio and reaction time; (b) reaction time and water loading; (c) water loading and ethanol molar ratio...	97
Figure 4.11: Soap in form of (a) emulsion and (b) particulate/granular	98
Figure 4.12: Overview of aqueous silver nitrate extraction of EPA and DHA from WSLO	101
Figure 4.13: Effects of process parameters on EPA and DHA recovery %; (a) at different reaction times and 30 wt.% AgNO ₃ concentration; (b) at different AgNO ₃ concentrations and 2 h reaction time.....	102
Figure 5.1: Process flow sheet for acid-catalysed transesterification of WSLO for the production of biodiesel.....	106
Figure 5.2: Process flow sheet for conventional biodiesel production (alkali-catalysed process) from refined vegetable oil	108
Figure 5.3 Process flow sheet of biodiesel production plant from palm oil with supercritical methanol at low molar ratio (Sakdasri <i>et al.</i> , 2018).....	115
Figure 5.4: The change in the NPV as functions of the purchase prices of (a) WSLO and methanol (b) rapeseed oil and methanol	117
Figure 5.5: The change in the NPV as functions of the biodiesel and glycerol selling prices for (a) the acid-catalysed plant using WSLO, and (b) the alkali-catalysed plant using vegetable oil (rapeseed oil).....	118

List of Tables

Table 2.1: Several processes for the silver ion-based extraction of omega-3 PUFAs	54
Table 2.2: Chemical and physical properties of squalene (Popa <i>et al.</i> , 2015a).....	55
Table 2.3: Experimental result for the squalene content and yields (Pietsch and Jaeger, 2007a) 57	
Table 2.4: A comparison of various EPA and DHA extraction techniques(Lembke, 2013b)	61
Table 3.1: Atomic number and nuclei spin (Pavia <i>et al.</i> , 2008).....	80
Table 3.2: Nuclei spin quantum and magnetic properties of selected nuclei (Pavia <i>et al.</i> , 2008)	81
Table 3.3: Laboratory equipment used and their errors	82
Table 4.1: Lipid classes as measured by Iatroscan MK-6	84
Table 4.2: Fatty acids profile of the WSLO	85
Table 4.3: Average molecular weights of WSLO	86
Table 4.4:Experimental and predicted conversion of WSLO to FAME at different conditions..	92
Table 4.5: Squalene recovery at different parameter spaces	95
Table 5.1: A summary of the raw materials used to produce biodiesel, and utilities including heating energy and cooling water.....	111
Table 5.2: Material balance and process conditions.....	112
Table 5.3: Economic analysis for the biodiesel production capacity of 12000 te/y.....	114
Table 5.4:The economic analysis results for biodiesel production from palm oil using SCM processe with different plant capacities in US\$ millions (Sakdasri <i>et al.</i> , 2018).	116

Nomenclature and Abbreviations

List of Abbreviations

AKG	Alkylglycerols
ALA	Alpha-Linolenic Acid
ASTM	American Society for Testing and Materials
CCC	Counter-current Chromatography
CFPP	Cold Filter Plugging Point
DAGE	Diacylglycerol Ether
DHA	Docosahexaenoic
DI	Deionised
DG	Di-glyceride
DoE	Design of Experiment
EPA	Eicosapentaenoic
FAEE	Fatty Acid Ethyl Ester
FAME	Fatty Acid Methyl Ester
FFA	Free Fatty Acid
FID	Flame Ionization Detector
FTIR	Fourier-transform infrared spectroscopy
GC	Gas Chromatography
GHG	Greenhouse Gases
GL	Glycerol
HPLC	High Performance Liquid Chromatography

IEA	International Energy Agency
IRR	Internal Rate of Return
LC	Liquid Chromatography
MAGE	Monoacylglycerol Ethers
MD	Molecular Distillation
MG	Mono-glyceride
MHz	Megahertz
MPa	Megapascal
MSHA	Mine Safety and Health Administration
Mtoe	Million Tonnes of Oil Equivalent
NMR	Nuclear magnetic resonance
NPV	Net Present Value
NRTL	Non-random Two Liquid
OBR	Oscillatory Baffle Reactor
OFR	Oscillatory Flow Reactor
OSHA	Occupational Safety and Health Administration
PEL	Permissible Exposure Limit
PPM	Parts per million
PUFA	Polyunsaturated Fatty Acids
RF	Radio frequency
RPM	Revolutions per minute
SBO	Seal Blubber Oil

SCCO ₂	Supercritical Carbon Dioxide
SCM	Supercritical methanol
SD	Standard deviation
SFC	Supercritical Fluid Chromatography
SFF	Supercritical Fluid fractionation
TCI	Total Capital Investment
TEA	Techno-economic Analysis
te/y	Tonne/Year
TG/TAG	Triglycerides
TLC	Thin Layer Chromatography
TMS	Tetramethylsilane
WSLO	Waste Shark Liver Oil

List of Nomenclature

ρ	Density (g/ml)
A_i	Peak area of methylheptadecanoate (mV.s)
C_i	Concentration of the methylheptadecanoate solution (mL)
I	Nuclei spin (-)
m	Mass of sample (mg)

P	Pressure (Pa)
P_c	Critical Pressure (Pa)
T	Temperature (K)
T_c	Critical Temperature (K)
V_i	Volume of the methylheptadecanoate solution (mL)
$(x_i - \bar{x})$	Deviation from the mean (-)
(N-1)	Total number of measurements minus one (-)

Chapter 1 Introduction

Globally, the main source of energy is fossil fuels. However, fossil fuel combustion leads to harmful environmental emissions and contributes to global warming, and these are a significant factor in climate change. Exploring renewable sources to replace fossil fuels is therefore an important task for scientists (Mathimani *et al.*, 2015). Figure 1.1 shows worldwide energy consumption in 2013, in which petroleum was the largest source of energy.

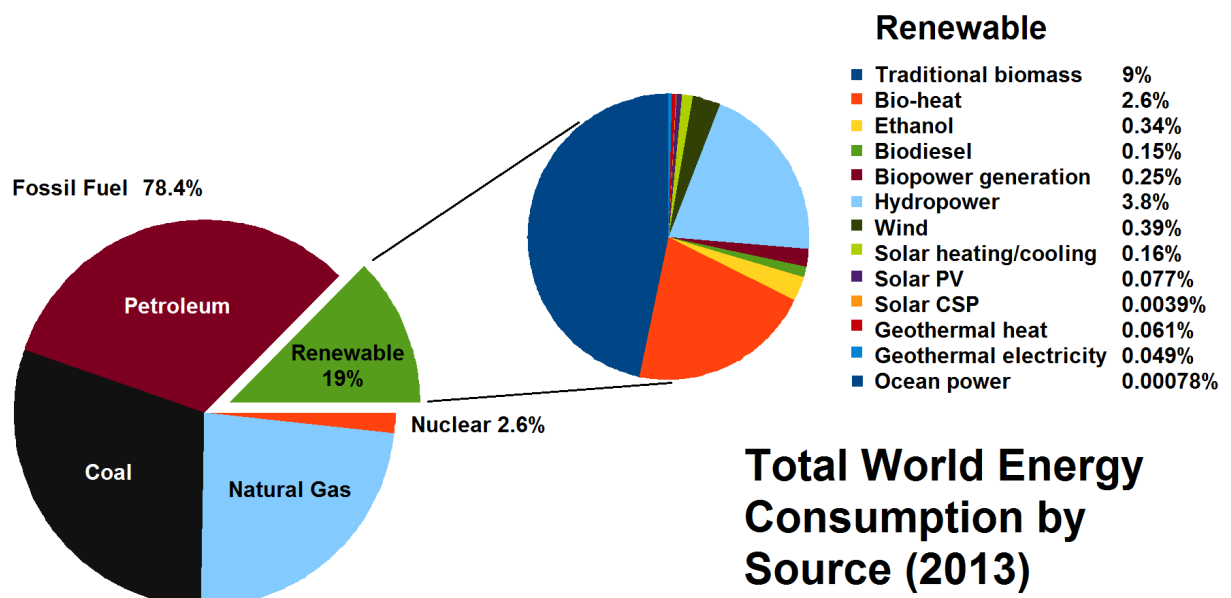


Figure 1.1: Worldwide energy consumption (Urban, 2015)

Energy is vital for the development of the world economy, and a major part of this energy is used for transportation. World transport fuel demand is expected to increase by approximately 30% in 2030, according to the World Energy Outlook (IEA, 2017). Figure 1.1 shows that almost 80% of the global energy consumed is fossil fuel-based, and 58% of this fossil fuel is used in the transport sector (Escobar *et al.*, 2009). Thus, for substantial changes in the composition of world transport energy consumption to be effected, the development of sustainable technology with low CO₂ emissions is required (Cuenot *et al.*, 2012).

To guard against the rise in fossil fuel-based transport energy consumption, numerous organisations and governments have promoted energy diversity and greenhouse gas (GHG) emission reduction through the use of biofuels. Figure 1.2 shows a projection of biofuel consumption in the transport sector (IEA, 2017). Clearly, the current production of transport biofuels needs to triple to achieve the 2030 Sustainable Development Scenario (SDS) target. This target can be driven by cost reductions of advanced biofuels, widespread sustainability governance and more adoption in aviation and marine transport (IEA, 2017). One of the main liquid biofuels used in the transportation sector is biodiesel.

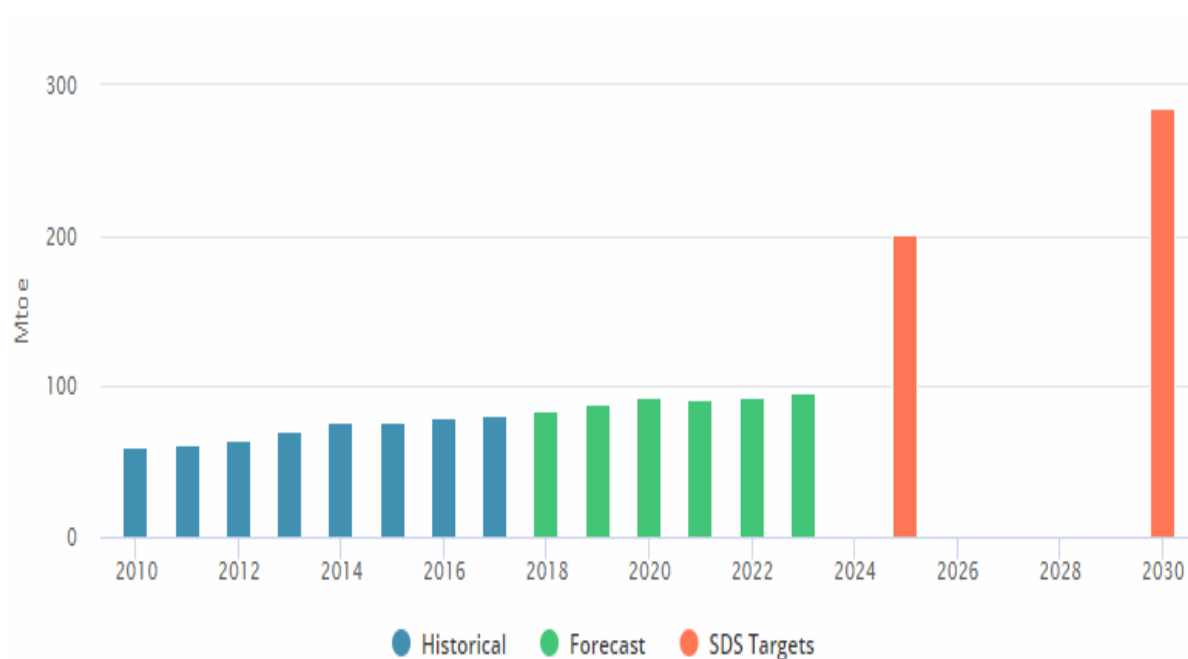


Figure 1.2: Projection regarding biofuel consumption in the transport sector in Million Tonnes of Oil Equivalent (Mtoe)(IEA, 2017)

1.1 Biodiesel

Biodiesel, derived from vegetable oils or animal fats, is a renewable replacement for petro-diesel in compression ignition engines. Its quality is dictated by ASTM D6751 (Burton and Biofuels, 2008) in the USA and Canada, and EN 14214 in the European Union. The main component is fatty acid methyl esters (FAMES) of long-chain fatty acids (Bryan, 2008). As a clean-burning alternative to diesel fuel, biodiesel has various environmental benefits, including biodegradability, very low toxicity, and a reduction in CO₂ emissions (Rasal *et al.*, 2019). Due to the environmental benefits of biodiesel combustion, various government policies have mandated the blending of biodiesel with petro-diesel, resulting in a growth in biodiesel production and consumption (Bin-Mahfouz *et al.*, 2018). This growth represents 15 times the production volume of biodiesel in the period from 2002 to 2012 (De Oliveira and Coelho, 2017). Biodiesel is commonly produced via triglyceride (usually vegetable oil) transesterification and/or free fatty acid (FFA) esterification reactions in the presence of alcohols (Kole *et al.*, 2012).

The main determining factor of the price of biodiesel is the cost of feedstock, which comprises 70–95% of total biodiesel production costs (Banković-Ilić *et al.*, 2012). Hence, the use of a cheap non-edible feedstock, such as waste shark liver oil (WSLO), would reduce biodiesel production costs and make the process more economically viable.

1.2 Waste Shark Liver Oil as a Feedstock for Biodiesel

Sharks have been consumed as a food in coastal regions for over 5,000 years (Vannuccini, 1999). In fact, they provide a variety of products including: meat (fresh, frozen or smoked), fins (shark fin soup), liver (cosmetics and boat coating), skin (leather and sandpaper), cartilage (ground and proposed as an anti-cancer treatment), jaws, and teeth (jewellery) (Vannuccini, 1999). Waste shark liver oil (WSLO), derived from discarded shark livers, has great potential for further processing into valuable products such as biodiesel, squalene and omega-3 polyunsaturated fatty acids (PUFA), including eicosapentaenoic (EPA) and docosahexaenoic (DHA). A shark's liver comprises 25-30% of its body weight (Popa *et al.*, 2015c), and WSLO is obtained by exposing the liver to the sun until it melts, so that the oil can be collected. The major constituents of WSLO are triglycerides (TG), diacylglycerol ethers (DAGE), and squalene (Wetherbee and Nichols, 2000). Lipid content varies among shark species and can be affected by factors such as fishing season, species, and the location of fishing (Navarro-Garcia *et al.*, 2000).

Generally, sharks form 50% of the by-catch (sharks that are caught unintentionally while catching certain target species and target sizes of fish) in the deep water fisheries of New Zealand and Australia, yet most of the sharks are discarded and the liver oil is unutilised (Wetherbee and Nichols, 2000). Historically, the discarded WSLO was used for to proof wooden boats (Jabado *et al.*, 2015), but now these applications are no longer required as modern boats are fibreglass. The excess WSLO derived from these discarded shark livers in the fishing industry could instead be processed to obtain valuable products like biodiesel, squalene, and omega-3 PUFAs –including EPA and DHA. While the TG components of the WSLO can be converted to biodiesel using existing biodiesel processing technologies, the squalene, EPA and DHA can be extracted and sold as value-added products through a biorefinery process in Oman.

The premise of this project is to utilise the waste from the discarded sharks' liver. Nowadays, shark liver oil is not utilised in Oman and it is usually wasted. Total shark landings by species for all governorates in Oman during 2016 was 7,507 tonnes (Ministry of Agriculture and Fisheries, 2014). Therefore, the proposed biorefinery project in Oman will focus in utilising the waste for the production of valuables products such as biodiesel, squalene, and omega-3 oil in Oman (Al Hatrooshi *et al.*, 2020).

There is a misconception between sharks finning which is prohibited internationally and shark fishing for local consumption. Shark finning is the act of removing fins from sharks and discarding the rest of the shark alive to the sea in order to have bigger space for storing the fins which is much valuable than the body (Fowler *et al.*, 2005).

Shark finning creates an extensive waste as the fin is about 5% of the total weight of a shark (Vannuccini, 1999). This waste is contrary to the code of conduct in the United Nations FAO which states the importance of avoiding waste and discards in fisheries (Code of Conduct for Responsible Fisheries (Article 7.2.2). Furthermore, the FAO International Plan of Action for the Conservation and Management of Sharks (IPOA- Sharks) encourages full utilisation of dead sharks. Thus, utilising shark liver oil obtained after fishing the sharks for local consumption is crucial as per the stated international laws and regulations.

1.3 Recovery of Squalene and Omega-3 PUFAs from Waste Shark Liver Oil

1.3.1 Omega-3 PUFAs Recovery

Among the valuable products that can be obtained from WSLO, there are omega-3 PUFAs, mainly the docosahexaenoic acid, DHA, (22 carbon atoms, 6 double bonds) and eicosapentaenoic acid, EPA, (20 carbon atoms, 5 double bonds) (Iagher *et al.*, 2013), as shown in Figure 1.3. In recent years, there has been an increase in the consumption of fish oil as a commercial source of omega-3 PUFA, resulting in a search for other fish species containing high amounts of PUFA, to substitute the increasing demand for this material (Navarro-García *et al.*, 2004). This increase is due to the health benefits of EPA and DHA; EPA is claimed to greatly reduce heart disease and inflammatory disorders, whereas DHA is used as a food supplement to enhance infant brain function (Navarro-Garcia *et al.*, 2000). Several methods are used to separate omega-3 concentrate from fish oil: high-performance liquid chromatography (HPLC/LC), molecular distillation (MD), supercritical fluid extraction (SFE), supercritical fluid chromatography (SFC), enzymatic enrichment, crystallisation at low temperatures, and urea precipitation. These technologies are discussed in more detail in the next chapter.

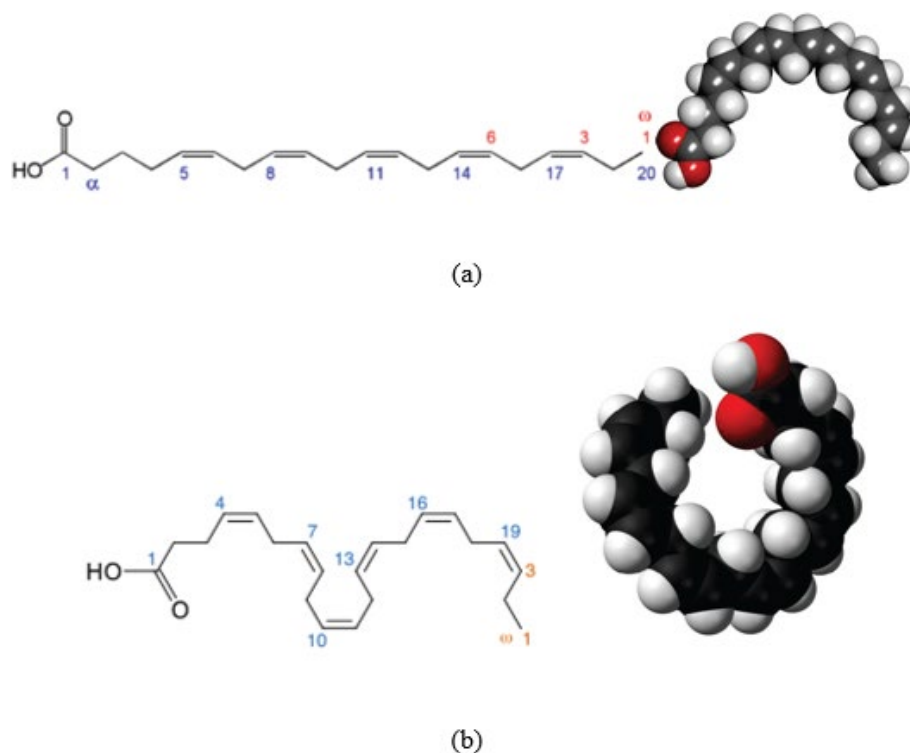


Figure 1.3: Structure of EPA (a) and DHA (b) (Holub and Holub, 2004)

1.3.2 Squalene Recovery and Novelty

Another major constituent of WSLO is squalene, which is an organic compound with the formula $C_{30}H_{50}$, as shown in Figure 1.4. It is mainly obtained from shark liver oil and can also be found in some vegetable oils (Kim and Karadeniz, 2012). The amount of hydrocarbon (squalene) present in WSLO varies widely depending on species. Deprez *et al.* (1990) reported quantities of squalene ranging from 1–88% of the overall lipids in eight shark species from Tasmanian waters. Squalene is used in various cosmetic applications, for example as a moisturiser, since it is able to penetrate the skin quickly and enhances skin absorption of cosmetics and medicaments (Davenport, 1989). Furthermore, it can be used as an adjuvant added to a number of vaccines, including the pandemic H_1N_1 vaccine (Fox, 2009). There are several methods used to extract squalene from shark liver oil including molecular distillation under high vacuum (short path distillation), counter current chromatography, and supercritical fluid extractions.

Controlled saponification for extraction of squalene is a newly proposed technique in this study. It was conducted for the first time for separation of squalene from WSLO using controlled saponification. No report has been published on the use of saponification for extraction of squalene from WSLO.

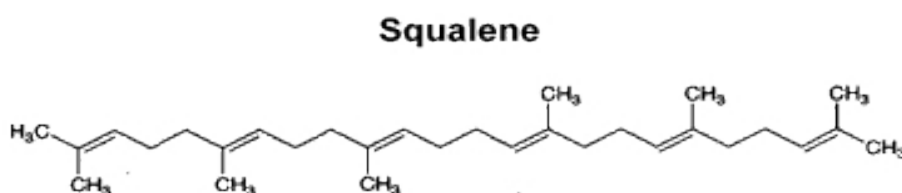


Figure 1.4: Squalene (Fox, 2009)

1.4 A General Overview of a Proposed WSLO-based Biorefinery

Producing biodiesel from discarded shark liver could lower the production cost of biodiesel. However, it is imperative to have a biorefinery rather than a single product-based plant, in order to utilise the various valuable products from processing the WSLO, such as squalene, EPA, DHA, and biodiesel, and to reduce waste and its associated environmental impacts.

A flow diagram of a possible marine waste biorefinery is shown in Figure 1.5. First of all, WSLO is collected in a feed storage tank after removing all solid waste and ashes from the feed materials. WSLO is then routed to a squalene separation unit to extract the squalene from the WSLO via a saponification reaction; that is, WSLO reacts with an alkali catalyst in the presence of alcohol (ethanol) and water to form soap. Squalene, which is un-saponifiable, is then extracted by adding a solvent such as hexane, since soap is insoluble in hexane. After separating the squalene, the remaining WSLO soap is neutralised with an acid catalyst to form free fatty acid (FFA). The FFA is then esterified using ethanol and an acid catalyst to form fatty acid ethyl esters (FAEE). The FAEE is forwarded to the omega-3 extraction unit, and long chain fatty acid ethyl esters DHA, (22 carbon atoms, 6 double bonds), as well as EPA (20 carbon atoms, 5 double bonds), are extracted from the short chain FAEE based on the complexation between the double bonds of EPA/DHA ethyl ester, and the silver ions using aqueous silver nitrate. In the final step, the remaining short chain FAEE are collected as biodiesel fuel.

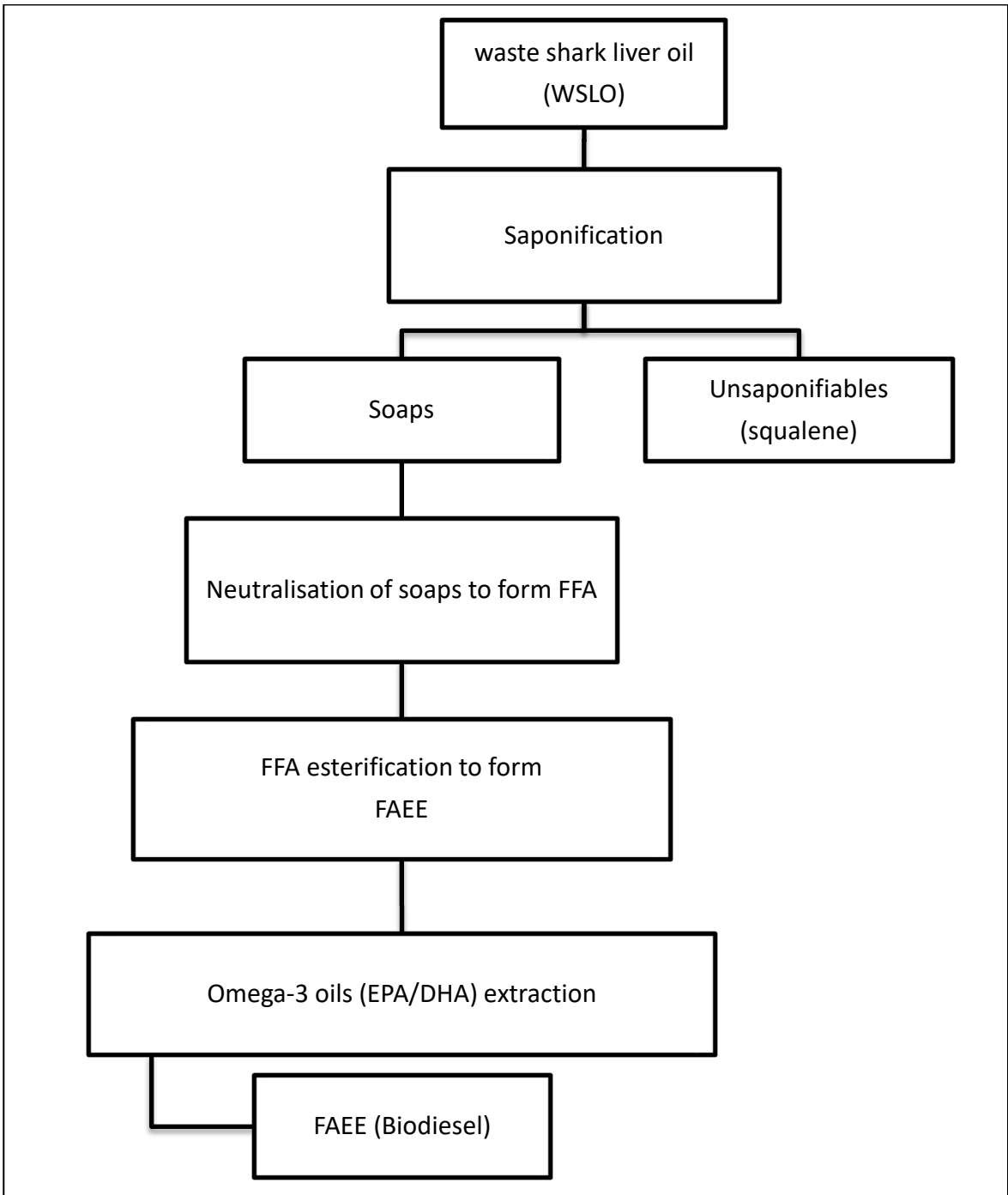


Figure 1.5: Flow diagram of WSLO Biorefinery

1.5 Research Aim and Objectives:

The aim of this work was to identify an efficient and cost effective technique to utilise waste shark liver oil (WSLO) for the production of biodiesel, squalene and omega-3 PUFAs, including EPA and DHA.

The following objectives were identified to achieve this research aim:

- 1) To survey the techniques used for squalene and omega-3 oil separation, to determine which can be integrated with biodiesel production;
- 2) To characterise WSLO, including the content of triglycerides, free fatty acids, moisture, squalene and omega-3 oils components (EPA and DHA);
- 3) To investigate the effect of using alkali and acid-catalysed homogeneous transesterification on FAME conversion from WSLO;
- 4) To carry out a parametric study on biodiesel production reaction from WSLO using both experimental investigations and statistical modelling, to obtain the conditions for highest FAME conversion from WSLO;
- 5) To determine the best technique for separating squalene, EPA and DHA from WSLO;
- 6) To simulate the conversion of WSLO to biodiesel using Aspen HYSYS-V9 and carry out a techno-economic analysis including net present value (NPV) and internal rate of return (IRR) to assess the potential economic feasibilities of the proposed plant;
- 7) To conduct a sensitivity analysis to show the effect of changing uncertain variables on the NPV of the proposed plant.

1.6 Thesis Layout

This section gives a brief overview of the thesis layout.

1) Chapter 1: Introduction

This chapter covers the background to the project on sources of energy and worldwide energy consumption, including transportation energy. It also shows the importance of promoting energy diversity and greenhouse gas (GHG) emission reduction using biofuels such as biodiesel. Furthermore, it presents the main determining factor in biodiesel production cost as feedstock, the cost of which comprises 70–95% of total biodiesel costs. Hence, the use of a cheap non-edible feedstock, such as waste shark liver oil (WSLO), would reduce biodiesel production costs and make the process more economically viable. This section also introduces value-added products obtained from this feedstock, such as squalene and omega 3 oils (EPA and DHA), via the biorefinery process. Finally, it presents the aim and objectives of this research.

2) Chapter 2: Literature Review

Initially, the technologies used to produce biodiesel and the factors that affect the biodiesel production reaction are reviewed. There is also a review of different squalene and omega-3 oils (EPA and DHA) extraction techniques.

3) Chapter 3: Materials and Methods

After reviewing biodiesel production technologies and identifying the extraction techniques for squalene and omega-3 oils (EPA and DHA), this chapter provides the details of all materials and methods used to carry out the experimental research, including the characterisation of WSLO, homogenous catalysed transesterification of WSLO, and squalene and omega-3 oils (EPA and DHA) extraction methods.

4) Chapter 4: Results and Discussion

This chapter describes the results obtained from the characterisation of WSLO, the alkali transesterification of WSLO, and the experimental design for acid-catalysed transesterification. It also presents and discusses the results of the experimental design for squalene extraction using saponification, before discussing the results of the EPA and DHA extraction experiments.

5) Chapter 5: Techno-economic Analysis

This chapter assesses and compares the commercial feasibility of an acid-catalysed biodiesel plant using WSLO, with conventional alkali-catalysed biodiesel production using refined vegetable oil (rapeseed oil). Aspen HYSYS-V9 was used to simulate both plants and accordingly the Net Present Values (NPV), internal rate of return (IRR), and breakeven price were evaluated. Finally, a sensitivity analysis was conducted to show the effect of changing certain variables on the NPV of both biodiesel plants.

6) Chapter 6: Conclusions and Further Work:

This chapter summarises the findings of the WSLO characterisation, the alkali transesterification of WSLO, and experimental design of the acid-catalysed transesterification. It also concludes from the findings of the experimental design for squalene extraction using saponification, and the EPA and DHA extraction experiments. The last section of this chapter recommends future work that needs to be undertaken.

Chapter 2 Literature Review

2.1 Biofuel Feedstock and Global Biofuel Production

There has been a continuous rise in global biofuel production since 2011, as shown in Figure 2.1. This growing interest in biofuel is mainly due to the concerns associated with petroleum-based fuels in terms of energy supply and cost, and climate change. Therefore, ensuring affordable and reliable energy sources with minimum adverse effects on the environment is crucial for world energy supply (Peters and Thielmann, 2008).

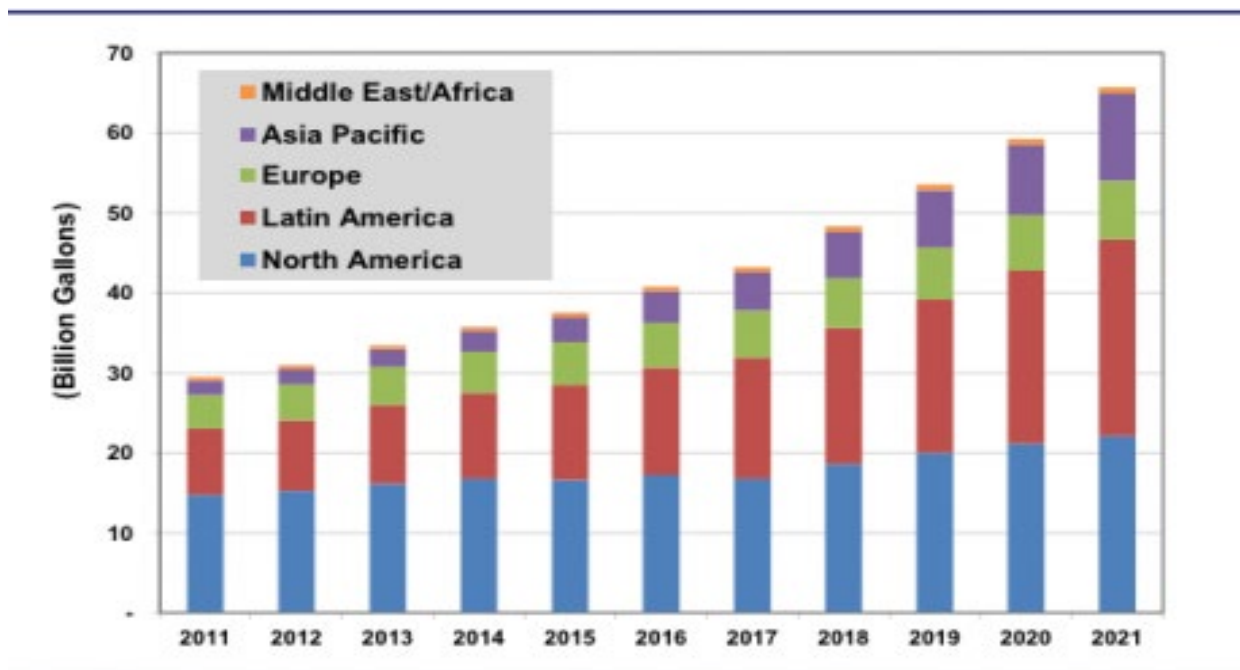


Figure 2.1: Biofuels production by region (PikeResearch, 2012)

Most biofuels are bio-ethanol and biodiesel and are used as liquid fuels for transportation. Generally, bioethanol is obtained from the fermentation of various feedstock that contains sugar and carbohydrates (Halder *et al.*, 2019) Figure 2.2 shows bioethanol yield from various feedstock. Bio-ethanol is produced commercially on an industrial scale, mainly in United States and Brazil due to the predominance of sugarcane and the abundance of land suitable for the cultivation of this raw material (Neto *et al.*, 2018). The production of world ethanol for transportation tripled from 17×10^9 L to 52×10^9 L between 2000 and 2007. The major producers of ethanol are United States and Brazil which account for 62.2% and 25% of global ethanol production, respectively (Singh and Dwevedi, 2019)

Ethanol fuel is used in blended state E10 (10% ethanol) which is recommended for all cars that are manufactured after 2000. Blended ethanol as fuel has been commonly used in Brazil, the United States, and Europe. The first car to run entirely on ethanol was a Fiat 147 in 1978 in Brazil. (Singh and Dwevedi, 2019).

In 2008, bio-ethanol consumption as a fuel for transportation surpassed gasoline in Brazil (Chaddad, 2010). Currently, more than 95% of all cars sold in Brazil are “flex-fuel” cars that can use any blend of gasoline and ethanol (Amorim *et al.*, 2011). Gasoline sold in Brazil contains 25% anhydrous bioethanol (Amorim *et al.*, 2011).

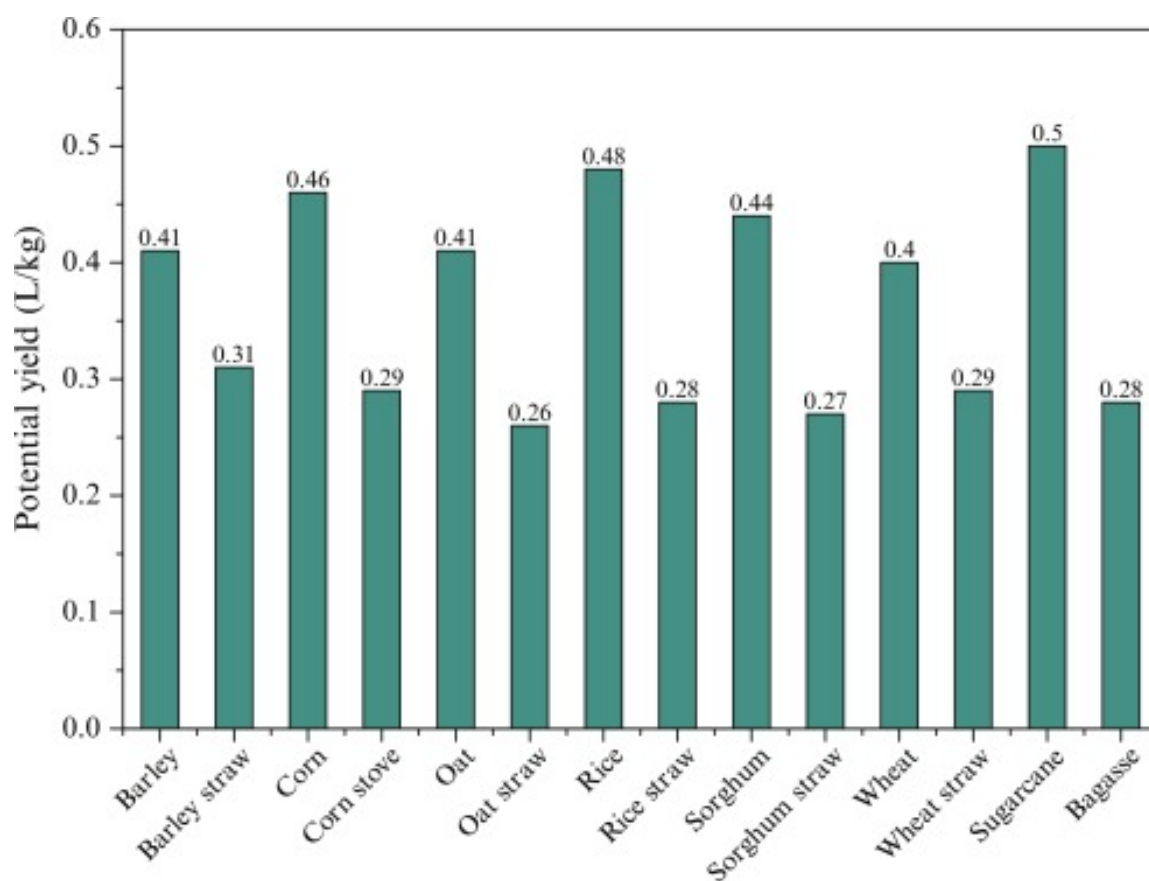


Figure 2.2: Bioethanol yield of different feedstocks (Halder *et al.*, 2019)

Biodiesel is the most common biofuel as a replacement for petrodiesel in compression ignition engines (Celante *et al.*, 2018). Biodiesel can be obtained from several sources, such as animal fat, vegetable sources (edible or non-edible oils), algae, waste cooking oil and grease (Singh and Singh, 2010). The selection of biodiesel feedstock depends on many factors, such as availability and climate. The main feedstock for biodiesel production in Europe is rapeseed and sunflower oils, whereas animal fats and soybean are predominantly used in the USA, and palm oil in Asia, respectively (Singh and Singh, 2010).

Non-edible vegetable oils and other sources of waste oils are potential low-priced feedstocks for biodiesel production, as there are concerns about the use of edible oil for biodiesel production due to the gap between demand and supply, which contributes to food shortages and the global food crisis (Yang *et al.*, 2014). Therefore, non-edible oils from crops that grow in wasteland and which do not compete with food crops could be considered as a sustainable feedstock for biodiesel production. Moreover, it is important that governmental policies and legislation should ensure a balance in ecosystems in the food and fuel supply chain (Yang *et al.*, 2014).

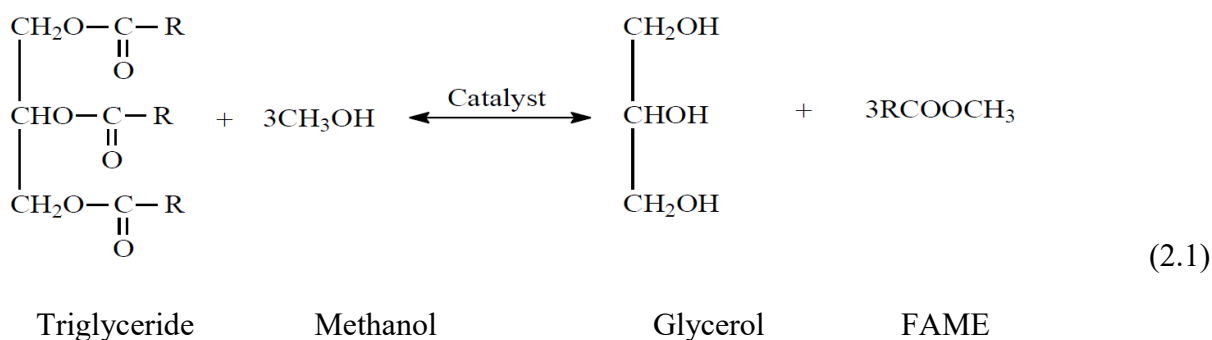
A major challenge to biodiesel production is the high production cost (Zhang *et al.*, 2003b), especially the high cost of feedstocks, which accounts for 70–95% of the total biodiesel production cost (Banković-Ilić *et al.*, 2012). Hence, using a cheap non-edible feedstock, such as waste oil, e.g. waste shark liver oil, could reduce production costs and make the process economically viable.

2.2 Biodiesel Production Technologies

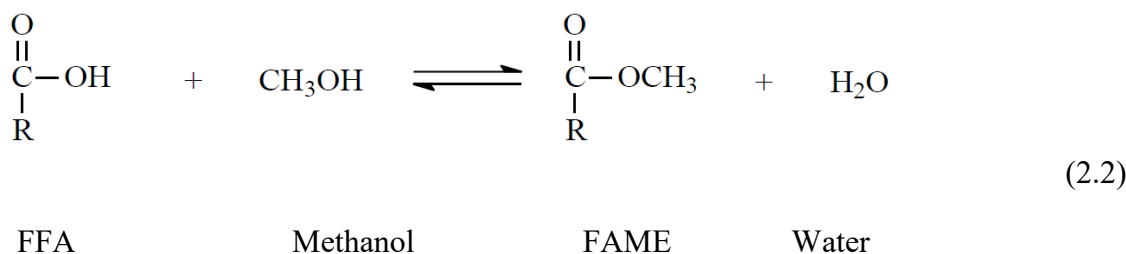
Biodiesel production technology is undergoing rapid technological reform in both industry and academia (Patil and Deng, 2009). The main challenge for commercial biodiesel production is its high cost compared to petroleum-based diesel (Radich, 1998). Therefore, several studies have been carried out to identify a cost effective biodiesel production technology (Patil and Deng, 2009). There are a number of technologies for producing biomass-derived biodiesels, such as direct use and blending of vegetable oils, micro-emulsions, thermal cracking (pyrolysis), and transesterification (Ma and Hanna, 1999b), but only the triglyceride transesterification and FFA esterification processes can be used to produce biofuel that meets the technical definition for biodiesel.

Transesterification for biodiesel production is the most common technique because it is cost effective, and the physical characteristics of the FAMES produced are very close to diesel fuel (Balat and Balat, 2010). Transesterification (alcoholysis) is an ester conversion process involving reactions of the triglyceride from animal fat or vegetable oils with an alcohol (e.g. methanol) to produce FAME and glycerol as a by-product, as shown in Equation 2.1. These reactions can be carried out with or without catalysts, but catalysts are routinely used to increase the reaction rates. Usually, excess alcohol is required to shift the equilibrium to the product side due to equilibrium limitations (Meher *et al.*, 2006). In biodiesel feedstocks containing high levels of free fatty acids, an esterification pre-treatment of the FFA may be required. Esterification is a reversible reaction of carboxylic acids with alcohol (e.g. methanol) to form alky esters and water in the presence of acid catalysts (Moser, 2009), as illustrated in Equation 2.2. This reaction has many commercial

applications such as in the production of intermediates for making cosmetic fragrances or lubricants and flavours (Hoydonckx *et al.*, 2004).



Where: R is an alkyl group of long-chain carboxylic acid



2.3 Factors that Affect Biodiesel Production Reactions

The rate of the biodiesel reaction is determined by a number of factors, including: catalyst type and concentration, alcohol/oil molar ratio, reaction time, temperature, moisture content of the oil, and mixing rate (Meher *et al.*, 2006).

2.3.1 Type of Catalyst

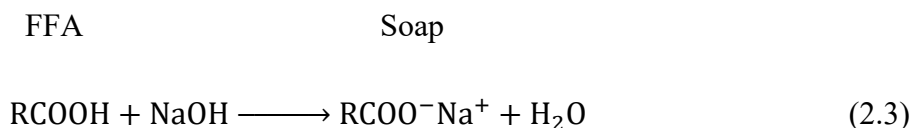
The catalytic transesterification of vegetable oil or animal fat with alcohol (methanol commonly) is an important process to enhance the reaction. Generally, catalysts used for transesterification are categorised into homogenous and heterogeneous catalyst, but this can be further classified as acid catalysts, base catalysts, and enzymes (Helwani *et al.*, 2009). Homogenous transesterification catalysis is the reaction of triglyceride from vegetable oil or animal fat with alcohol, where the

catalyst is in the same phase as the reactant. Among the homogenous catalysts used for transesterification are alkali catalysts, such as the hydroxides and methoxides of sodium and potassium (de Lima and Mota, 2019). Among the acid catalysts, the most commonly used homogenous acid catalysts are sulphuric, phosphoric and hydrochloric acids (Ma and Hanna, 1999b).

The use of heterogeneous catalysis in transesterification reactions has the advantages of preventing saponification reaction, and lower processing cost by eliminating the additional steps for removing the catalyst, as is the case in the homogenous catalyst (de Lima and Mota, 2019). Hence, heterogeneous catalysts have been reported as substitutes for homogeneous catalysts, as heterogeneous catalysts are less corrosive and easier to separate and handle (Helwani *et al.*, 2009). However, homogenous transesterification catalysis has significantly accelerated transesterification reaction rate in comparison with the heterogeneous reaction (Georgogianni *et al.*, 2009). Furthermore, transesterification can be conducted in the absence of catalyst (non-catalytic transesterification), but this process is not economically viable for the production of biodiesel due to the high energy requirement (Zabeti *et al.*, 2009).

2.3.2 Alkali Catalyst

For alkali-catalysed transesterification, low levels (>2.5%) of free fatty acid (FFA) are required to avoid soap formation and catalyst deactivation (Leung *et al.*, 2010), as shown in Equation 2.3. Sodium hydroxide and potassium hydroxide are the most common alkali catalysts in the transesterification reaction (Leung *et al.*, 2010). However, Freedman *et al.* (1984) found that sodium methoxide was more efficient than sodium hydroxide, because when sodium hydroxide is mixed with methanol, a small amount of water is formed which may affect the yield of biodiesel by hydrolysing the triglyceride to diglyceride and FFA, as shown in Equation 2.4 (Leung and Guo, 2006). The oil and alcohol feedstocks are also required to be substantially anhydrous with total water content less than 0.06 wt.%, as water may favour the saponification reaction (Atadashi *et al.*, 2012b). Water also promotes esters (FAME) hydrolysis to form FFA, as shown in Equation 2.4, leading to catalyst deactivation and saponification reactions (Atadashi *et al.*, 2012b).

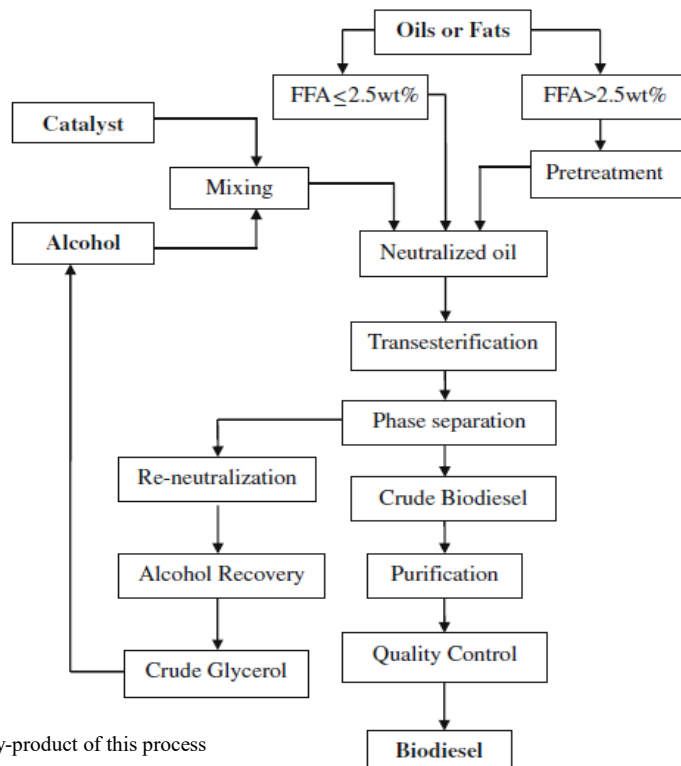




FAME Water FFA Methanol

Alkaline catalysis is advantageous because of its higher reaction rate, which is 4,000 times faster than acid-catalysed transesterification, and the relatively simple process requirements (Lam *et al.*, 2010; Atadashi *et al.*, 2013). However, there are some drawbacks of this type of catalyst, such as the difficulty of extracting the catalyst from the product and recovering by product (glycerol); these are an extra steps with cost and energy implications (Leung *et al.*, 2010). Current purification technologies for crude glycerol are proven effective technologies. However, due to the cost and high energy requirement, it is believed that glycerol purification technologies are viable for large scale plants and unfeasible for small and medium plants due to the energy and cost restraints (Thompson and He, 2006; Ardi *et al.*, 2015).

Figure 2.3 shows that feedstock with an FFA percentage higher than 2.5% requires pre-treatment before using an alkali catalyst. The oil may be esterified with an acid catalyst to reduce the amount of FFA, but if the amount of free fatty acid in the biodiesel feedstock is less than 2.5% then an alkali catalyst is suitable for the reaction (Leung *et al.*, 2010).



Crude Glycerol is a by-product of this process

Figure 2.3: Alkali-catalysed biodiesel production (Leung *et al.*, 2010)

2.3.3 Acid Catalyst

Acid-catalysed transesterification is not as often used in industrial applications for biodiesel production as its counterpart, the alkali-catalysed transesterification. The main reason for this is that the homogenous acid-catalysed transesterification reaction is about four thousand times slower than the homogenous base-catalysed transesterification (Leung, Wu *et al.* 2010). Nevertheless, acid-catalysed transesterification has an advantage over the base-catalysed process as it has a high tolerance for high FFA in the feedstock. Some of the acid catalysts used for transesterification are sulphuric, phosphoric, hydrochloric and organic sulphuric acids.

In alkali-catalysed transesterification, the presence of high FFA and water results in soap formation and, hence, partially shifts the reaction from transesterification to saponification. To avoid these problems, oil from animal fat, or fish oil with a high FFA content, requires an FFA esterification pre-treatment step using an acid catalyst to reduce the FFA content before the application of alkali-catalysed transesterification (Canakci and Sanli, 2008).

Existing studies have shown the positive effect of using an acid-catalysed pre-treatment method followed by alkali-catalysed transesterification. For example, acid-catalysed pre-treatment steps were applied to a yellow grease with 12% FFA and a brown grease with 33% FFA, to reduce their FFA content to less than 1% FFA (Enweremadu and Mbarawa, 2009).

2.3.4 Enzyme Catalyst

Enzymatic catalysts such as lipases can catalyse the transesterification of a variety of triglycerides, including waste oils and fats with high levels of FFA. For instance, sunflower oil has been successfully catalysed by lipases from *C. antarctica* and *R. miehei*. Furthermore, rapeseed oil has been transesterified using lipases from *M. miehei*, *M. circinelloides* and *T. lanuginose* (Gog *et al.*, 2012). Feedstock with high FFA, such as tallow, was transesterified using *M. miehei* and *C. antarctica* lipases (Gog *et al.*, 2012). Using enzymatic catalysts to produce biodiesel can overcome the drawbacks associated with alkali-catalysed transesterification, such as extracting the catalyst from the product and avoiding soap formation. The main drawback of enzymatic transesterification is the high cost and longer reaction time, and so it is not common to use lipases to produce biodiesel commercially (Leung *et al.*, 2010).

2.3.5 Alcohol Quantity

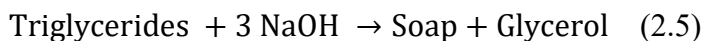
Researchers have investigated the effect of the molar ratio of alcohol to triglycerides in the yield of biodiesel and found that one of the important factors influencing ester yield is the quantity of alcohol (Leung and Guo, 2006). The stoichiometric molar ratio of alcohol to oil is 3:1, where the reaction needs three moles of alcohol for one mole of triglycerides to produce three moles of FAME and one mole of glycerol. However, since the reaction is reversible, excess alcohol is required to ensure triglycerides have been converted to FAME. Although increasing the amount of alcohol enhances the ester yield, this also increases the cost of alcohol recovery (Musa, 2016). The higher energy required for alcohol recovery has a huge effect on the processing of feedstocks containing a high level of FFA, such as waste cooking oil, which requires higher molar ratios of alcohol to triglycerides of up to 15:1 for acid-catalysed transesterification (Ali *et al.*, 1995). Furthermore, molar ratios of 3:1 to 15:1 were investigated in the transesterification of Cynara oil using ethanol, where the yield of biodiesel increased with the ethanol molar ratio up to a value of 12:1. The best biodiesel yield was obtained with molar ratios of 9:1 and 12:1, whereas an incomplete reaction was observed for molar ratios below 6:1. However, for a molar ratio of 15:1, the glycerol separation was difficult and the yield of esters decreased due to the fact that a part of the glycerol remains in the biodiesel phase (Lee and Saka, 2010).

2.3.6 Reaction Temperature and Catalyst Concentration

It has frequently been reported that the temperature of the transesterification reaction influences the ester yield. The transesterification of soybean oil with methanol molar ratio 6:1 has been investigated using 1% of NaOH at three different temperatures. After 0.1 hr the ester yields were 94%, 87% and 64% for 60°C, 45°C and 32°C, respectively (Ma and Hanna, 1999a). Researchers demonstrated that, depending on the oil feedstock used, the optimal temperature ranges from 50°C to 60°C, and it has to be lower than the boiling point of alcohol used to avoid vaporisation of alcohol (Ma and Hanna, 1999a).

The conversion of triglycerides to fatty acid esters can also be affected by the amount of catalyst used in the reaction. Eevera *et al.* (2009) investigated the influence of catalyst concentrations on transesterification using sodium hydroxide catalyst in methanolysis of refined canola oil and used frying oil. The conversion of triglyceride to FAME was shown to increase with catalyst concentration, while an insufficient amount of sodium hydroxide resulted in incomplete conversion of triglycerides to FAME, resulting in lower ester contents (Eevera *et al.*, 2009). The study also showed that, sodium hydroxide catalyst at 1.5 wt. % based on the oil reached the optimal value biodiesel yield. However, a further increase in catalyst concentration decreased ester

conversion and a large amount of soap was noticed (Eevera *et al.*, 2009). This is because the addition of excess alkaline catalyst resulted in greater triglyceride participation in the saponification reaction with sodium hydroxide, as shown in Equation 2.5. Therefore, the amount of soap production increased and consequently ester conversion decreased (Eevera *et al.*, 2009).



2.3.7 Moisture Content and Free Fatty Acid Content

Oil and alcohol feedstocks are required to be substantially anhydrous with total water contents below 0.06 wt.% for alkali-catalysed transesterification. Having excess water above 0.06 wt.% in alkali-catalysed transesterification leads to hydrolysis of the triglycerides and production of FFA, which react with the alkaline catalyst to form soap. Consequently, it will affect the biodiesel yield and render the separation of glycerol (Dorado *et al.*, 2002). Furthermore, soap formation deactivates the catalyst activity, which will reduce the biodiesel yield (Atadashi *et al.*, 2012a).

Feedstocks with FFA percentages above 2.5% require pre-treatment before using an alkali catalyst. The oil may be esterified with an acid catalyst to reduce the amount of FFA, but if the amount of free fatty acid in the biodiesel feedstock is less than 2.5% then the alkali catalyst is suitable for the reaction (Leung *et al.*, 2010). Generally, feedstock with high FFA and water result in soap formation and, hence, shift the reaction partially from transesterification to saponification. Therefore, to avoid these problems, an esterification pre-treatment step using an acid catalyst is required to reduce the FFA content before the application of alkali-catalysed transesterification (Canakci and Sanli, 2008).

2.4 Types of Reactors for Biodiesel Production

Commercial biodiesel producers use continuous stirred tank reactors (CSTR) for the transesterification of animal fat or vegetable oils in the presence of acid or base catalyst to produce biodiesel. CSTR is the most common continuous-flow system in biodiesel production (Regalado-Méndez *et al.*, 2015). The continuous-stirred tank reactor has constant input and output of material where the reactants are continuously added and the product are continuously removed as shown in Figure 2.4.

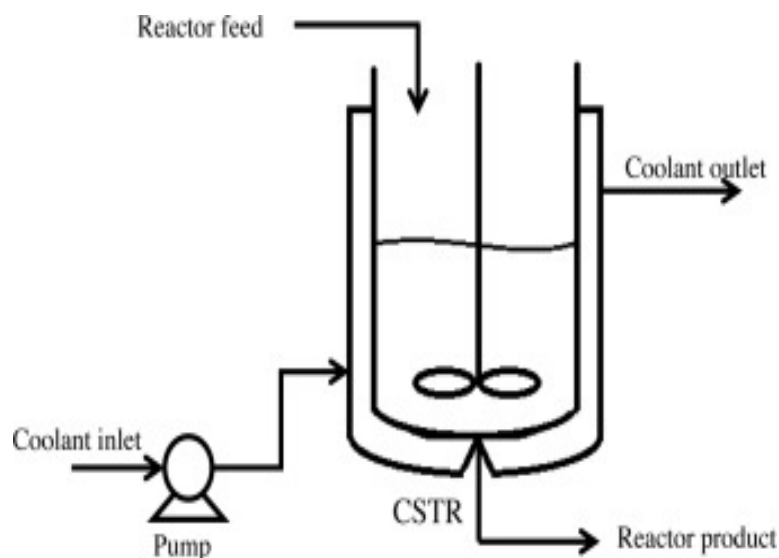


Figure 2.4: CSTR diagrammatic sketch (Zhao *et al.*, 2015)

CSTR is usually used for larger plants (>4 million L/year) whereas batch reactors are used for small biodiesel production plants (Gerpen, 2005). The batch reactor consists of a tank and some type of agitation. The tank contains the reactants for the process which are oil, alcohol, and catalyst in the case of biodiesel process.

Batch reactors are operated with all the reactants placed in the reactor before the start of reaction, and all are removed after the completion of reaction. There is no addition or removal of material during the reaction process as shown in Figure 2.5 (Foutch, 2003).

The main advantages of the batch reactor are simplicity of design, which allows for high flexibility to accommodate variations in feedstock type, composition, and quantity. The major drawbacks of the batch process include low productivity, larger variation in product quality, and labour that is more intensive and energy requirements (Foutch, 2003).

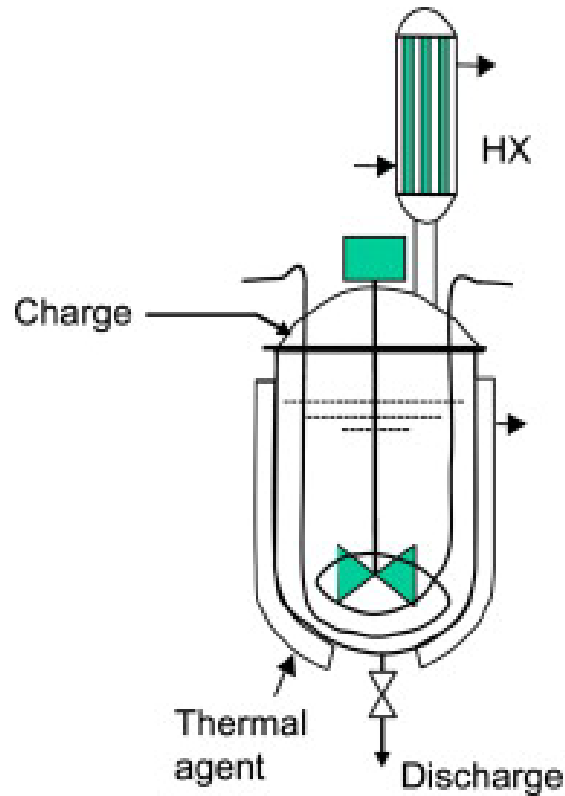


Figure 2.5: Batch reactor (Dimian *et al.*, 2014)

There are technical challenges facing biodiesel production via transesterification, which include: long residence times, high operating cost, high energy consumption and low production efficiency (Qiu *et al.*, 2010). Therefore, several studies were carried out to develop process intensification technologies to overcome the aforementioned challenges in biodiesel production. These process intensification technologies enhance reaction rate, reduce molar ratio of alcohol to oil and lower the energy needed by intensification of mass transfer and heat transfer in addition to the in situ product separation. Implementing these process intensification technologies result in achieving the desired products for successful commercial production (Qiu *et al.*, 2010).

Some aspect of the development of process intensification technologies that is highlighted in this review are the utilisation of novel reactors. These reactors are used to enhance the reaction rate and thus the residence time.

2.4.1 *Static mixers reactor*

Static mixers consist of specially designed motionless geometric elements enclosed within a pipe or a column. They create efficient radial mixing of two immiscible liquids as they flow through the mixer. Static mixer system has been used as a continuous-flow reactor to produce biodiesel

from canola oil with methanol and sodium hydroxide as catalyst (Thompson and He, 2007). The experimental setup is shown in Figure 2.6. The static mixer system consists of two stainless steel static reactors (4.9 mm ID \times 300 mm long) including 34 fixed right- and left-hand helical mixing elements. After optimising the experimental parameters, high quality biodiesel which met the ASTM D6584 standard was successfully obtained. The optimum conditions for this reaction were 60 °C reaction temperature, 1.5% sodium hydroxide catalyst concentration, and reaction time of 30 min. and 6:1 molar ratio of methanol to oil (Qiu *et al.*, 2010)

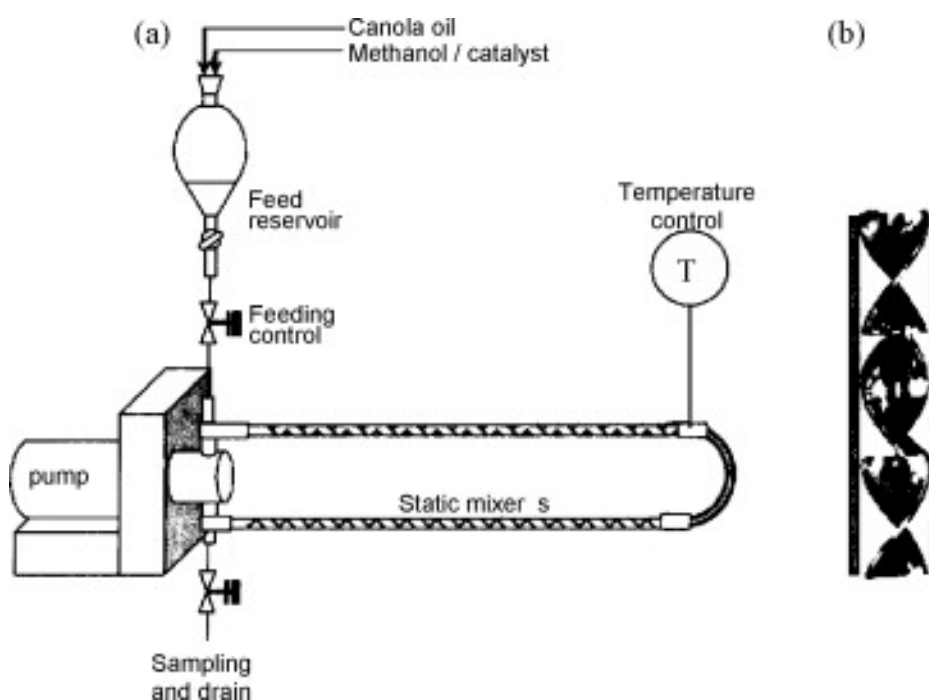


Figure 2.6: Experimental setup: (a) static mixer closed-loop system, and (b) internal structure of static mixer (Qiu *et al.*, 2010)

2.4.2 Micro-reactors

The micro-reactor device has a very small internal diameter 10-50 μm (Dessimoz *et al.*, 2008), with high interfacial area to reactor volume 10,000-50,000 m^{-1} (Jähnisch *et al.*, 2004). Its high interfacial area can increase the agitation between the liquid-liquid particles, to improve the heat and mass transfer (Dessimoz *et al.*, 2008; Mazubert *et al.*, 2013). The liquid intensity inside the reactor depends on flow regime, physical properties of the reactants and the reactor geometry (Dessimoz *et al.*, 2008). Due to its millimetre volume, low quantity of reagents are used therefore, the reaction is always either in slug flow or parallel flow (Dessimoz *et al.*, 2008).

In slug-flow, the mixing can be enhanced by either increasing of interfacial area (i.e. using zigzag channel) or increasing the recirculating diffusion (Wen *et al.*, 2009). In parallel flow regime, the mass transport depends only on the particles diffusion inside the reactor, because there is no recirculating diffusion (Mazubert *et al.*, 2013).

This reactor was employed in the transesterification reaction of biodiesel production. Rahimi *et al.* (2014) reported that 98% of yield can be obtained from methanolysis of soybean oil at 9:1 of (MeOH: soybean oil) molar ratio, 1.2 (catalyst KOH : oil) wt.% , 60 °C reaction temperature and 180s reaction time (Rahimi *et al.*, 2014). While, only 28s and 56°C were required to complete the same reaction under the same operating conditions when the reactor was modified to zigzag channel (240µm) (Wen *et al.*, 2009). Zigzag shape can increase the internal surface area which in turn leads to increase the contact between the reaction particles and improve triglyceride to FAME conversion. 78.3% of FAME yield was obtained from supercritical conditions of refined palm oil with ethyl acetate at 330-370°C reaction temperature , under 200 bar pressure in micro- reactor and 1:50 of ethyl acetate to oil molar ratio (Sootchiewcharn *et al.*, 2015).

To sum up, biodiesel synthesis can be intensified in a micro reactor, as this reactor can reduce the required time and energy with high efficiency of production. However, due to reactor small volume, using solid catalyst can cause many technical problems such as plugging.

2.4.3 Oscillatory flow reactors

Oscillatory flow reactors (OBR) are tubular reactors which contain equally spaced orifice plate baffles and produce oscillatory flow using a piston drive as shown Figure 2.7. When a fluid is introduced into the OBR reactor, an oscillatory motion interacts with it, intensifies radial mixing which enhance mass and heat transfer, and maintain plug flow.

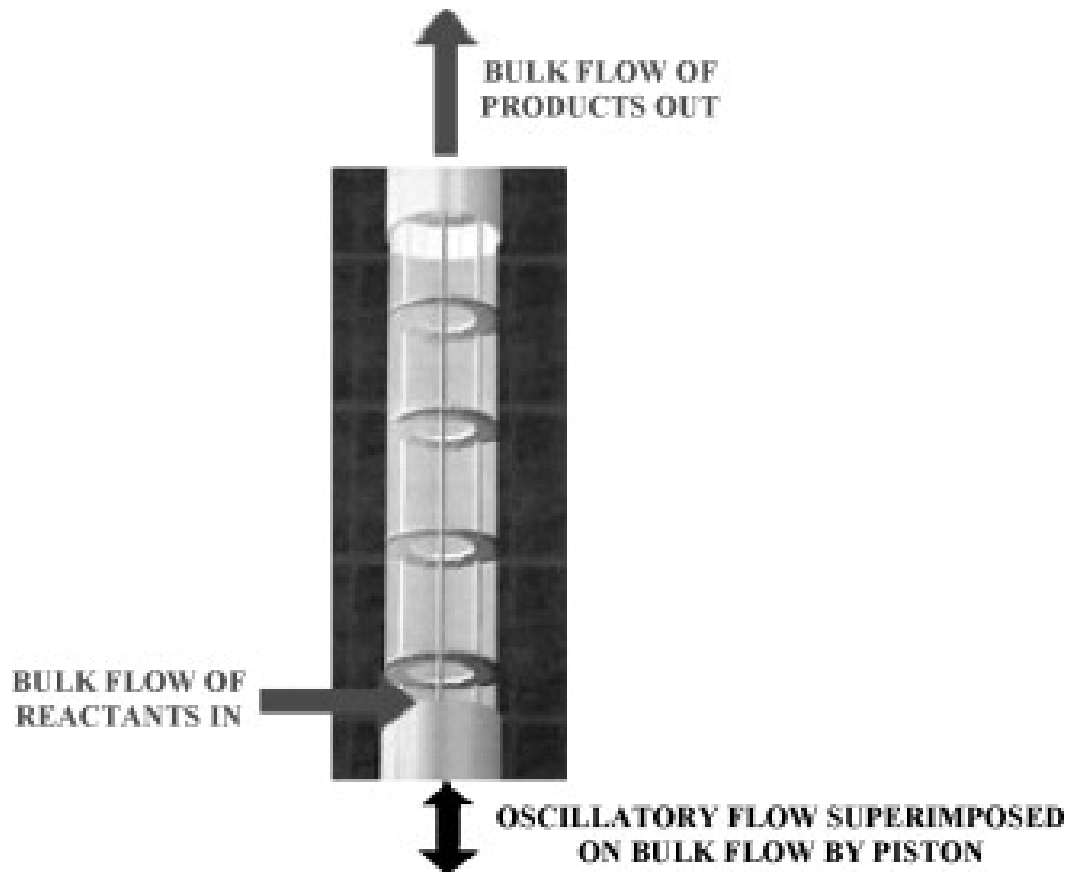


Figure 2.7: The configuration of oscillatory flow reactor (Harvey and Lee, 2012)

A continuous oscillatory flow reactor (OFR) was developed to produce biodiesel from rapeseed oil in a pilot-scale plant shown in Figure 2.8. The reactor consists of two vertically positioned jacketed tubes of 1.5 m length and 25 mm internal diameter. Biodiesel conversion of 99% were achieved after 30 min at 50 °C using a molar ratio of methanol to rapeseed oil of 1.5 and in the presence of a sodium hydroxide catalyst. Conversions of biodiesel up to 99% were achieved after 30 min at 50 °C using a molar ratio of methanol to rapeseed oil of 1.5 and in the presence of a sodium hydroxide catalyst (Harvey and Lee, 2012).

One of the advantages of OFR technology is that it requires a very low molar ratio of methanol to oil in comparison to the stoichiometric ratio (3:1) which reduces significantly the operating cost. Furthermore, the short length-to-diameter of this reactor decreases capital cost and allows scale up of the process (Harvey and Lee, 2012).

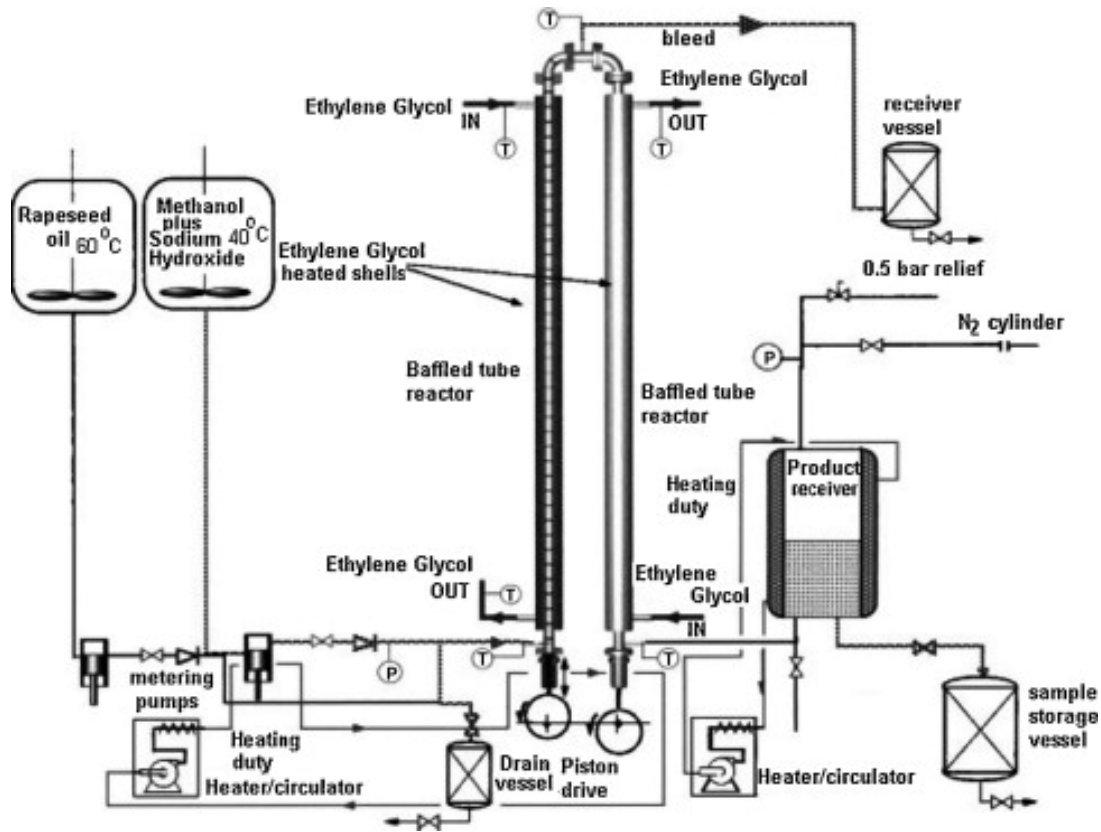


Figure 2.8: Schematic of oscillatory flow reactor for biodiesel production (Harvey and Lee, 2012)

2.4.4 Spinning reactors

The spinning reactor is disc or tube rotates fast depending on centrifugal force. The reactants fed from the top of the reactor, from which a thin layer travel along the disc and help to enhance the mixing as shown in Figure 2.9 **Error! Reference source not found.**(de Caprariis *et al.*, 2012; Pask *et al.*, 2012).

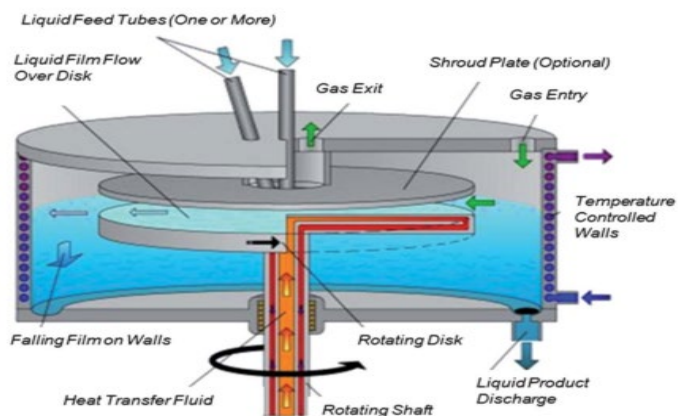


Figure 2.9: A schematic view of a spinning disk reactor (Pask *et al.*, 2012).

More than 98% of FAME yield was attained after 40s from methanolysis of canola oil in the presence of NaOH catalyst under 40 - 65 °C for a reaction carried out in a rotating tube reactor (Lodha *et al.*, 2012). In comparison with batch reactor, a few seconds were required to convert 80% of canola oil to FAME conversion at 40°C reaction temperature, 6:1 (methanol : canola oil), 1 wt.% of (NaOH : oil) catalyst concentration and 1000 rpm stirring speed (Qiu *et al.*, 2012).

The disadvantage of this reactor is the difficult handling of solid catalyst in this reactor. The only way that can be used to overcome this difficulty is by coating the reactor tube by a catalytic material which is a very expensive and time consuming technique.

2.4.5 Acoustic reactors

Acoustic reactor or ultrasound reactor is a type of intensification reactor that produces an acoustic energy with a frequency ranged from 20-50 kHz to mix the reactants together. This frequency can create a cavity in the reaction mixture which enables establishment of a uniform and intense mixing inside the reactor (Gole and Gogate, 2012). This reactor has been employed to produce biodiesel due to its excellent performance to enhance the mixing and increase the interfacial area between the liquid-liquid reaction (Mazubert *et al.*, 2013).

It was found that the transesterification reaction carried out in an acoustic reactor is shorter and more economic in terms of reducing the required reagents to achieve the same conversion of triglyceride to methyl ester compared with batch reactor. (Kumar *et al.*, 2010) found that more than 98% of free fatty acid ethyl ester yield can be obtained from ethanolysis of coconut oil at 6:1 of ethanol : oil molar ratio, 0.75 wt % (KOH : oil) catalyst concentration in an acoustic reactor. Furthermore, the required time in ultra-sonication reactor was 7 min. compared with 1-4 h to achieve the same conversion in a batch reactor (Kumar *et al.*, 2010). Similarly, only 50 min was required in the transesterification reaction of canola oil to methanol (1:5), 0.7 wt.% of potassium hydroxide in ultrasonic reactor at room temperature to get >99% of canola oil conversion to FAME (Thanh *et al.*, 2010). Ultrasound reactor was also used in the transesterification reaction in heterogeneous phase. Mild reaction conditions were required to obtain more than 90 % yield of methyl ester at 90 min reaction time, 65°C reaction temperature, (9:1) of methanol to soybean oil and 1wt% loading of calcium methoxide catalyst (Deshmane and Adewuyi, 2013).

In summary, even the obtained free fatty acid alkyl ester from this type of reactor has a good quality with high conversion, but the required time to establish the reaction (7 and 90 min) which is high compared with that required in micro-reactor (180 s) and spinning disc (40 s).

2.5 Bio-refining of Waste Shark Liver Oil

2.5.1 Biodiesel Production from Waste Shark Liver Oil

There are limited studies on biodiesel production from WSLO, and there is currently no existing work on producing biodiesel from *Carcharhinidae* shark liver oil used in this study. Most existing research is focused on physical and chemical properties, characterisations of lipids, separation of squalene and discrimination against diacylglycerol ethers (DAGE). A lipase-catalysed ethanolsis of squalene-free shark liver oil was investigated by Fernández *et al.* (2013), who used the ethanolsis of shark liver oil for the discrimination of ether lipids such as alkylglycerols (AKG), monoacylglycerol ethers (MAGE), and DAGE, as shown in

Figure 2.10. Ether lipids (AKG, MAGE, and DAGE) are valuable components. They have been used as a therapy for cancer since they are potent antineoplastic agents that inhibit growth, show anti-metastatic activity and induce differentiation and apoptosis in cancer cells (Diomedea *et al.*, 1993).

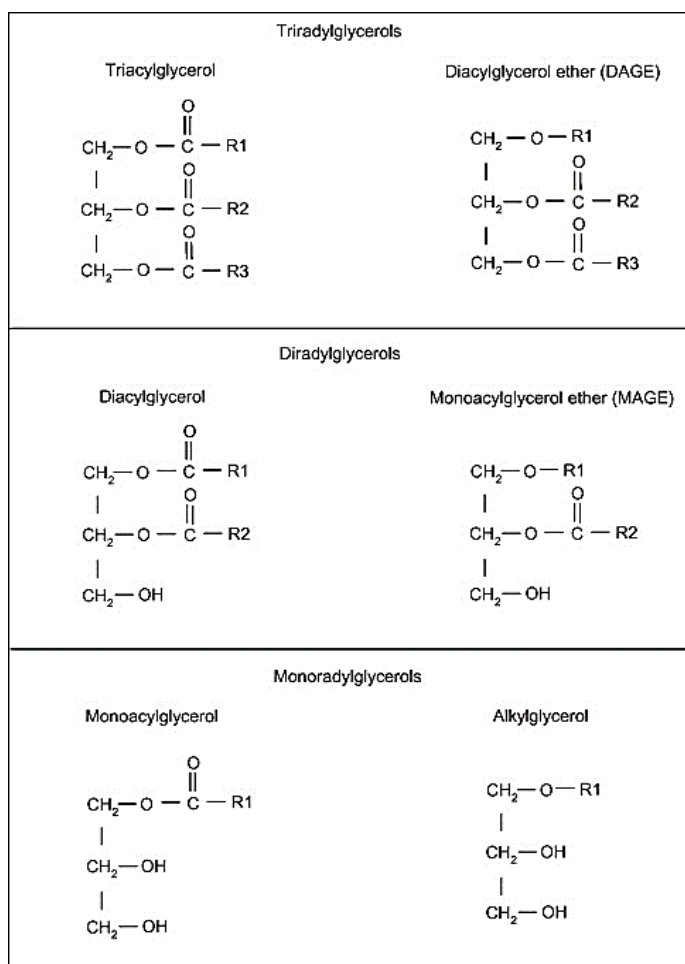


Figure 2.10: Ether lipids (Fernández *et al.*, 2013)

2.5.2 Extraction Process of Omega-3 Polyunsaturated Fatty Acids (PUFAs)

Omega-3 fatty acids are long-chain polyunsaturated fatty acids ranging from 18 to 22 carbon atoms, with the first double bonds starting at the third carbon from the methyl end group. WSLO is one source of omega-3 PUFA, mainly the docosahexaenoic acid, DHA, (22 carbon atoms, six double bonds) and eicosapentaenoic acid, EPA (20 carbon atoms, five double bonds), as shown in Figure 2.11 (Iagher *et al.*, 2013). Omega-3 fatty acid can also be found as alpha-linolenic acid (ALA) in plant oil like walnut and algal oil. The degree of unsaturation (number of double bonds) in the fatty acid determines the degree of susceptibility to oxidation. DHA has six double bonds and EPA has five double bonds which are very susceptible to several types of reaction, especially oxidation, due to the high number of double bonds. Furthermore, the hydrolysis reaction can occur in the presence of moisture and heat, where the PUFA triglycerides will break down into free fatty acids, mono, and di-glycerides (Hernandez, 2005).

The isomerisation reaction also occurs in fish oil when there is a change in the configuration of fish oil fatty acid from cis- to trans-isomers, especially when fish oil deodorisation is conducted at unusually high temperatures and for long periods of time (Hernandez, 2005). Other isomerisation reactions occur when the double bond in fatty acids changes position due to high heat exposure, resulting in the formation of conjugated double bonds (Hernandez, 2005).

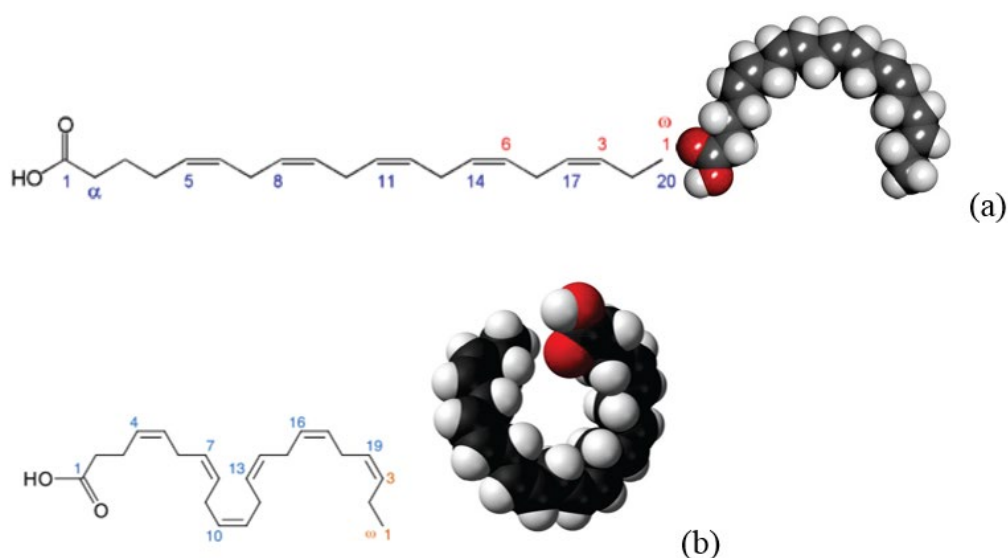


Figure 2.11: Structure of EPA (a) and DHA (b) (Holub and Holub, 2004)

In terms of applications, there is a high demand for omega-3 PUFA due to their health benefits, after their importance to human health was realised in the 1980s when several authors published epidemiological studies about the relation between an omega-3 enriched diet and the prevention of diseases like myocardial infarction or bronchial asthma (Kromann and Green, 1980). Subsequently many studies have investigated the effect of EPA and DHA in human health (Rubio-Rodríguez *et al.*, 2010). The health benefits of EPA include the prevention of coronary heart disease, while DHA is useful for the improvement of brain and retina functions (Navarro-García *et al.*, 2004). Ruxton *et al.* (2005) concluded that there is strong evidence of the clinical benefit of long chain omega-3 fatty acid on cardiovascular diseases or rheumatoid arthritis. Moreover, it has the ability to inhibit a number of aspects of inflammation (Calder, 2013), and decreases the risk of arrhythmias, which can lead to sudden cardiac death (Rubio-Rodríguez *et al.*, 2010). Due to the proven health benefits of omega-3 fatty acids, these products are now widely used in infant formula as essential nutrients for infant growth (Li and Li, 2008). The above applications strongly suggest the importance of consuming omega-3 fatty acid either through natural food products or as a supplement (Lands, 2008). Thus, any new sources of omega-3 are valuable, especially if the source is currently under-utilised, as is the case with waste shark liver oil (Navarro-García *et al.*, 2010).

There are a number of methods of extracting omega-3 PUFAs from fish oils, as shown in Figure 2.12, most commonly: molecular distillation (MD), high-performance liquid chromatography (HPLC/LC), supercritical fluid extraction (SFE), supercritical fluid chromatography (SFC), enzymatic enrichment, crystallisation at low temperatures, and urea precipitation.

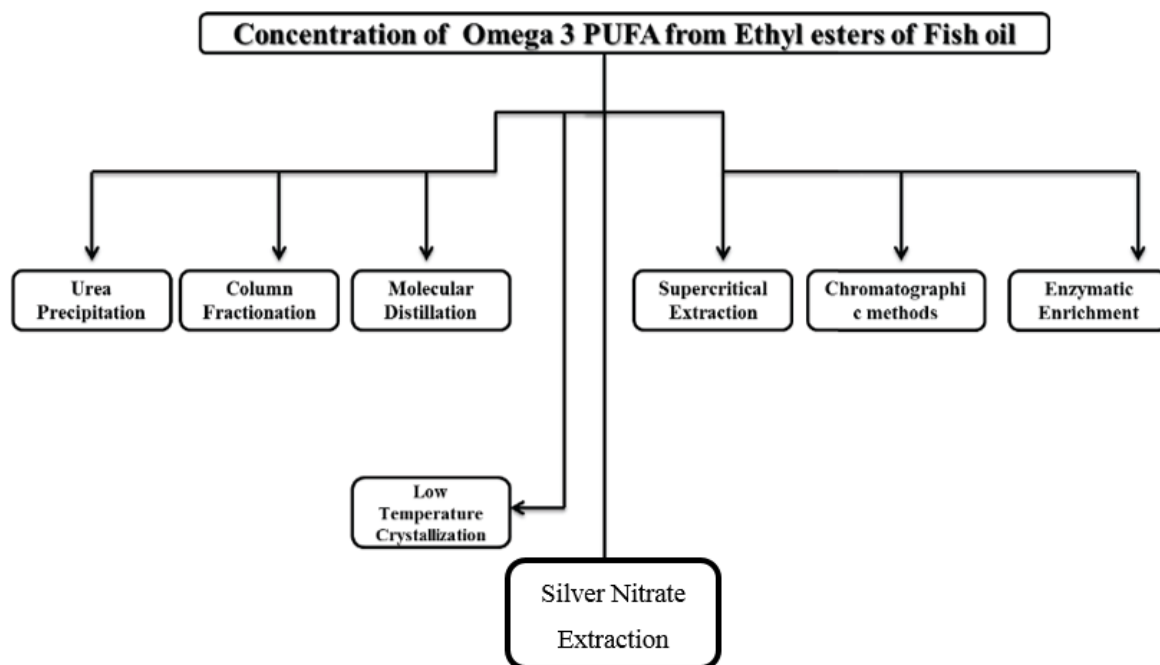


Figure 2.12: General overview of common omega-3 extraction methods (Lembke, 2013a)

2.5.2.1 Urea Precipitation

Urea precipitation is used to extract omega 3 PUFA from fish oil, and was first reported by Domat *et al.* (1955). The process depends on the formation of crystals that contain urea-complex with saturated fatty acids.

Figure 2.13 shows the formation of urea crystals in the absence and presence of long chain fatty acids. This crystal is removed by centrifugation or filtration, and subsequently produces an effluent liquid stream with a high concentration of unsaturated fatty acid. The drawback of this extraction process is the moderate extraction efficiency and potential formation of carbamate, which is a carcinogenic compound (Shahidi and Wanasundara, 1998; Canas and Yurawecz, 1999).

The use of urea complexation in pilot scale for the concentration of omega-3 fatty acid has been demonstrated by Ratnayake *et al.* (1988). The production of omega-3 fatty acid from seal blubber using urea complexation was optimised by Wanasundara and Shahidi (1999). A maximum production of omega-3 fatty acid (88.2%) at a urea : fatty acid ratio of 4.5:1, a crystallisation time of 24 h, and a crystallisation temperature of -10°C (Wanasundara and Shahidi, 1999).

UREA COMPLEXATION

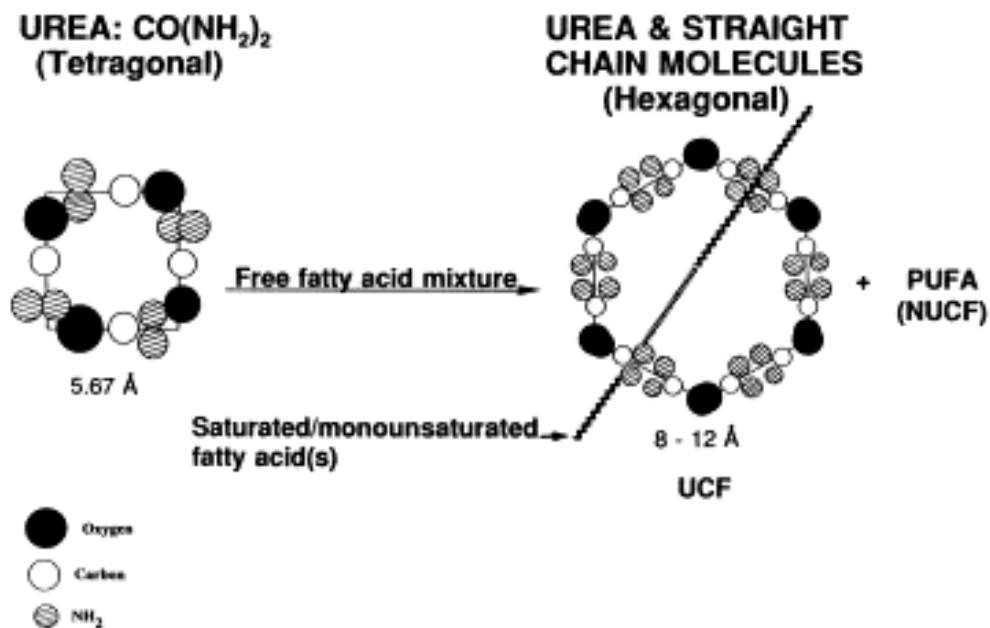


Figure 2.13: Formation of urea crystals in the absence and presence of long chain fatty acids (Shahidi and Wanasundara, 1998)

2.5.2.2 Low Temperature Crystallisation

The low temperature crystallisation method is one of the techniques used for the separation of omega 3 PUFA from fish oil. The method depends on the melting point of the fatty acid in a different organic solvent at low temperature (-50°C to -70°C), such as methanol, ethanol and hexane. In order to attain the required low temperatures, a heavy refrigeration load is required, and this is the main shortcoming of this extraction process for large industrial applications(Lembke, 2013a). It has been reported that use of different organic solvents and temperatures affects the concentration of PUFA (Yokochi *et al.*, 1990). Therefore, it is necessary to select carefully the right solvent and temperature in order to achieve the optimum concentration of ω3-PUFA.

Preparation of ω3-PUFA concentrates from seal blubber oil (SBO) by low-temperature crystallisation has been reported (Wanasundara, 2001). The SBO in TAG form was subjected to solvent crystallisation at different temperatures. Figure 2.14 (A) shows the extraction of total ω3-PUFA following low-temperature crystallisation of SBO using hexane and acetone as solvents. It was observed that the content of ω3-PUFA in the non-crystalline fraction (the concentrate) was increased with lowering of the crystallisation temperature. Acetone afforded the highest concentration of total ω3-PUFA at all of the temperature conditions.

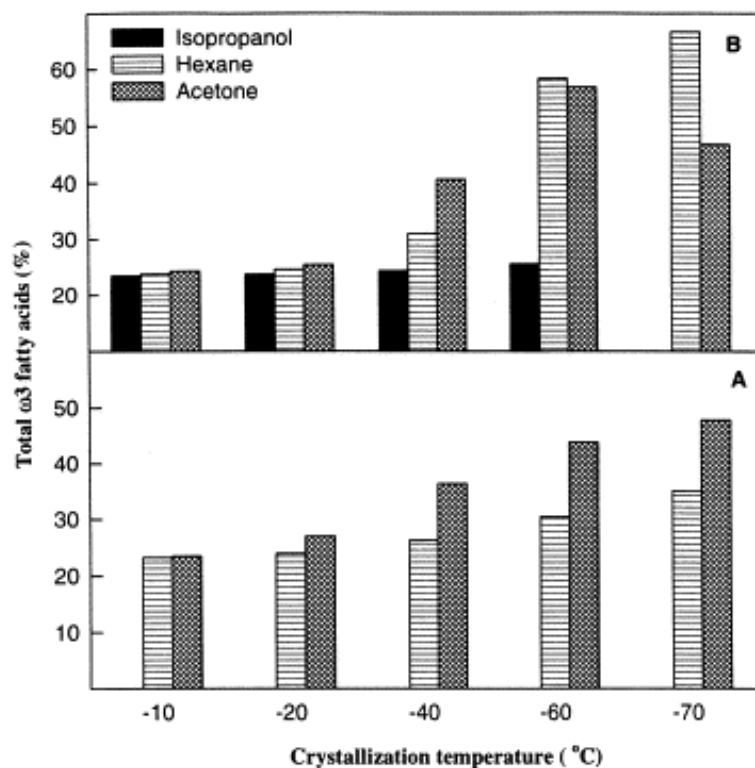


Figure 2.14: Enrichment of total ω 3-fatty acids of seal blubber oil upon low temperature crystallization. A, triacylglycerol form; B, free fatty acid form (Wanasundara, 2001).

Low-temperature crystallization of SBO, in the free fatty acid form resulted in total ω 3-PUFA content of up to 58.3 and 66.7% at -60 and -70°C temperature using hexane with concentrate recoveries of 39.0 and 24.8%, respectively as shown in Figure 2.14 (B). However, the content of total ω 3-PUFA in acetone increased up to 56.7 and 46.8%, but the recovery of the concentrate was 15.9 and 12.9%, respectively (Wanasundara, 2001).

2.5.2.3 Enzymatic Enrichment

Enzymatic enrichment can be used to extract EPA and DHA from fish oil. The process depends on liberating the FFA from the glycerol backbone using specific enzymes such as lipase B from *Candida antarctica*, which can cleave in the sn1 and sn3 positions of the glycerol; alternatively, they can cleave in the sn2 position specifically, as most fish oils have EPA and DHA in position sn2 of the triglycerides. Consequently, the FFA can be removed by molecular distillation (MD) and the remainder is the concentrated EPA and/or DHA fraction. Using enzymatic enrichment technology, around 50% omega-3 concentrations (EPA + DHA) can be achieved (Lembke, 2013b).

Enzymatic hydrolysis of sardine oil for enriching omega-3 fatty acid in small scale with *Candida rugosa*, *Mucor javanicus*, and *Aspergillus niger* were investigated by Okada and

Morrissey (2007). It was concluded that *Candida rugosa* is more effective compared to other lipases (Okada and Morrissey, 2007).

Mbatia *et al.* (2010) examined the enzymatic enrichment of omega-3 fatty acid with Nile perch viscera oil. It has been found that the temperature can affect the reaction rate of lipase and consequently affect the enrichment. Therefore, the increase in enrichment level is proportional to the EPA and DHA losses (Mbatia *et al.*, 2010). Chen and Ju (2000) reported that using immobilised enzymes is time consuming and in order to PUFA, oxidation at relatively low temperature reaction, additional time is recommended (Chen and Ju, 2000).

The main factors that affect the production ω -3 fatty acids concentrates via lipase-assisted hydrolysis are: enzyme concentration, reaction time, temperature and pH. Furthermore, the temperature of the reaction medium and the reaction time are vital due to the influence on the oxidative state of the prepared ω -3 concentrates (Sun *et al.*, 2002).

2.5.2.4 Liquid Chromatography

Liquid Chromatography (LC) is a separation technique with high selectivity for the chain length and degree of unsaturation of the fatty acid. However, isolation of the fatty acid fraction requires a large amount of organic solvents (mobile phase) in the separation column and these organic solvents have to be removed from the isolated fatty acid, which makes it a costly process (Lembke, 2013a). The other drawback of LC is that the final product may still have traces of the undesired organic solvents. Nevertheless, the LC technique has been used for many years to produce very highly concentrated omega-3 products, mostly in combination with other concentration techniques like urea precipitation, MD, and low temperature crystallisation (Lembke, 2013a)

2.5.2.5 Molecular Distillation

The basic principle of molecular distillation as shown in Figure 2.15 is the difference of compound volatility under vacuum to allow operation at lower temperatures. The difference in volatility of the shorter chain (16- and 18-carbon fatty acids esters) and longer chain (20- and 22-carbon EPA/DHA ethyl ester) enables the short path distillation process to concentrate EPA and DHA ethyl esters to levels of over 50% (Breivik *et al.*, 1997). Further concentration of omega-3 over 50% using the same method can be achieved by repeatedly running the oil through the same process, which costs more energy and exposes the product to a very high temperature, consequently shortening product stability and shelf life (Breivik *et al.*, 1997).

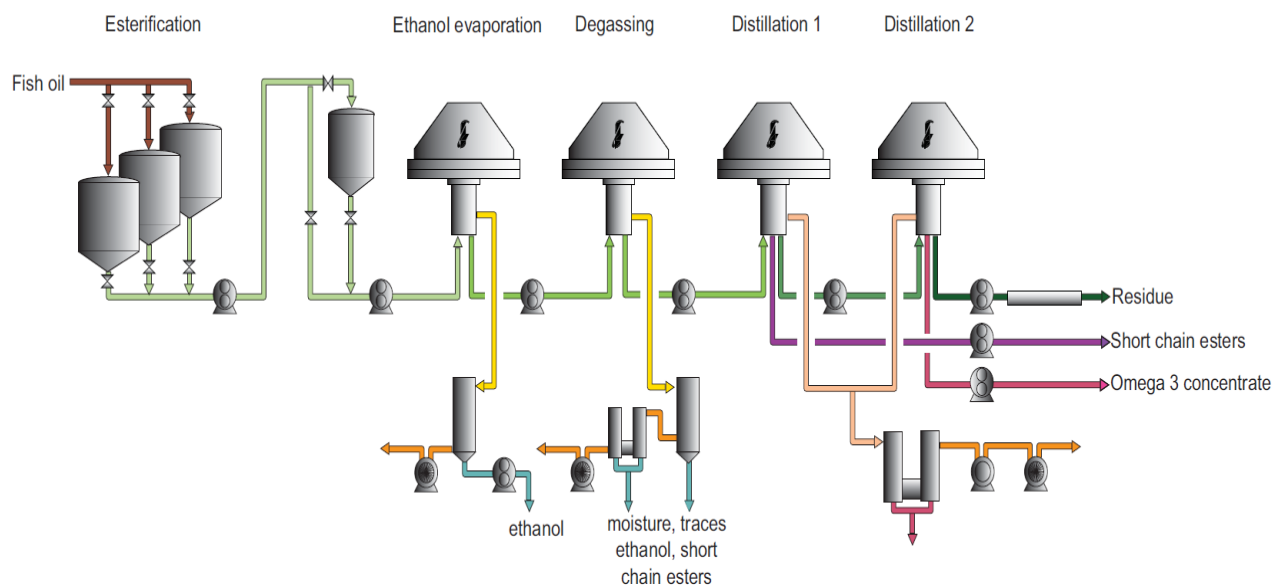


Figure 2.15: Molecular distillation for production of omega 3 ester (Flavourtech, 2009; Atadashi *et al.*, 2013)

2.5.2.6 Supercritical Fluid Extraction

A supercritical fluid state exists when the pressure and temperature are both above the critical values (i.e. $T > T_c$ and $P > P_c$), as shown in Figure 2.16. Supercritical fluid extraction uses supercritical carbon dioxide (“SCCO₂”) as the medium of extraction. This is considered a green solvent because CO₂ is non-toxic, non-flammable, inexpensive, and has mild critical conditions ($T_c = 31.1^\circ\text{C}$ and $P_c = 73.8$ bar) (Rubio-Rodríguez *et al.*, 2010); all this allows for the processing of thermo-labile compounds such as omega-3 PUFAs. CO₂ is easily separated from the product after processing because it is gaseous at ambient conditions (Rubio-Rodríguez *et al.*, 2010).

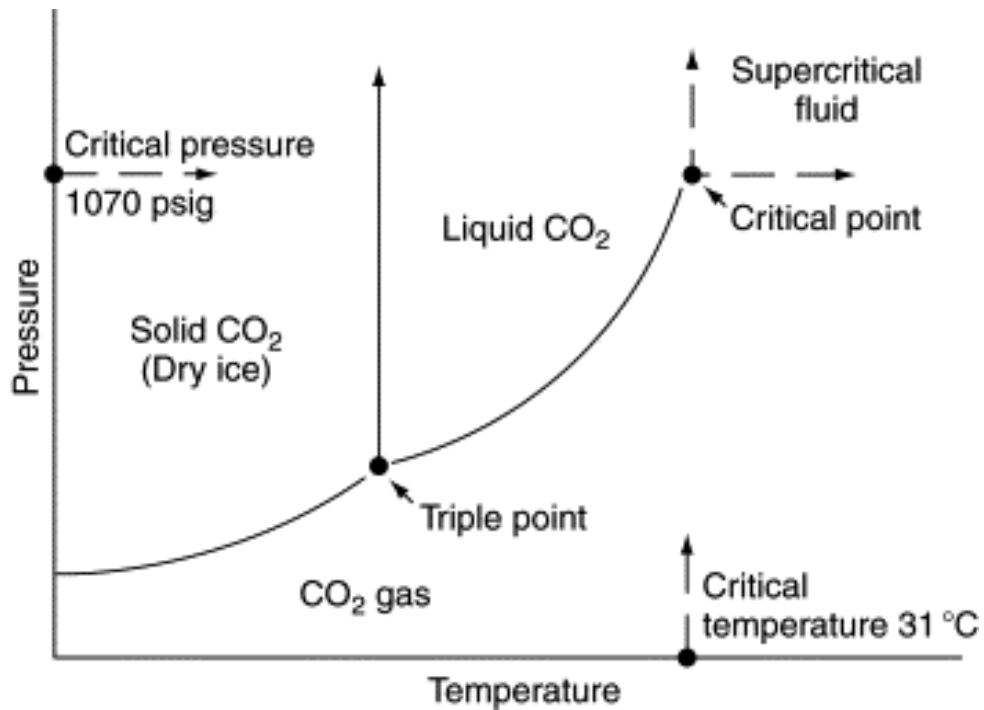


Figure 2.16: Pressure-temperature phase diagram for CO₂ (Grandison and Lewis, 1996; King, 2003)

The principle of the SFE technology is the different solubility of the fatty acid ethyl ester in the SCCO₂. The solubility of short chain FAEEs is greater than the solubility of long chain ones, while the solubility dependence on the number of unsaturated chemical bonds is almost negligible (Fiori *et al.*, 2014). Figure 2.17 shows a flow scheme of the SFF process. The SFF operates in a high pressure extraction column, where the fatty acid ethyl ester mixture flows counter-current to the supercritical carbon dioxide. The liquid FAEE mixture flows downwards and the SCCO₂ flows upwards. The short chain FAEEs are solubilised into SCCO₂ and, consequently, the liquid FAEE mixture is enriched in long chain FAEEs, which include the EPA and DHA concentrate (Fiori *et al.*, 2014).

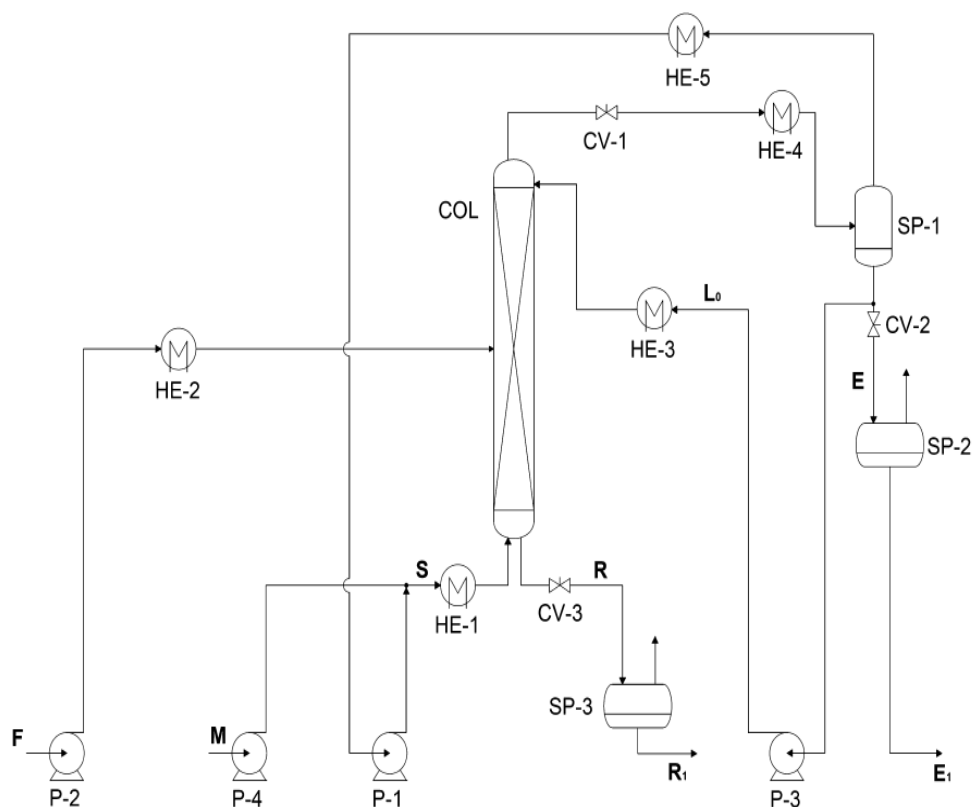


Figure 2.17: Flow scheme of the SFF process (Fiori *et al.*, 2014) Streams: F=FAEE feed, M=CO₂ make up, S=CO₂ to column, E=extract, E₁=extract CO₂ free, L₀=reflux, R= raffinate, R₁=raffinate CO₂ free. Equipment: COL=fractionation column, SP=separator, HE=heat exchanger, CV=control valve

2.5.2.7 Supercritical Fluid Chromatography

The SFC technique operates at temperatures in the range of 40–50°C, and these low temperatures prevent thermal stress on EPA and DHA, which are highly temperature sensitive (Lembke, 2013a). This makes the SFC one of the most appropriate technologies for the concentration of polyunsaturated fatty acids. The low temperature and efficient performance of the SFC is due to the high selectivity of both the supercritical fluid and the stationary phase, like packed or capillary columns (Lembke, 2013a). Omega-3 PUFA from fish oil has been separated at a bench scale, to achieve an ester mixture with 90% purity of EPA, using silica gel as the stationary phase and supercritical chromatography with SC-CO₂ as the mobile phase (Pettinello *et al.*, 2000). The SFC process is already installed at the industrial scale, and there are some companies like KD-Pharma or Solutex which are separating omega-3 to EPA at concentrations of 95% and DHA up to 80%, using this technology (Rubio-Rodríguez *et al.*, 2010).

2.5.2.8 Aqueous Silver Nitrate Extractions

Silver nitrate has been previously reported for concentration of the ethyl ester of PUFAs by Yazawa *et al.* (1995). A US patent also shows that silver nitrate solution can be used to extract omega-3 PUFA from marine oils (Breivik *et al.*, 2015). The extraction process depends on the interaction of the silver ions (Ag^+) with the double bonds of EPA and DHA to produce complexes that are soluble in the ionic or polar carrying phases (Shanmugam and Donaldson, 2015). The same extraction principle has been reported by Fagan *et al.* (2013), in which EPA and DHA was isolated at more than 88% purity from esterified tuna oil in chromatography-based separations.

Teramoto *et al.* (1994) examined the effect of temperatures on the extraction of PUFA ethyl ester using silver nitrate solution, and found that PUFA ethyl ester extraction decreased with the temperature. The advantage of using silver nitrate extraction is the ability to extract the omega-3 PUFAs at moderate temperatures and pressures, compared to other techniques which need significant changes in temperature and pressure to extract the omega-3 PUFAs. The other advantage of this technique is the ability to achieve high product purity. Furthermore, the silver nitrate in this technique can be recovered since silver nitrate is an expensive material and toxic. The cost of silver nitrate with $\geq 99.0\%$ purity is 1,262 US\$/kg (Patil *et al.*, 2013). The Occupational Safety and Health Administration (OSHA) and the Mine Safety and Health Administration (MSHA) reported the Permissible Exposure Limit (PEL) of the silver compounds to be 0.01 mg/m³ (Drake and Hazelwood, 2005).

The recovery methods for silver nitrate include multi-effect evaporation, electrochemical oxidation using a copper electrode, and a chemical reaction method using sodium hydroxide and nitric acid (Shanmugam *et al.*, 2015). The recovered silver nitrate will reduce the material cost and improve the economic process of this technique (Murphy, 1991; Rawat, 1986).

Over the past decade, micro/mini-fluidic technology has also been incorporated into the solvent extraction of PUFA ethyl esters, to enhance mass transfer rates, extraction performance, and low solvent inventory requirements, as compared to other conventional extraction techniques (Shanmugam and Donaldson, 2015). Generally, PUFA extraction can be carried out using ionic liquid containing silver salt or silver nitrate solution, with the former having better extraction performance than the latter (Li *et al.*, 2009a).

Despite its superior extraction performance, AgNO_3 in ionic liquid has a number of limitations, such as difficulties of preparation where it requires inert gas atmospheres and heating at 70°C (Li *et al.*, 2009a).

Furthermore, ionic liquid silver salts can decompose in harsh environments, for instance, AgNO_3 in ionic liquid is light-sensitive and must be stored under dark conditions (Li *et al.*, 2009a). Table 2.1 summarises the existing processes for the silver ion-based extraction of omega-3 PUFAs in terms of flow pattern, residence time and extraction efficiency.

Table 2.1: Several processes for the silver ion-based extraction of omega-3 PUFAs

System	Flow pattern	Residence time	Extraction efficiency	Reference
Ionic Liquids based AgBF_4 in Mistral Multi-Mixer	Mixing	30 mins at 20°C	80% in solvents	Min Li <i>et al.</i> 2008
Imidazolium-based ionic liquids containing silver tetra fluoroborate	Mixing	25 mins at 20°C	Distribution ratio-320	Min Li <i>et al.</i> 2009
Silver ion-loaded porous hollow fibre membrane	Flow through packed column	-	100% recovery	Akio Shibasaki <i>et al.</i> 1999
II Complexing sorbents	Solid phase extraction in Mistral Multi Mixer	30 mins at 20°C	89-91% Stripping in Solvents	Min Li <i>et al.</i> 2009
Aqueous silver nitrate solutions	Micro reactor slug flow	20 s	N/A	Eiji Kamio <i>et al.</i> , 2009
Silver nitrate solution	Hydrophobic Hollow fiber membrane	N/A, 303K	N/A	Kubota <i>et al.</i> ,1997
Silver nitrate solution	Slug flow based Mini-fluidic	36 s at 10°C	80%	A.Donaldson ,2013

2.5.3 Squalene Extraction Process

Squalene is an organic compound with the formula $C_{30}H_{50}$. It is mainly obtained from shark liver oil and can also be found in some vegetable oils (Kim and Karadeniz, 2012). Although numerous efforts have been made to produce squalene from plant sources such as olive oil, wheat germ and rice bran, the squalene contents of these materials have been too low for commercial purposes (Nakazawa *et al.*, 2012). The Japanese researcher Dr. Mitasumaru Tsujimoto discovered squalene in 1906 while working at the Tokyo Industrial Testing Station as an oil and fat expert. He extracted the unsaponifiable fraction from the shark liver oil and discovered the presence of squalene, a highly unsaturated hydrocarbon (Popa *et al.*, 2015a). In 1916, Mitasumaru successfully obtained unsaturated hydrocarbon $C_{30}H_{50}$ from two deep-sea shark species. He named it squalene in reference to the shark family name Squalidae (Tsujimoto, 1916). In the following years, many researchers confirmed the chemical formula proposed by Mitasumaru with the chemical structure as shown in

Figure 2.18 and chemical and physical properties as in Table 2.2 (Popa *et al.*, 2015a).

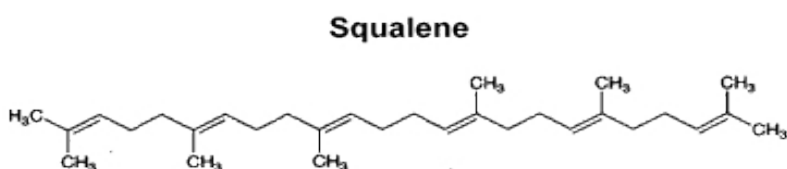


Figure 2.18: Squalene chemical structure (Popa *et al.*, 2015a)

Table 2.2: Chemical and physical properties of squalene (Popa *et al.*, 2015a)

Properties	Value
Molecular weight	410.7 g/mol
Melting point	-75 °C
Viscosity at 25°C	12 cP
Density	0.858 g/mL
Boiling point at 25°C	285 °C
Flash point	110 °C

It has been reported that squalene can be used to protect the skin to promote the effects of some cholesterol-lowering drugs (Smith *et al.*, 1998). Therefore, the importance of squalene in the cosmetic and pharmaceutical industries was the driving force to develop new technology to isolate squalene from different sources (Vázquez *et al.*, 2007). Several technologies have been studied for the separation of squalene, including molecular distillation under high vacuum (short path distillation), counter current chromatography, and supercritical fluid extractions.

2.5.3.1 Short Path Distillation

The short path distillation process for squalene extraction operates based on the compound volatility at different temperature ranges from 170 to 180°C under a high vacuum of 0.01 mbar, as shown in Figure 2.19.

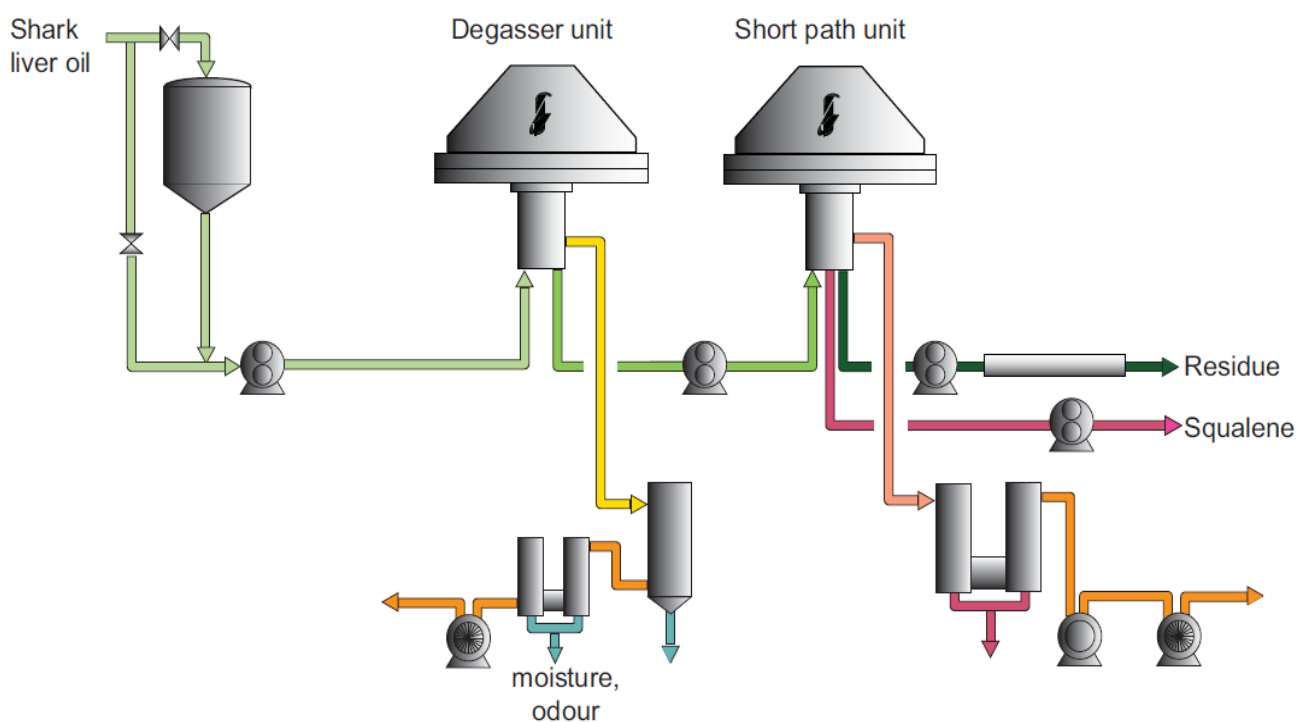


Figure 2.19: Short path distillation (Flavourtech, 2009)

The shark liver oil is pumped from a feed tank to the degassing unit to eliminate water and other high volatile compounds. From the bottom of the degasser, the oil is piped to the distillation unit (short path distillation).

The feed oil to the distillation unit makes contact with a fast rotating disk and then a thin film is obtained, which flows down the inner wall of the distillation unit. High volatile components are vaporised and condensed on the compensator surface inside the distillation unit. After this, the squalene-rich stream (distillate) and the triacylglyceride-rich stream (residue) flow to the bottom of the short path distillation unit, where they are retrieved and collected separately (Flavourtech, 2009). However, due to the unsaturated bonds (number of double bonds) of squalene it is considered to be thermolabile. Thus, squalene should be processed at a moderate temperature.

Pietsch *et al.* (2007) have investigated the optimum conditions to obtain the highest yield of highly concentrated squalene at the lowest feasible temperature and economically visible. Eight experiments were conducted at different operational parameters (temperatures, pressures and mass flows) of shark liver oil containing 60% of squalene.

Table 2.3 shows the experimental results for the squalene content and yields. The squalene concentration was increased from 60% to above 95% in all eight investigated cases. The result also showed that 99% squalene concentration has been achieved by lowering the temperature but the yield has been reduced as it is clear in case 7 (Pietsch and Jaeger, 2007a).

Table 2.3: Experimental result for the squalene content and yields (Pietsch and Jaeger, 2007a)

No.	Feed flow	Pressure	Temperature	Yield distillate of total feed	Squalene content in distillate	Yield squalene
5	4 kg/h	0.01 mbar	185 °C	43.3%	98.0%	68%
6			190 °C	55.6%	98.0%	88%
4			200 °C	58.0%	97.2%	91%
3			230 °C	57.8%	96.5%	90%
1	7 kg/h	0.1 mbar	215 °C	56.6%	98.7%	90%
2			230 °C	59.0%	97.6%	93%
7			190 °C	42.6%	>99%	69%
8			230 °C	58.0%	96.5%	90%

2.5.3.2 Supercritical Fluid Extraction

Another common technique for refining squalene is supercritical fluid extraction (SFE). Continuous extraction of squalene from WSLO in a packed column using supercritical carbon dioxide was performed at the laboratory and pilot scales by (Catchpole *et al.*, 1997), who examined the SFE for concentrating squalene from WSLO as shown in Figure 2.20. Different experiments were carried out which involved passing supercritical carbon dioxide through a high-pressure counter-current column (H column = 7.5 m, ID = 40 mm), while the WSLO flows downwards as a film covering the Sulzer BX packing elements inside the column. The extract (squalene) is dissolved in supercritical carbon dioxide and leaves the top of the column and the residue (triacylglyceride) at the bottom of the column.

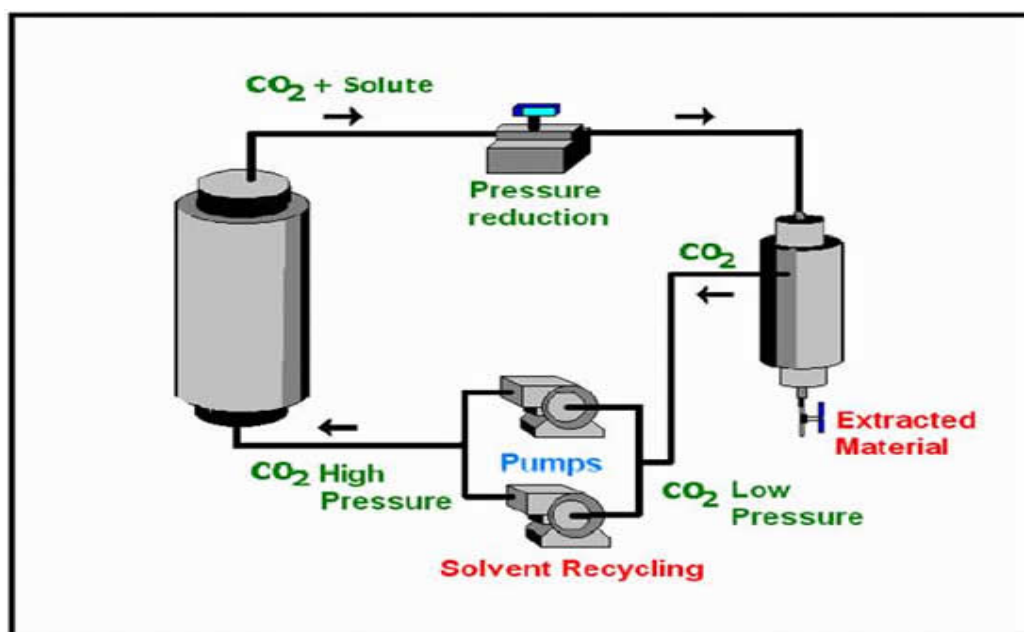


Figure 2.20: Supercritical carbon dioxide extraction (FluidsScience, 2015)

Compared to short path distillation techniques, moderate temperatures can be applied in supercritical fractionation. However, supercritical carbon dioxide fractionation has higher energy requirements than short path distillation, i.e. short path distillation requires 2 kW/kg squalene as compared to 9 kW/kg squalene for the supercritical extraction (Pietsch and Jaeger, 2007a). Furthermore, the investment costs of supercritical carbon dioxide fractionation are three times higher than short path distillation (Pietsch and Jaeger, 2007a).

2.5.3.3 Counter-Current Chromatography

Counter-current chromatography (CCC) is a technique for separating many natural compounds using a support free liquid stationary phase or “solid phase” (Berthod *et al.*, 2009). The main principle of CCC is to split a sample into two immiscible liquid phases prepared by mixing two or more solvents, where one of the liquid phases is used as the stationary phase and the other is pumped through the column as the mobile phase. This allows the components to be separated, based on their solubilities, into the two phases (Berthod *et al.*, 2009). Purification of squalene from micro algae was successfully performed using counter-current chromatography (Lu *et al.*, 2003).

There are several advantages of the CCC technique in comparison to the classical liquid chromatography. These are that solvent usage is far lower than in solid phase chromatography systems (Graham *et al.*, 2001), and that sample components can be completely recovered, as the CCC technique is a solid free phase. This means that there is no possibility of component losses from irreversible adsorption onto the solid matrix, as is the case with liquid chromatography (Skalicka-Woźniak and Garrard, 2014).

The drawbacks associated with the CCC technique are that it is time consuming to employ solvent selection systems as both phases are liquid, and any change in one phase directly affects the other. Although the analysis of solvent selection systems can be achieved by an automated liquid-handling, it still requires several hours to complete (Skalicka-Woźniak and Garrard, 2014). Another drawback is that a single CCC run operates over a low polarity range in comparison with the high polarity range in the liquid chromatography. The low polarity range is useful to remove a compound from a complex mixture, but it is a disadvantage when many pure compounds are required from the mixture in a single purification run (Skalicka-Woźniak and Garrard, 2014).

2.6 Summary

Using a cheap non-edible feedstock, such as waste shark liver oil, could reduce production costs and make the process economically viable. Waste shark liver oil could instead be processed to obtain valuable products such as: biodiesel, squalene, and omega-3 PUFAs– including EPA and DHA.

Squalene C₃₀ H₅₀ can be separated from WSLO using several technologies, such as molecular distillation (short path distillation), counter current chromatography, and supercritical fluid extractions. The other added-value product that can be obtained from WSLO is omega-3 oils (EPA and DHA). Various techniques have been investigated or used for the extraction of EPA and DHA

from WSLO, such as: molecular distillation, high-performance liquid chromatography, supercritical fluid extraction, supercritical fluid chromatography, enzymatic enrichment, crystallisation at low temperatures, silver nitrate extraction, and urea precipitation. Table 2.4 compares various EPA and DHA extraction techniques, and the silver nitrate extraction technique is recommended in this work due to the following advantages:

- (i) The ability to extract omega-3 PUFAs at moderate temperatures and pressures, compared to other techniques, which require high temperatures and pressures to reach the supercritical conditions which would incur higher operating and capital costs.
- (ii) It has a high extraction efficiency of 88-91%, after liquid chromatography and supercritical fluid extraction, which both have up to 99% extraction efficiency. However, the silver nitrate extraction technique has a lower capital investment cost in comparison to liquid chromatography and supercritical fluid extraction.
- (iii) Silver nitrate can be recycled, which will reduce the materials costs and improve the overall process economics.

Table 2.4: A comparison of various EPA and DHA extraction techniques(Lembke, 2013b)

	Molecular distillation	Supercritical fluid chromatography	Liquid chromatography	Supercritical extraction	Urea precipitation	Low temperature crystallization	Silver Nitrate Extraction
Selective mechanism	Chain length (boiling point)	Chain length and C=C	Chain length and C=C	Chain length	Saturated fat	Melting point (chain length and C=C)	Silver ion Complexation with C=C
Process condition	T= 220 °C P=0.001 mbar	35-50 °C >140bar	20-50 °C 1 bar	35-50 °C >140 bar	-10 to -90 °C 1 bar	0-70 °C 1 bar	20-30 °C 1 bar
Use of toxic solvent	No	No	Organic solvent	No	No	No	No
Extraction efficiency	65-75%	99%	99%	78-85%	45-65%	>90%	88-91%
Decontamination efficacy	Very high	Very high	High	Medium	Low	Low	Low
Product oxidation	Low	Very Low	Possible	Very low	Possible	Possible	Very low
Capital investment	Low	High	High	High	Low	Low	Low

Chapter 3 Materials and Methods

3.1 Introduction

This chapter describes the project's materials and methods. The feedstock used was waste shark liver oil (WSLO), which was characterised by measuring its density, water content and chemical composition.

The transesterification of WSLO was investigated using alkali and acid catalysts. Saponification of the WSLO was also investigated for extracting squalene from it, while aqueous silver nitrate (AgNO_3) was employed for extracting eicosapentaenoic acid (EPA) and docosahexaenoic acid (DHA) from fatty acid ethyl esters produced by the WSLO.

3.2 Materials

The feedstock used for this study was WSLO obtained from the *Carcharhinidae* family. The oil was sourced from Sur, Sultanate of Oman, which is one of the largest collection centres for WSLO in Oman. Sulfuric acid (H_2SO_4 , 98% purity, Sigma-Aldrich, UK) was used as an acid catalyst and granulated sodium hydroxide (NaOH , 97% purity, Sigma-Aldrich, UK) as an alkali catalyst. The alcohols used were anhydrous methanol (99.8% purity, Sigma-Aldrich, UK) and anhydrous ethanol (96% purity, Alfa Aesar, UK). Methyl heptadecanoate (99% purity, Sigma-Aldrich, UK) was used as an internal standard for gas chromatography (GC) analysis of the FAME produced. Acetic acid (99.5% purity, Sigma-Aldrich, UK) and powdered calcium oxide anhydrous (99.9% purity, Sigma-Aldrich, UK) were used for quenching the reactions.

A standard grain FAME Mix—10 mg/mL in dichloromethane, part number: CRM47801, from Sigma-Aldrich, UK—was used for identifying the FAME peaks in the chromatogram. Hexane (98% purity, Alfa Aesar, UK) was used as a solvent for EPA and DHA extractions. Silver nitrate (AgNO_3 , 99% purity, Sigma-Aldrich, UK) was used to prepare the silver nitrate solution for EPA and DHA extraction.

3.3 Experimental Methods

3.3.1 Determinations of the Density of the Waste Shark Liver Oil

The WSLO density was determined using the following steps. The oil was heated to 30°C and transferred into a dry, 25 mL volumetric flask of known weight. The weight of the oil was recorded using an AND HR-200 weighing balance (± 1 mg), and the density of the WSLO was calculated using Equation 1.1. The density is calculated to obtain the amount of alcohol (molar ratio of alcohol to WSLO) needed for the transesterification of WSLO.

$$\text{Density of WSLO } (\rho) = \frac{\text{Weight of the WSLO (g)}}{\text{Volume of flask (mL)}} \quad (1.1)$$

3.3.2 Water Content by Karl Fischer Titration

Karl Fischer Titration is an analytical technique for determining the amount of water in organic substances. The water content analysis was performed using a C30 Karl Fischer Titrator with HYDRANAL™ - Coulomat AG as a titration reagent as shown in Figure 3.1 (Mettler Toledo, UK). The titration reagent was titrated until a steady background endpoint of 20 $\mu\text{L}/\text{min}$ was achieved, followed by additions of 0.2 g of the WSLO sample using a 1mL syringe. The added samples were then titrated until a stable endpoint was achieved to obtain the WSLO water content.



Figure 3.1: C30 Karl Fischer Titrator (Mettler Toledo, UK)

3.3.3 Determination of Lipid Classes, Squalene and Free Fatty Acids

The glycerides (TG, DG and MG), squalene and FFA contents of the WSLO were determined using the Iatroscan method. Iatroscan thin-layer chromatography (TLC)–flame-ionization classes were analysed (by Callaghan Innovation, an external laboratory) using an Iatroscan MK-6s as shown in Figure 3.2.

The basic principle of Iatroscan is to scan the adsorbent-coated chromarods where the flame jet of the flame ionisation detector (FID) is used to drive the rod holder carrying the developed chromarods at a chosen speed from one end to the other. The fractions resolved on each of the rods are successfully vaporised, and the ionisable carbon is converted to ions that are detected in the collector electrode. Finally, the FID signals obtained from each fraction are amplified and recorded as separate peaks (Sherma and Fried, 2002).

The amounts of TG, DG, MG, squalene and FFA in the WSLO were quantified from the Iatroscan FID peaks. The lipid classes were quantified based on the internal standards which were triolein (Sigma T-7140) for the TG, stearic acid (Sigma S4751) for the FFA, 1, 2-dipalmitin (Fluka 42555) for the DG and 1, 2-monopalmitoyl-rac-glycerol (MP Biomedicals) for the MG.

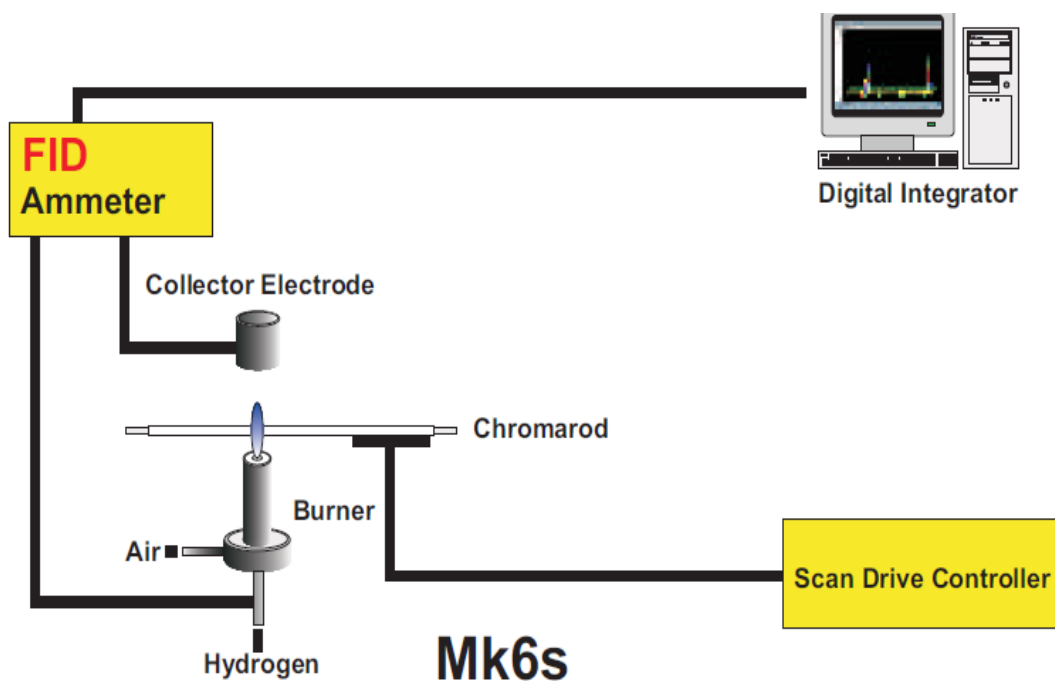


Figure 3.2: Iatroscan MK-6 (Scientifique, 2014)

3.3.4 Alkali-Catalysed Transesterification

Homogeneous alkali-catalysed transesterification of the characterised WSLO using methanol was conducted in a 250 mL, three-neck batch reactor equipped with a condenser, a sampling point connection and a thermocouple to measure the temperature. The round-bottomed reactor was seated on a metal block attached to a heater-stirrer (Stuart UC152, UK), which did both the heating and the mixing. Prior to the reactions, 1.5 wt.% NaOH, based on the WSLO, was dissolved in methanol and heated to the reaction temperature in a separate vessel. The methanol-catalyst solution was transferred into the batch reactor that contains WSLO, which had already been heated to the reaction temperature inside the batch reactor.

These reactions were carried out at a mixing speed of 720 rpm, a reaction temperature of 60°C and 6:1 methanol to WSLO molar ratio. The methanol to oil molar ratio of 6:1 is the usually accepted alcohol-to-glyceride molar ratio (Musa, 2016). It has been reported that soybean methanolysis using an H₂SO₄ catalyst has increased the ester formation sharply from 77%, at a 3.3:1 methanol to oil molar ratio, to 87.8%, at a 6:1 methanol to oil molar ratio, with only moderate improvement to a maximum value of 98.4% ester formation at a 30:1 methanol to oil molar ratio (Balat and Balat, 2008). During the experiments, 1mL sample was collected from the reaction mixture at different time intervals (1, 2, 4, 8, 15, 20, 40, 50 and 60 min) using a 1000 µL micropipette. The samples were dispensed into a 2mL, pre-weighed vial containing 0.05 mL acetic acid 0.1 M to quench the reaction. All samples were kept in the freezer at -20°C for GC analysis.

The experiments were carried out using a three-neck batch reactor. The reactor was a round-bottomed glass flask with three necks connected with a condenser, a sampling point and a thermocouple. The round-bottomed three-neck reactor was attached with a heating block designed to transfer the heat and magnetic stirring from the hotplate stirrer to attain the heating and mixing required for the experiment, as shown in Figure 3.3.



Figure 3.3: Experimental set up

3.3.5 Acid-Catalysed Transesterification

The acid-catalysed transesterification of the WSLO was investigated, using Design of Experiments (DoE), by a response surface method. DoE is a statistical tool used to evaluate, and optimise, the relations between variables and system responses. The advantage of DoE lies in minimising the number of experimental trials required to cover a particular parameter space (Abdullah *et al.*, 2009).

DoE was not conducted for the alkali-catalysed transesterification of WSLO because the alkali catalyst was clearly inferior to the acid for this process, based on the screening results. This was because the alkali catalyst is not appropriate for high-FFA feedstocks, as it reacts with the FFA forming soap and water “saponification” (Pullen and Saeed, 2015).

The reaction variables studied for the acid catalysis were reaction time in the range of 1 to 7 h, H₂SO₄ catalyst loading from 1 to 6 wt.% and methanol to oil molar ratios from 6:1 to 30:1. The experiments were carried out using the batch reactor setup described earlier for the homogeneous alkali-catalysed process and a similar experimental procedure, with a reaction temperature of 60°C and a mixing speed of 720 rpm. The amount of H₂SO₄ catalyst calculated for each experiment was dissolved in the matching required amount of methanol and heated to the reaction temperature in a separate vessel, and this solution was transferred into the batch reactor containing each experiment’s desired amount of WSLO already heated to the reaction temperature. For every experiment, 1mL of the sample was collected from the reaction mixture at different time intervals (15, 30 min; 1, 1.5, 2, 3, 4, 5, 6 h) using a 1000 µL micropipette, and the sample was transferred to a 2mL, pre-weighed vial, where the reaction was quenched using a saturated solution of calcium oxide. All the collected samples for the experiments were kept in the freezer at -20°C for GC analysis.

3.3.6 Squalene Extraction by Saponification

The amount of squalene present in WSLO varied widely depending on the species (Hall *et al.*, 2016). In this research, saponification for extracting squalene was investigated. The principle applied in this extraction technique was to extract the un-saponifiable squalene from the saponifiable WSLO. Fatty acids can react with alkali catalyst such as NaOH and turn into many polar carboxylic salts (soap), which are insoluble in solvents such as hexane and accordingly the un-saponifiable squalene can be extracted from the saponifiable WSLO .

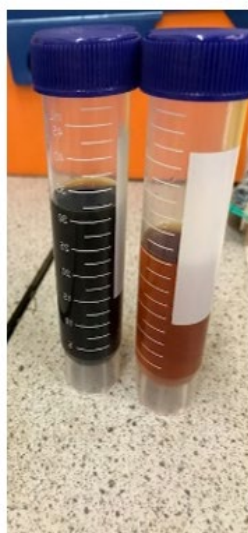
DoE was conducted for the squalene extraction to obtain the operating conditions for the highest squalene extraction. The DoE was conducted over the following parameter space: (i) alcohol to

WSLO molar ratio of 20:1 to 100:1; (ii) reaction times of 5 to 60 min; (iii) water content in the range of 0 wt.% to 20 wt.%.

The WSLO saponification was carried out using 25 g of WSLO in the experimental set-up as shown in Figure 3.3. The alkali catalyst concentration was 25 wt.% of NaOH based on WSLO; the reaction temperature was 60°C; and the mixing speed was 720 rpm. These conditions for the saponification reaction were selected based on other studies, which assessed the saponification reaction with sodium hydroxide and potassium hydroxide catalysts in alcohol (Eze *et al.*, 2014; Eze *et al.*, 2015). Squalene was added to the WSLO to make up 1.2 g of squalene in order to create a reliable squalene-containing feedstock. After the reaction, the reaction mixture was transferred to a 100 mL separating funnel to settle by gravity. The bottom layer, containing soap and glycerol as shown in Figure 3.4, was then transferred into a 50mL tube, and 25 mL of hexane was added for the first washing (Figure 3.4 (a)). Then the tube was centrifuged at 4000 rpm using a Sigma 2-6 Compact Centrifuge (Sigma Model 2-6, UK) to separate the liquid from the solid. The solid was transferred to another 50 mL tube, and 25 mL of fresh hexane was added for the second wash (Figure 3.4 (b)). This process was repeated again for the third wash (Figure 3.4 (c)). The liquid from all three washes was combined, and the extracting solvent (hexane) was recovered using a rotary evaporator. After that, 200 mg of the sample was weighed into a 2 mL vial and mixed with 1mL of methyl heptadecanoate (C17) prepared in hexane at a concentration of 10 mg/mL for GC quantification of the squalene recovery.



(a) After the experiment



(b) Washing 1 and 2



(c) Washing 3

Figure 3.4: WSLO saponification

3.3.7 EPA and DHA Extraction Using Aqueous Silver Nitrate

Solvent extraction has been widely used for separating fatty acid ethyl esters (FAEE) based on the complexation between the double bonds of PUFA ethyl ester and silver ions (Shanmugam and Donaldson, 2015). This separation was achieved through a chemical reaction between the silver nitrate ions and the five to six unsaturation sites of Omega-3/6 PUFA. Silver nitrate salt-solutions have previously been used as solvents for the purification of the ethyl ester of PUFA ethyl ester. (Yazawa *et al.*, 1995). In this process, silver ions interact with the double bonds in unsaturated fatty acids to produce complexes that are soluble in ionic/polar carrying phases, as shown in Figure 3.5.

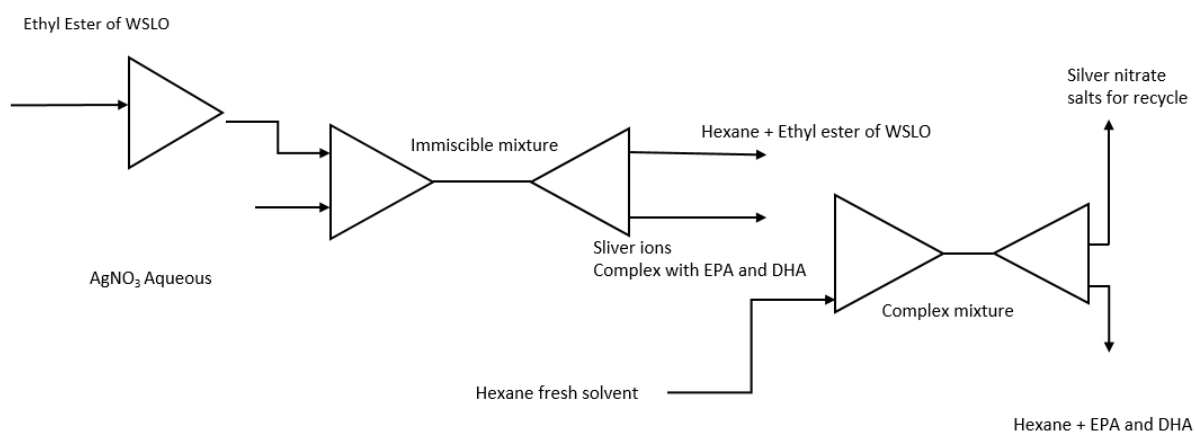


Figure 3.5: General overview of EPA and DHA extraction (Shanmugam and Donaldson, 2015)

Extraction was carried out by mixing aqueous silver nitrate with the FAEE produced from the WSLO in a ratio of 3:1 silver nitrate to FAEE. The mixing was performed using an IKA incubator, model KS 4000i, at a mixing speed of 300 rpm and a temperature of 20°C. The silver nitrate solution was prepared by adding solid silver nitrate to DI water at different concentrations (15, 30 and 50 wt.%) to obtain the concentration profile (Shanmugam and Donaldson, 2015). The reaction times were varied at (0.5, 1, 2 and 4 h) to screen the highest extraction of EPA and DHA. The selected ranges of reaction times were based on studies conducted for the extraction of EPA and DHA from tuna methyl esters using aqueous silver nitrate (Huong, 2007). The catalyst concentrations ranges were based on studies elsewhere including (Shanmugam and Donaldson, 2015).

The overall EPA and DHA recovery process is summarised in Figure 3.6. After mixing in the incubator, the reaction mixture was transferred to a separating funnel to separate the residual oil layer, as shown in Figure 3.7 (a). Subsequently, 10mL of hexane was added to the aqueous/emulsion layer obtained after gravity separation to de-emulsify the oil droplets. The resulting organic layer was recovered via gravity separation. This is the ‘de-emulsification’ step, and the recovered organic layer is referred to as ‘Fraction 1’ (F1), as illustrated in Figure 3.7 (b). Deionised water was added to the remaining aqueous solution from the de-emulsification step at a volume ratio of 10:1, which caused the complexed omega-3 to de-complex. This was followed by the addition of 10 mL of hexane and recovery of the organic layer via gravity separation. This is the ‘de-complexation’ step, and the recovered layer is referred to as ‘Fraction 2’ (F2). This step is shown in Figure 3.7 (c). Samples from F1 and F2 were weighed into 2 mL vials, to which was

added 1 mL of C17—the internal standard for GC analysis—to determine the percentage of EPA and DHA recovery.

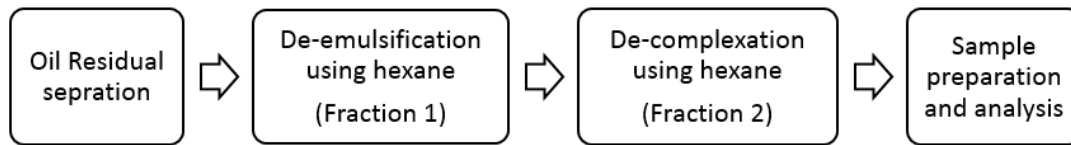
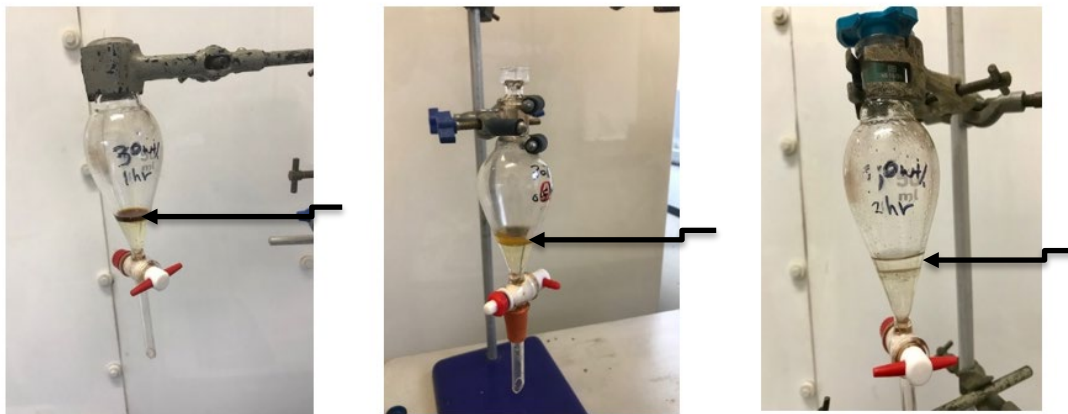


Figure 3.6: process for recovery of EPA and DHA from aqueous and emulsion phases



(a) Residual oil

(b) De-emulsification

(c) De-complexation

Figure 3.7: Experimental steps for the EPA and DHA extractions. Arrow in Figure 3.7 (a) refers to the residual oil layer, arrow in Figure 3.7 (b) refers to the de-emulsification layer and the arrow in Figure 3.7(c) refers to the de-complexation layer.

3.3.8 Analysis of FAME, EPA, DHA and Squalene Contents Using Gas Chromatography

Gas chromatography, as shown in Figure 3.8, is a technique used to analyse/separate mixtures of gases or liquid. FAME contents in the samples collected from the transesterification reaction were analysed using a Hewlett Packard 6890 Series II Gas Chromatograph (Hewlett Packard, USA), equipped with a fused silica (15QC3/BPX5-0.25, SGE Analytics, UK) capillary column 0.25 μ m in film thickness, 15m in length and 0.32mm in diameter.

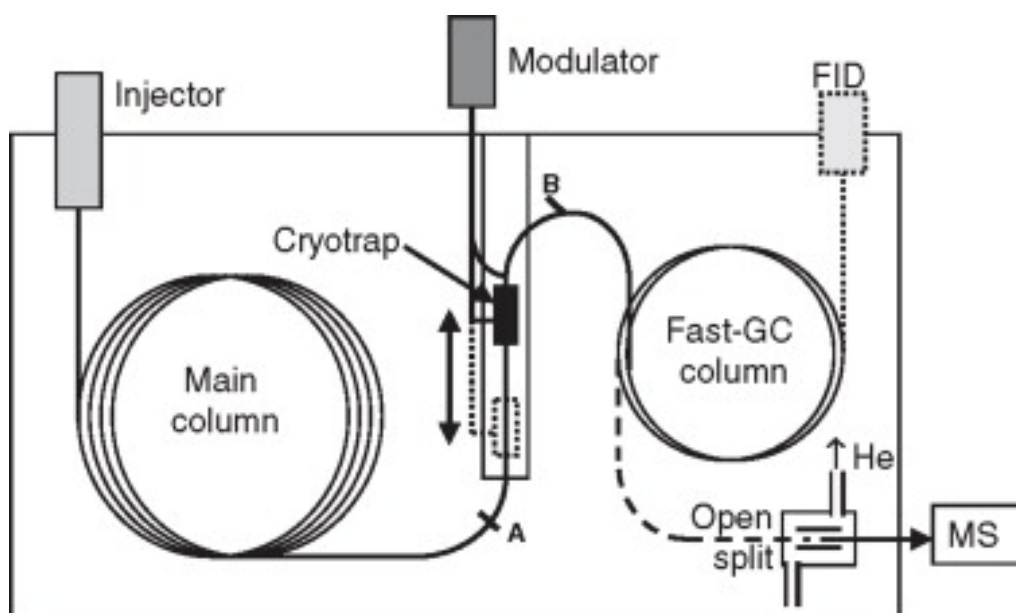


Figure 3.8: Gas chromatography (Chaintreau, 2007)

50mg of each sample was carefully weighed in a 2 mL vial using an A&D HR-200 weighing balance (± 1 mg). Then 1mL additions of a solution of 10 mg/mL methyl heptadecanoate prepared in heptane were added to the samples. 0.5 μ L of the prepared sample solution was injected into the GC using a 5 μ L micro-syringe (SGE Analytics, UK). The GC analysis was programmed, beginning with an initial oven temperature of 120 $^{\circ}$ C (held for 5 min.). This temperature was increased to 210 $^{\circ}$ C, at a rate of 30 $^{\circ}$ C/min, and held for 17min (total run time of 25 min). The GC injector and FID temperatures were set at 250 $^{\circ}$ C and 260 $^{\circ}$ C, respectively, while the carrier gas used was helium at pressure of 10.0 psi.

FAME contents and yields for the samples were calculated using the procedure of BS EN 14103, as shown in Equations 1.2 and 1.3.

$$\text{FAME content in the sample (\%)} = \frac{\sum A_i}{A_i} * \frac{C_i * V_i}{m} * 100\% \quad (1.2)$$

Where $\sum A$ is the sum total of the all the peak areas of all the FAMES in the sample from the GC chromatogram.

A_i = Peak area of methylheptadecanoate.

C_i = concentration, in mL, of the methylheptadecanoate solution.

V_i = volume, in mL, of the methylheptadecanoate solution.

m = mass, in mg, of the sample.

$$\text{FAME yield (\%)} = \frac{\text{FAME content in the sample}}{\text{Maximum theoretical FAME}} * 100\% \quad (1.3)$$

Squalene recovery was quantified using GC. A 200 mg sample was obtained after combining all three washes from the saponification reaction and after removing the hexane by rotary evaporator. The 200 mg sample was weighed into a 2 mL vial using an A&D HR-200 weighing balance (± 1 mg), and the sample was then mixed with 1mL of methyl heptadecanoate (C17) prepared in hexane at a concentration of 10 mg/mL. 0.5 μ L of the prepared sample, solution was injected into the GC using a 5 μ L micro-syringe (SGE Analytics, UK). The GC analysis was programmed, beginning with an initial oven temperature of 120°C (held for 5 min.). As before, this temperature was increased to 210°C, at a rate of 30°C/min, and held for 17 min (total run time of 25 min). The GC injector and FID temperatures were again set at 250°C and 260°C, respectively, while the carrier gas used was helium at a pressure of 10.0 psi. Squalene content in the samples was calculated using Equation 1.4, based upon the line equation, $y = 0.8827x + 0.0225$, from the calibration curve shown in Figure 3.9. The squalene recovery was calculated using Equation 1.5, where the total mass of squalene in the experiment was obtained using the volume and density after the reaction.

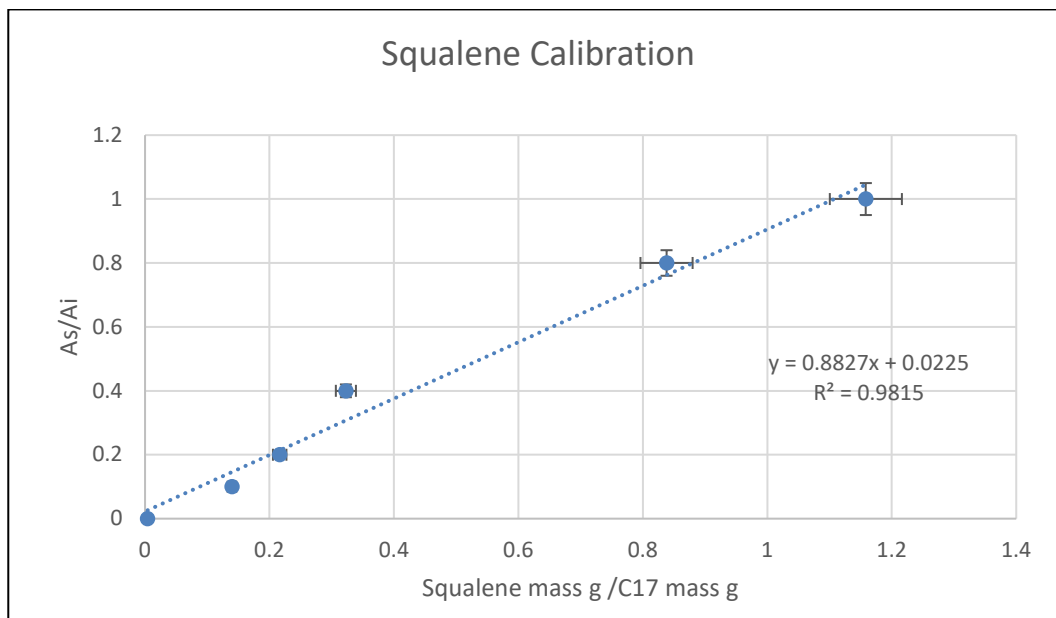


Figure 3.9: Squalene calibration curve

$$\text{Squalene Content (\%)} = \frac{A_s}{A_i} * \frac{C_i * V_i}{m} * \frac{1}{\text{Slop}} * 100 \quad (1.4)$$

Where: A_s is the peak area of squalene in the sample

A_i = Peak area of methylheptadecanoate

C_i = concentration, in mL, of the methylheptadecanoate solution

V_i = volume, in mL, of the methylheptadecanoate solution

m = mass, in mg, of the sample

$$\text{Squalene Recovery (\%)} = \frac{\text{total mass of squalene after the reaction}}{\text{total mass of squalene before reaction}} * 100 \quad (1.5)$$

EPA and DHA content, as well as EPA and DHA recovery, were also quantified using GC. The samples from F1 and F2 were weighed into 2 mL vials using an A&D HR-200 weighing balance (± 1 mg), and the samples were then injected with 1 mL of C17 prepared in hexane at a concentration of 10 mg/mL. 0.5 μ L of the prepared sample was injected into the GC using a 5 μ L micro-syringe (SGE Analytics, UK). The GC analysis was programmed, beginning with an initial oven temperature of 120°C (held for 5 min.). This temperature was, as before, increased to 210°C, at a rate of 30°C/min, and held for 17 min. (total run time of 25 min). The GC injector and the FID temperatures were set at 250°C and 260°C, respectively, while the carrier gas used was helium, again at a pressure of 10.0 psi.

EPA and DHA content were calculated using Equation 1.6, where A_s is the peak area of EPA and DHA in the sample, A_i is the peak area of methylheptadecanoate, C_i is the concentration (mg/mL) of the methylheptadecanoate solution, V_i is the volume (mL) of the methylheptadecanoate solution, and m is the mass (mg) of the sample.

$$\text{EPA/DHA Content (\%)} = \frac{A_s}{A_i} * \frac{C_i * V_i}{m} * 100\% \quad (1.6)$$

3.3.9 Fourier Transform Infrared Spectroscopy

Fourier transform infrared spectroscopy (FTIR) is a technique used for the identification and structural analysis of organic materials. The principle of this technique is the absorption of infrared radiation of the spectrum which results in changes in the vibrational energy of the molecules. There are different energy levels where the spectroscopy measures differences between stationary quantum states. The energy of a photon is equal to Planck's constant times the oscillation frequency of the electromagnetic radiation. Figure 3.10 illustrates the relationship of the vibrational infrared region (wavelengths between 2.5 mm and 25 mm) to others types of energy transition included in the electromagnetic spectrum. Generally, the nature of the molecules in the absorption process are excited to a higher energy state on the range of 8 to 40 kJ/mole when they absorb infrared radiation (Pavia *et al.*, 2008).

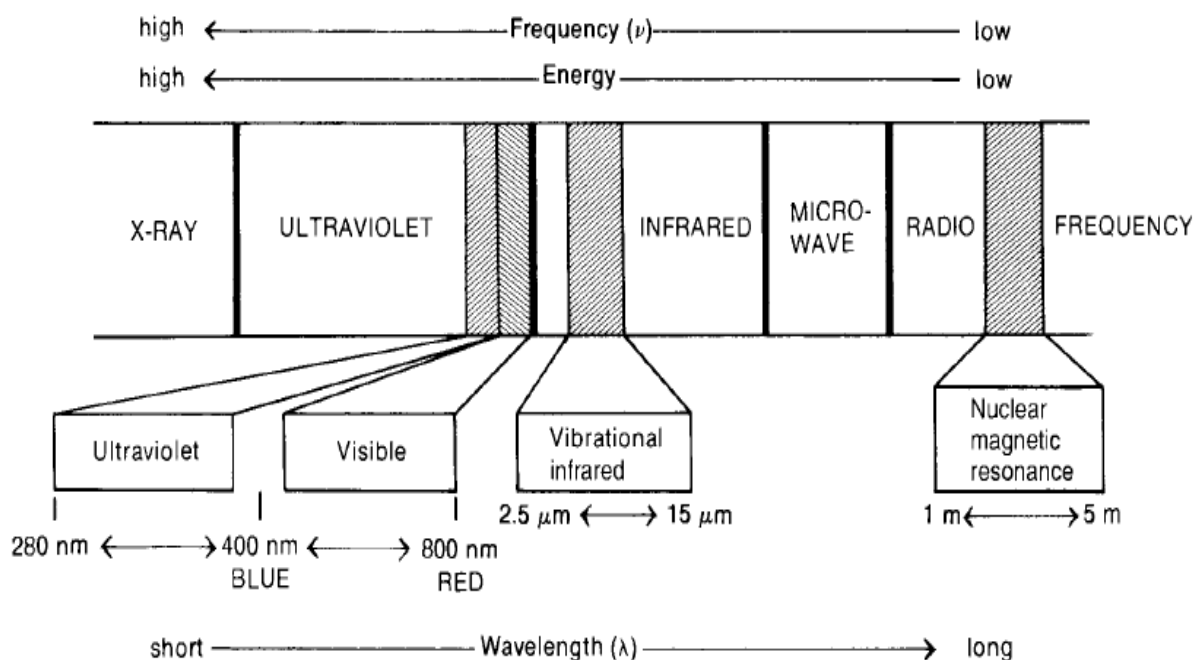


Figure 3.10: The relationship of the vibrational infrared region to others types of energy transition (Pavia *et al.*, 2008).

The absorbed energy will increase the amplitude of the vibrational motions of the bonds in the molecule. Every type of bond has a different natural frequency of vibration therefore; infrared radiation is used for the identification of the molecules. Other use of infrared spectrum is the structural analysis of the molecules because each type of bond (N-H, C-H, O-H, C=O, C-O, C=C, etc.) are found in specific vibrational infrared region. For example, any infrared absorption in the range of $1715 \pm 100 \text{ cm}^{-1}$ is typically due to the existence of a C=O bond (carbonyl group) in the molecule (Fifield and Kealey, 1995). Figure 3.11 illustrates different type of bond with the infrared absorption range.

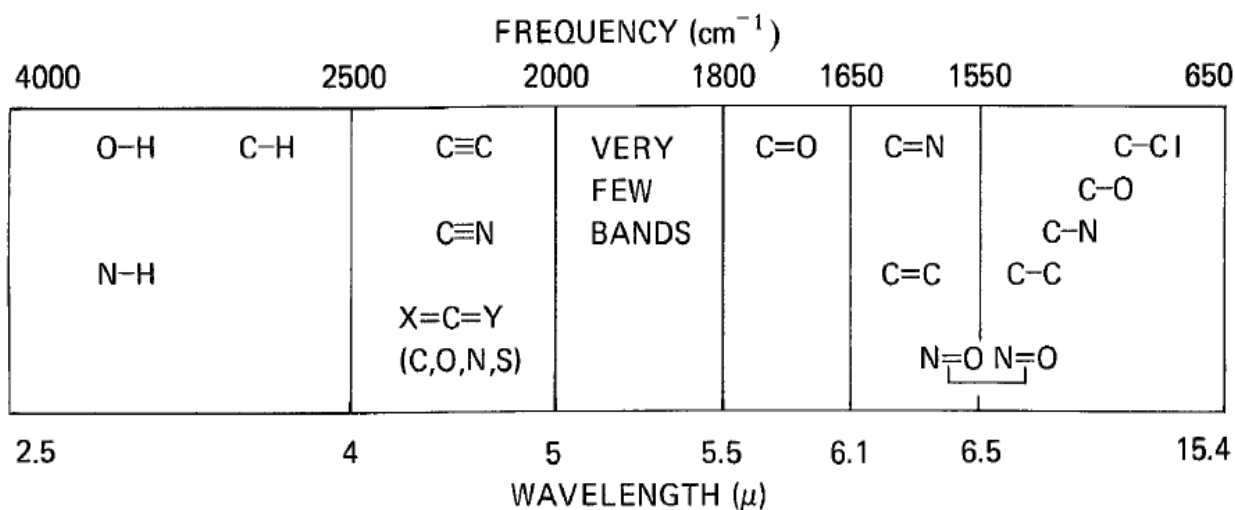


Figure 3.11: Different types of bond with the infrared absorption range (Pavia *et al.*, 2008).

Infrared active molecules have different mode of vibrational motion. The typical modes of vibrational motion in a molecule that absorb infrared radiation are stretching and bending as shown in Figure 3.12. Stretching vibrations arise at higher frequencies than bending vibrations. Any group contains three or two atoms where at least two are identical; there are two modes of stretching vibration: asymmetric stretching vibrations and symmetric stretching vibrations. Furthermore, various bending vibration are executed and can be observed at characteristic wave number.

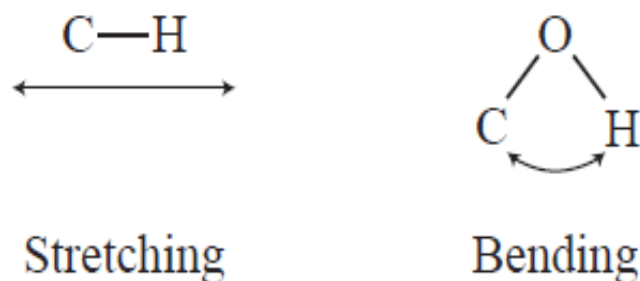


Figure 3.12: Stretching and bending modes (Pavia *et al.*, 2008).

Figure 3.13 shows stretching and bending modes of methyl group. In general, symmetric stretching vibrations occur at higher frequencies than asymmetric stretching vibrations. For instance, the methyl group gives rise to a symmetric stretching vibration at 2872 cm^{-1} and an asymmetric stretch at 2962 cm^{-1} . The bending vibration terms such as scissoring, rocking, wagging, and twisting are used to designate the origins of infrared bands as it is clear in Figure 3.13.

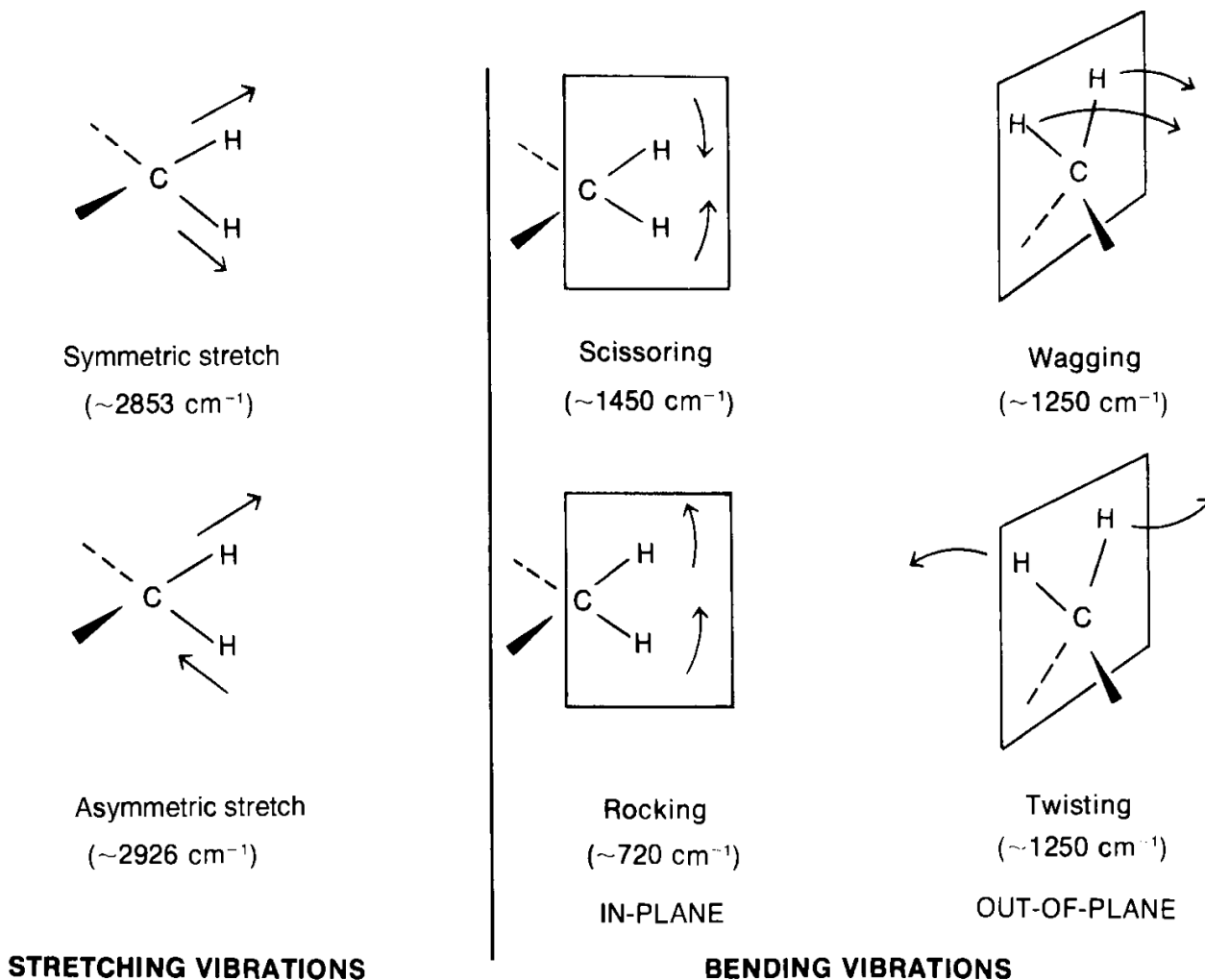


Figure 3.13: Stretching and bending vibration of methyl group (Pavia *et al.*, 2008).

A schematic diagram of an FTIR is shown in Figure 3.14 where an interferometer is used to process the energy sent to the sample where the source energy passes through a beam splitter. Incoming radiation will pass through a mirror positioned at a 45° angle and then separates it into two perpendicular beams; one at a 90° angle and the other is undeflected. The 90° angle beam goes to a stationary mirror and is returned to the beam splitter, whereas the undeflected beam goes

to a moving mirror and then returned to the beam splitter. The two beams are recombined when they meet at the beam splitter. Different wavelength content of the two beams causes both constructive and destructive interferences. The combined beam containing these interference patterns is called the interferogram which contains all of the radiative energy coming from the source and has a wide range of wavelengths oriented toward the sample by the beam splitter. The wavelength (frequencies) that are found in the infrared spectrum are absorbed by the sample simultaneously. After that, the modified interferogram signal reaches the detector with the amount of energy absorbed at every wavelength (frequency). The modified interferogram is compared with a reference laser beam by a mathematical process called a Fourier transform by the computer. Then, the individual frequencies are reconstructed and plotted as a typical infrared spectrum. Infrared spectrum of a compound is obtained by subtracting the spectrum of the background which contains infrared-active atmospheric gases such as carbon dioxide and water vapour from the sample spectrum automatically by the computer software.

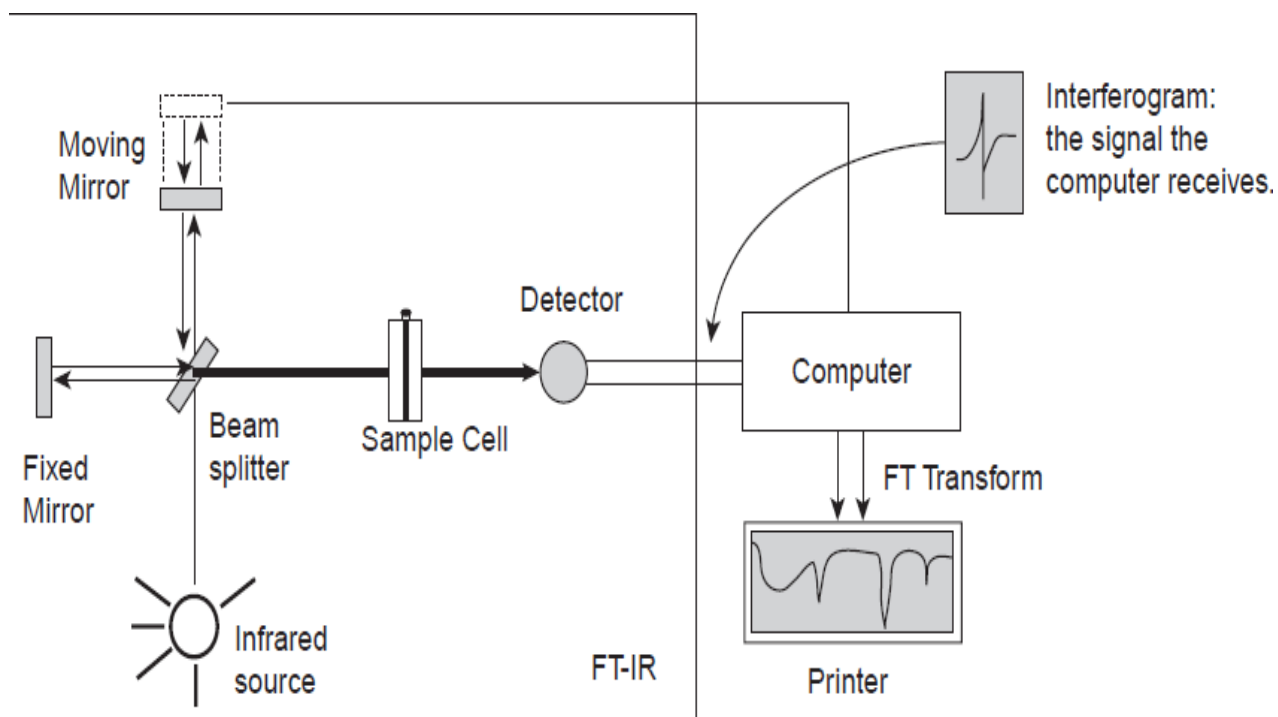


Figure 3.14: A schematic diagram of an FTIR (Pavia *et al.*, 2008).

3.3.10 Nuclear Magnetic Resonance

Nuclear magnetic resonance (NMR) is a physical phenomenon used to investigate the molecular properties of matters by irradiating atomic nuclei in a magnetic field with radio waves. The principle of NMR is the absorption of electromagnetic radiation in the radio magnetic region of the spectrum which leads to change in the orientation of the spinning nuclei in the magnetic field. Not every proton in a molecule has absorption of the electromagnetic radiation at exactly the same frequency. This is because the protons in a molecule are surrounded (shielded) by electrons that exist in different electronic (magnetic) environment from one proton to other. After exposing the protons to a magnetic field, the valence electrons of the protons are caused to circulate and create a counter magnetic field that opposes the applied magnetic field. This circulation of valence electrons called diamagnetic shielding or diamagnetic anisotropy as it is shown in Figure 3.15.

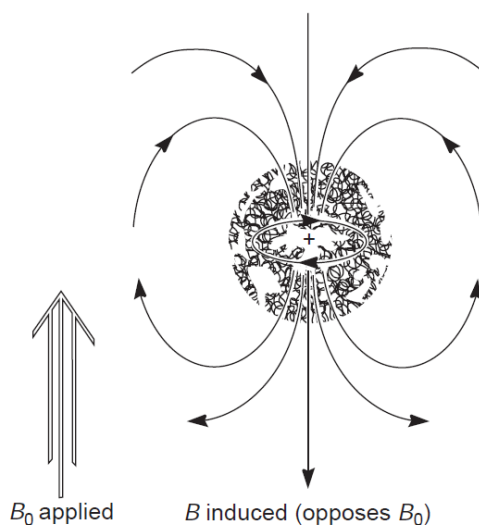


Figure 3.15: Diamagnetic shielding or diamagnetic anisotropy (Pavia *et al.*, 2008)

The difference between the amounts of a given proton resonance from the standard reference substance TMS (tetramethylsilane) is called the chemical shift. The TMS has been chosen as a reference substance because the methyl groups protons are more shielded than most of other compounds. Thus, when the resonance of other compound is measured, its proton resonance is obtained in term of how far is (in Hertz) from those of TMS. The shift from TMS for a given proton is proportional to the strength of the applied magnetic field. For instance, in an applied magnetic field of 1.41 Tesla, the resonance of a proton is 60 MHz, whereas if the applied magnetic field is 2.35 Tesla, the resonance is 100 MHz.

The chemical shift unit is reported as ppm (parts per million) because the TMS is used as a reference substance for other compound protons absorption. Thus, the resonance of the protons in TMS comes at exactly 0.00 ppm in a typical chemical shift scale on NMR spectrum chart as it is shown in Figure 3.16.

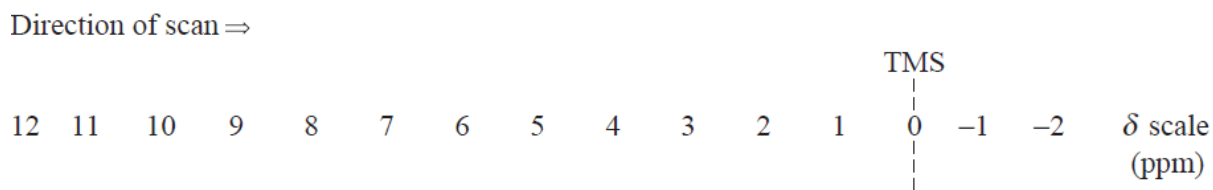


Figure 3.16: A typical chemical shift scale on NMR spectrum chart (Pavia *et al.*, 2008)

The nuclei spin (I), has different values such as 0, $\frac{1}{2}$, 1, $1\frac{1}{2}$. The actual value of nuclei spin depends on the atomic number and the mass number of the nuclei as it is clear in Table 3.1. Only non-zero spin quantum numbers can produce NMR spectra. When the nucleus has a charge, spinning about its own axis may produce a magnetic momentum in the axis.

Table 3.1: Atomic number and nuclei spin (Pavia *et al.*, 2008)

Mass number	Atomic number	Nuclei spin(I)
Odd	Even or odd	$\frac{1}{2} \dots$
Even	Even	0
Even	Odd	1, 2, 3.

The nucleus possesses angular momentum, where for each isotope, the value of magnetic moment along the axis and the angular momentum determine the frequency at which the energy can be absorbed. Furthermore, the sensitivity of the technique for a specific nucleus is determined by the value of its magnetic moment. As shown in Table 3.2, the ^1H has the highest sensitivity,

whereas ^{12}C and ^{16}O have spin quantum numbers of zero and they are inactive. Therefore, proton magnetic resonance is very useful in the identification of organic compounds as many organic compounds consist of only these three atom (Pavia *et al.*, 2008) .

Table 3.2: Nuclei spin quantum and magnetic properties of selected nuclei (Pavia *et al.*, 2008)

Nucleus	Nucleus spin quantum number	Magnetic moment	Resonance frequency	Sensitivity
^1H	1/2	14.09	60.000	1.00
^{12}C	0	-	-	-
^{13}C	1/2	3.53	15.08	1.8 x-410
^{16}O	0	-	-	-

Figure 3.11 schematically illustrates the main elements of an NMR spectrometer. First of all, the sample is dissolved in a solvent, then a small amount of internal reference TMS is added. The sample cell is a small cylindrical glass suspended in the gap between the faces of the pole pieces of the magnet. The sample is turned around its axis to ensure uniform magnetic field to all part of the solution. A coil attached to a 60-MHz radiofrequency (RF) generator in the magnet gap. This coil in the magnet gap is attached to the 60-MHz radiofrequency (RF) generator in order to supply the electromagnetic energy used to change the spin orientations of the protons. A detector coil is positioned perpendicularly to the RF oscillator coil. When there is no absorption of energy taking place, detector coil will not pick up any of the energy given off by the RF oscillator coil. However, if the sample absorbs energy, radiofrequency signal is induced by the reorientation of the nuclear spins. Finally, it is recorded as a peak or resonance signal (Pavia *et al.*, 2008).

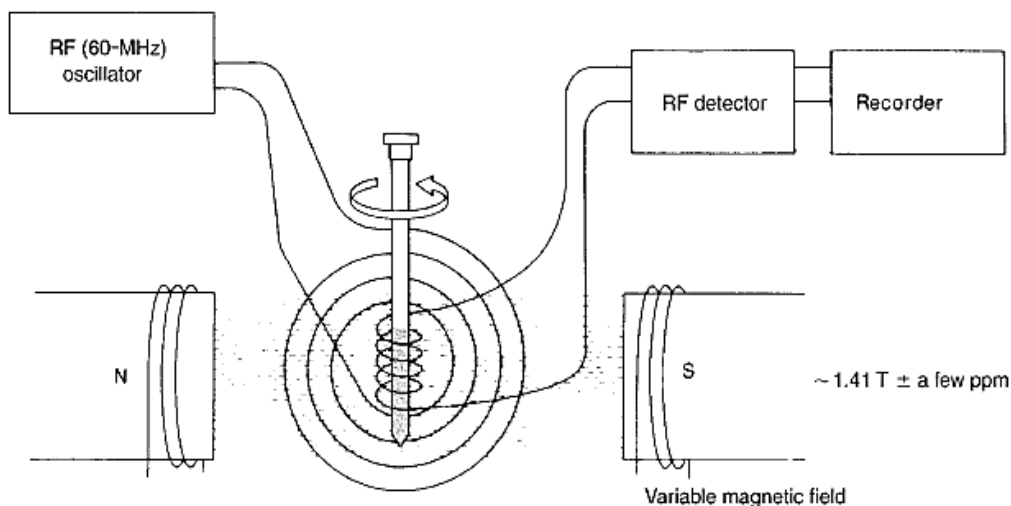


Figure 3.11 a schematic diagram of an NMR (Pavia *et al.*, 2008).

3.3.11 Error Analysis

There are three main categories of error. These three types are systematic error (determinate errors), random error (indeterminate errors) and gross errors. The systematic errors are instrumental, methodological, which is consistently deviated in one direction from the true value. Table 3.3 shows the errors for the laboratory equipment used in this project.

Table 3.3: Laboratory equipment used and their errors

Laboratory equipment	Error
Weighing balance A&D HR-200 weighing balance	($\pm 0.05 \text{ mg}$)
Pipette 100-1000 μL	$\pm 8 \mu\text{L}$ @ISO8655
Measuring flask/ cylinder	$\pm 0.25 \text{ mL}$
rpm mixing speed	$\pm 10 \text{ rpm}$
Hotplate temperature controller	$\pm 0.5^\circ\text{C}$

The second category of error is the random error. Random errors are caused by uncontrollable fluctuations in variables which result in a change in the experimental results. A multiple number of measurements result in evenly distributed data scattered around an average value or mean. This

positive and negative scattering of data is characteristic of random errors. Some examples of random error include: incomplete drying of sample before weighing, material loss during transfer of precipitates, and errors in transfer of solutions etc. Standard deviation (SD) is often reported to smooth out the random error for a set of values mainly higher than 4 measurements.

$$SD = \pm \sqrt{\frac{\sum (x_i - \bar{x})^2}{N - 1}}$$

Where $(x_i - \bar{x})$ is the deviation from the mean, the difference between the individual experimental value and the mean value. $(N-1)$ is the total number of measurements minus one (number of degrees of freedom).

The standard deviation for FAME conversion, squalene recovery and EPA/DHA recovery, are obtained from the repeated runs at the central points.

Chapter 4 Results and Discussion

4.1 Waste Shark Liver Oil Characterisation

The Karl Fischer Titration of the WSLO indicated a water content of $0.08 \pm 0.01\%$, and the measured WSLO density was 0.916 g/mL at 30°C . The glyceride (TG, DG and MG) and FFA content of the WSLO was determined by the Iatroscan MK-6, as shown in Table 4.1 and chromatograms for the lipid classes is showing in Appendix B.

Table 4.1: Lipid classes as measured by Iatroscan MK-6

Lipid classes	WSLO composition wt.%
TG	44.0
DG	14.3
MG	21.1
FFA	19.9
Squalene	0.7

The WSLO composition suggests that this feedstock can be used for biodiesel production. However, due to the high FFA content, it is envisaged that homogeneous alkali catalysis will not be effective. Earlier studies have shown that alkali-catalysed transesterifications require low levels of FFA ($< 2.5\%$) to avoid soap formation and catalyst deactivation (Leung *et al.*, 2010). Therefore, an acid-catalysed transesterification, which tolerates high FFA in the feedstock, would be recommended for one-step biodiesel processing from WSLO. The water content of the WSLO was slightly higher than the $0.06 \text{ wt.}\%$ required for homogeneous catalysis, indicating that glyceride and FAME saponification might occur (Phan *et al.*, 2012; Eze *et al.*, 2014; Eze *et al.*, 2018).

Table 4.2 shows the fatty acid profile of the WSLO, obtained by complete conversion to FAME via acid-catalysed transesterification with methanol and quantification by the GC, and analysed using the BS EN 14103:2003 standard (Wang; Wang and McCurry, 2006). Full fatty acid profile can be found in Appendix A.

Table 4.2: Fatty acids profile of the WSLO

Type of fatty acids	Systematic Name	Weight % of fatty acid
14:0	Myristic acid	5.0
15:0	Pentadecanoic acid	0.6
16:0	Palmitic acid	19.5
16:1n-7	Palmitoleic acid	6.0
16:2n-4	9,12-hexadecadienoic acid	1.0
18:0	Stearic acid	6.3
18:1n-9	Oleic acid	11.4
18:1n-7	Vaccenic acid	4.0
18:2n-6	Linoleic acid	1.1
20:1n-9	Eicosenoic acid	1.9
20:4n-6	Arachidonic acid	2.2
22:1n-11	Cetoleic acid	1.8
22:4n-6	Adrenic acid	1.0
22:5n-3	Clupanodonic acid	3.7
22:5n-6	Osbond acid	1.8
20:5n-3 (EPA)	Eicosapentaenoic acid	6.1
22:5n-3	Docosapentaenoic acid	3.7
22:6n-3 (DHA)	Docosahexaenoic acid	15.0

The fatty acid profile in Table 4.2 shows that the WSLO contains 21.1% PUFAs, constituting 15% DHA and 6.1% EPA. The European biodiesel standard, EN 14214 as shown in Appendix D, limits the content of polyunsaturated (\geq four double bonds) methyl esters to 1% (m/m). However, the FAME produced from the WSLO could be directly used as biodiesel in the USA and Canada, as the ASTM D6751 standards as shown in Appendix E do not specify the percentage of PUFAs allowable in biodiesel. Nevertheless, it is recommended that the PUFAs in WSLO be separated to obtain EPA and DHA for pharmaceutical application. The remaining FAME after EPA and DHA separation meets the EN 14214 standards and can be used as a biodiesel.

The average molecular weights obtained from the WSLO fatty acids profile are shown in Table 4.3. Where, the molecular weight for TG, DG and MG are calculated as below:

$$TG = 3 \Sigma \text{FAME} + GL - 3CH_3OH$$

$$DG = 2 \Sigma \text{FAME} + GL - 2CH_3OH$$

$$MG = \Sigma \text{FAME} + GL - CH_3OH$$

Table 4.3: Average molecular weights of WSLO

Glyceride/FAME	WSLO average molecular weight (g/mol)
Triglyceride (TG)	910
Di-glyceride (DG)	698.4
Mono-glyceride (MG)	393.7
Fatty acid methyl esters(FAME)	304.7

4.2 NMR Analysis for FAME Produced from Acid Catalysed Transesterification

FAME produced from acid catalysed transesterification was analysed by using NMR. Figure 4.1 shows an NMR spectrum of the FAME from WSLO. The purpose of this test was to investigate if the triglycerides have been totally converted to FAME or not. Furthermore, NMR analysis was used to check the presence of squalene in the WSLO sample after reaction.

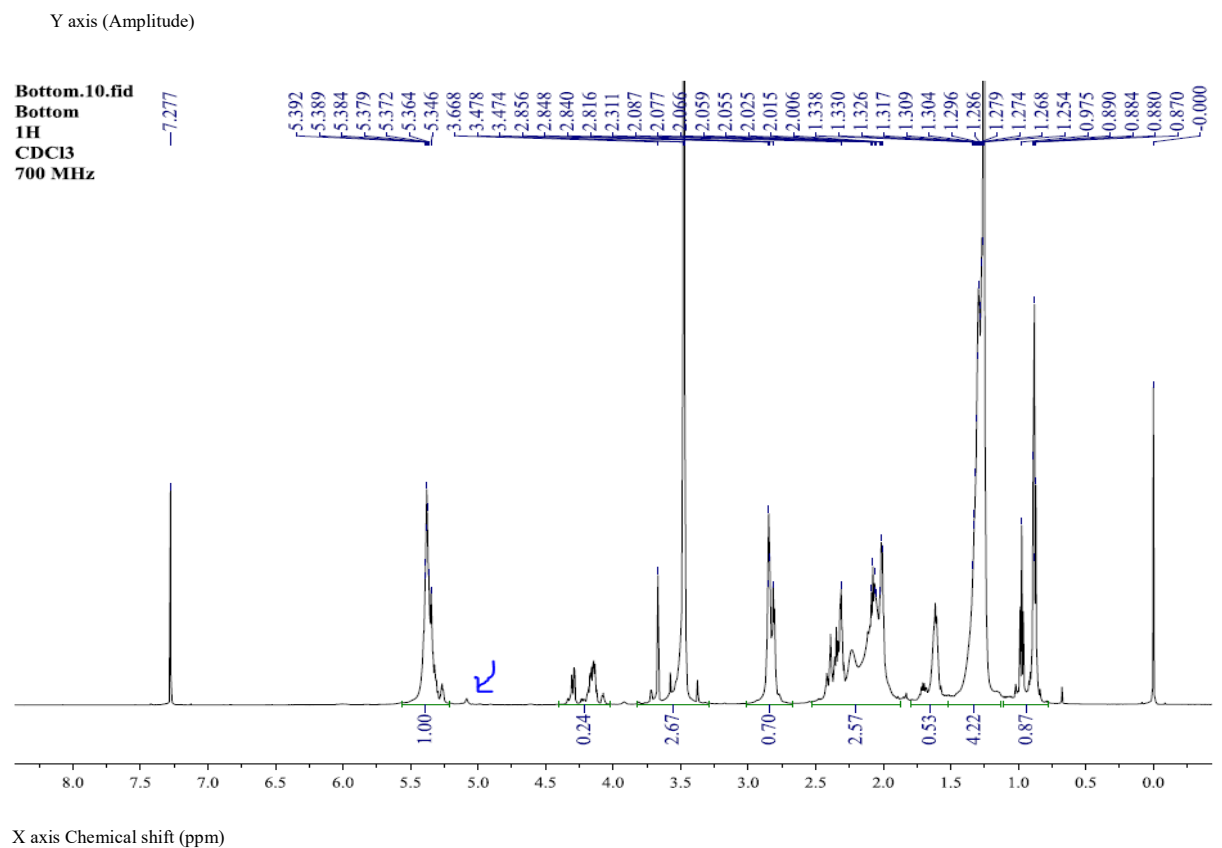


Figure 4.1: NMR spectra of the FAME from WSLO

Figure 4.1 shows that there are some unconverted triglyceride peaks at 4.28 ppm and 4.131 ppm for “c” proton (H₂C) as shown in Figure 4.2 which indicate that complete conversion was not achieved for the FAME produced from WSLO.

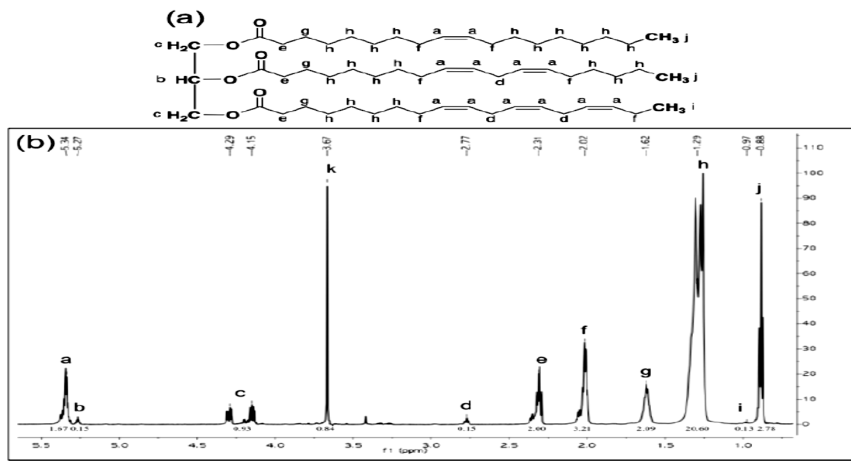
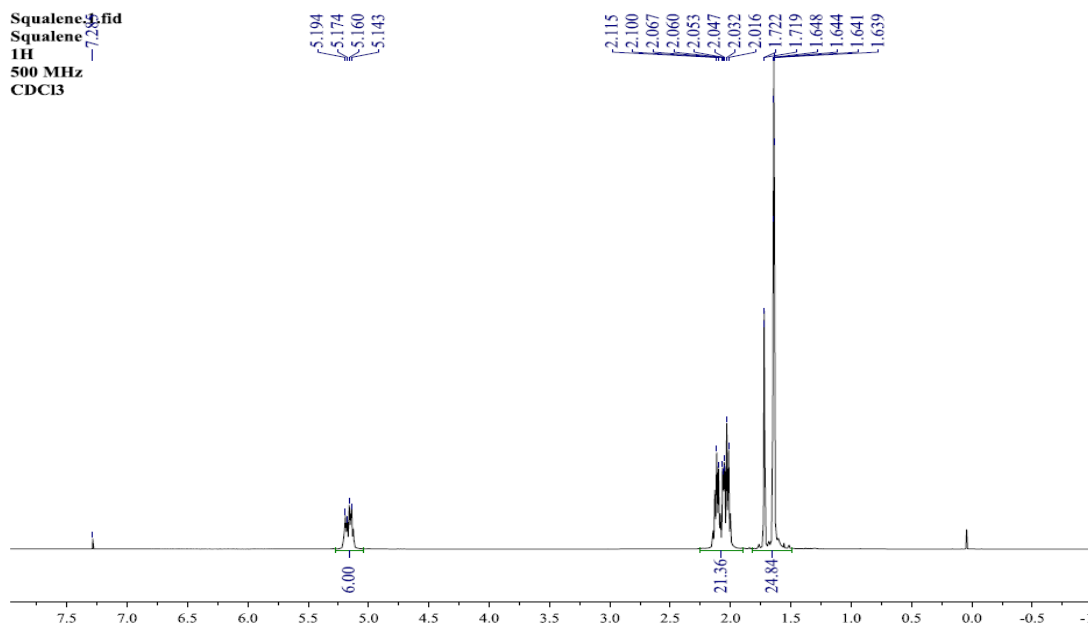


Figure 4.2: Proton NMR Chart

Figure 4.3 shows NMR spectra for pure squalene (99% purity). This spectrum has been used to determine the presence of squalene in WSLO fatty acid methyl ester NMR spectra. The NMR spectra of the FAME from WSLO in Figure 4.1 showed a presence of a small peak at 5.201 ppm (=C-H) assigned to squalene, which is consistent with the Iatroskan chromatogram result for WSLO about the presence of squalene in the WSLO sample.

Y axis (Amplitude)



X axis Chemical shift (ppm)

Figure 4.3: NMR spectra for pure squalene

4.3 Monitoring Waste Shark Liver Oil Transesterification Using FTIR

FTIR was used to monitor transesterification using an acid catalyst as shown in Figure 4.4 and Figure 4.5. The results illustrate that the FTIR technique was not a reliable method for on-line monitoring of conversion of triglyceride to FAME using transesterification reaction for WSLO samples. There was no real indication of FAME produced because the methyl peak at wave length 1438 cm^{-1} may represent FAME and methanol as well. Likewise, the carbonyl functional group observed at wave length 1749 cm^{-1} could be from either triglyceride or FAME. Therefore, the result in Figure 4.4 is not indicating a firm conclusion about FAME production at different time intervals for this reaction. However, GC analysis of the samples confirmed that FAME was produced from the transesterification of WSLO using acid catalysts.

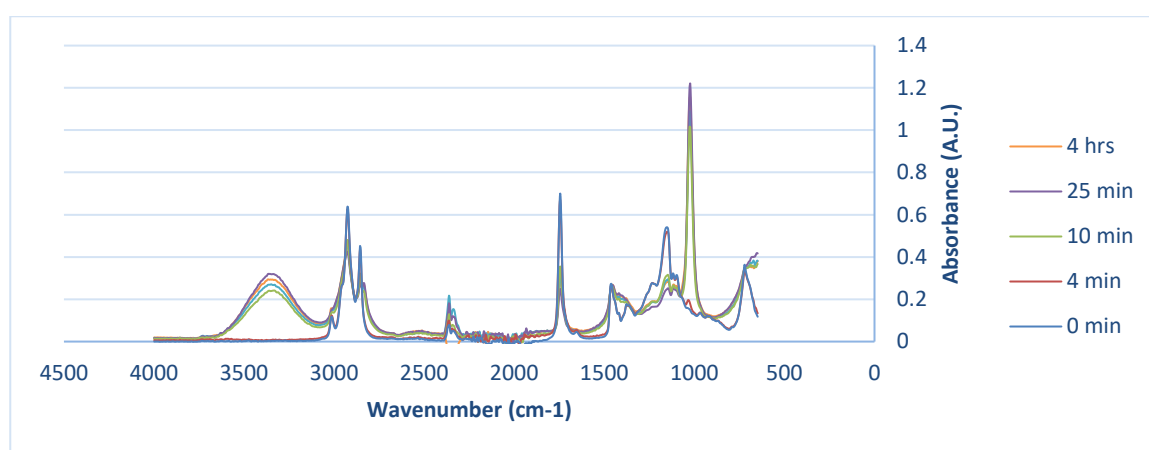
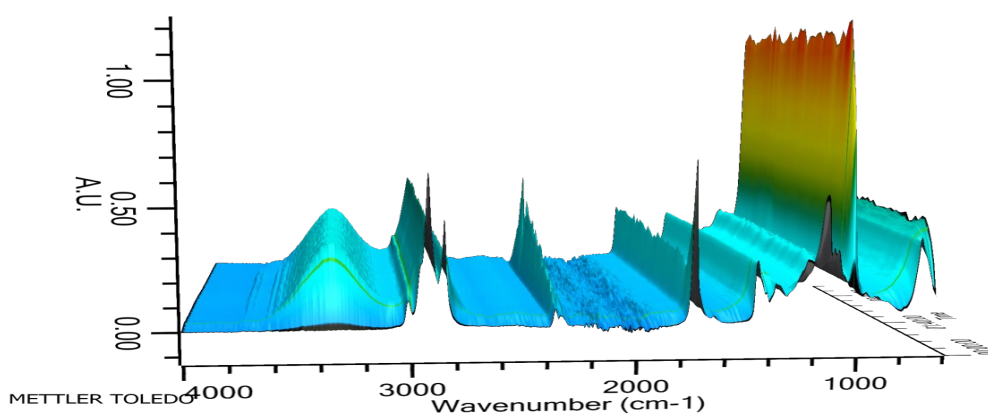


Figure 4.4: FTIR 4 hrs transesterification reaction using acid catalyst



Axes (X=Wavenumber ,Y= Absorbtion,and Z-time)

Figure 4.5: 3-D FTIR transesterification reaction using acid catalyst

4.4 Waste Shark Liver Oil Transesterification and FAME Conversions with the Catalysts

The effects mixing has on WSLO transesterification are shown in Figure 4.6 for reactions at 60°C with a reaction time of 6 h, a 30:1 methanol to oil molar ratio and using a 3 wt.% of sulfuric acid (H₂SO₄) catalyst. The FAME conversions against time for different mixing speeds (400, 720 and 1080rpm) clearly indicate that the reaction was mixing independent at 720 rpm and above, while, at speeds above 400 rpm, there was a mass transfer-controlled reaction. The WSLO transesterification reaction overcomes the mass transfer dependent region at speeds of 720 and 1080 rpm, becoming kinetically controlled.

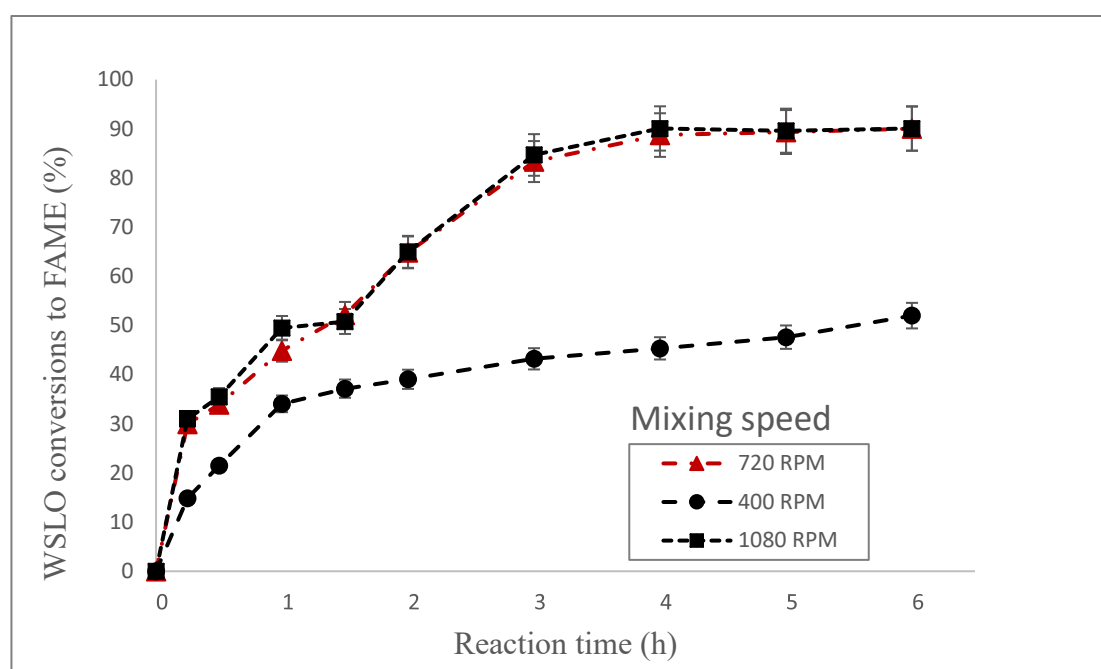


Figure 4.6: Effect of mixing intensity on WSLO transesterification at 60°C, with a 6h reaction time, a 30:1 methanol to oil molar ratio and using a 3wt.% of the H₂SO₄ catalyst.

Figure 4.7 shows the results of the preliminary investigations of the WSLO transesterification using both acid and base catalysts. The maximum FAME conversion obtained for the homogeneous alkali-catalysed process was 40%, using the typical transesterification conditions of 60°C temperature, a 60 min reaction time, a mixing speed of 720 rpm, 1.5 wt.% NaOH, and a 6:1 methanol to oil molar ratio (Figure 4.7 (a)). The FAME conversions increased only slightly from 15% at 3min to reach the maximum after 15min. This was followed by a period of continuous decrease in the FAME conversions, with only 12% FAME conversion after the full 60min reaction time. The trend in the FAME conversions for the NaOH catalyst was attributed to the effect of the

high FFA content (19.9%) in the WSLO, which results in the catalyst being deactivated by reacting with the FFA to form soap and water (saponification) (Pullen and Saeed, 2015). Moreover, the presence of water in the reaction mixture also leads to glyceride and FAME saponification, resulting in the observed period of decrease in FAME conversions after achieving the maximum conversion.

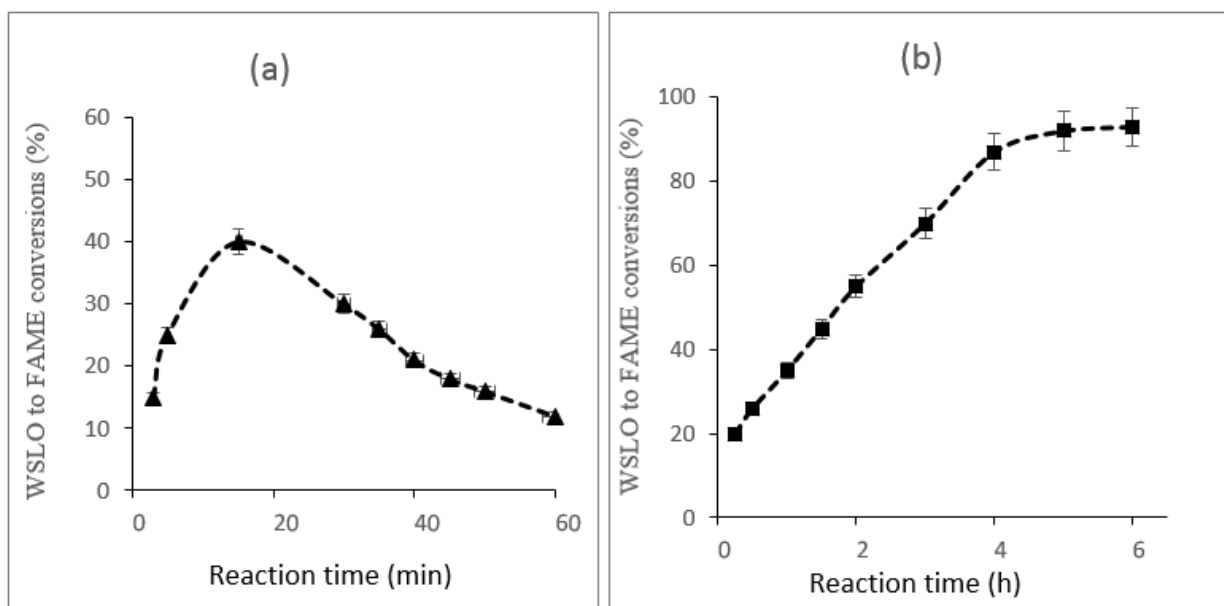


Figure 4.7: FAME conversions for transesterification of WSLO at 720rpm mixing speed using, (a) 1.5 wt.% NaOH at 6:1 methanol to oil molar ratio, 60^oC temperature and 60min reaction time, (b) 1.5 wt.% H₂SO₄ at 30:1 methanol to oil molar ratio, 60^oC temperature and 6h reaction time.

As shown in Figure 4.7 (b), the FAME conversions increased with the reaction time, achieving 93% conversion after 6h. Acid-catalysed transesterification has an advantage over the base-catalysed process, as it can tolerate high FFA in the feedstock (Issariyakul *et al.*, 2007). It is expected that either a longer reaction time or an increase in catalyst concentration would be required to reach the maximum equilibrium of FAME conversion for acid-catalysed WSLO transesterification. Therefore, a parametric study and optimisation of the acid-catalysed WSLO transesterification was carried out, as discussed in the following section.

4.5 Parametric Study and Optimisation of Acid-catalysis of WSLO Transesterification

Parametric studies of the reaction conditions for the acid-catalysed transesterification of the WSLO were evaluated at 1 to 7 h reaction times, H₂SO₄ catalyst loading from 1 to 6 wt.% and methanol to oil molar ratios from 6:1 to 30:1. These studies used a response surface methodology in DoE with a central composite design.

Table 4.4 shows the experimental and predicted conversion of WSLO to FAME at different parameter spaces. The main effects were caused by the reaction times and catalyst concentrations, while the molar ratios showed only moderate effects on FAME conversion. An experimental error of $\pm 1.1\%$ was obtained for the data in Table 4.4, based on the three repeats on central points which are 18 molar ratio of methanol to WSLO, 3.5wt. % of H₂SO₄ catalyst loading and 4 hrs reaction time.

Table 4.4: Experimental and predicted conversion of WSLO to FAME at different conditions

Run	Molar Ratio (methanol/WSLO)	H ₂ SO ₄ catalyst loading (wt. %)	Time (h)	Experimental conversion of WSLO to FAME	Model predicted conversion of WSLO to FAME
1	30	6	7	99.6	99.8
2	18	6	4	95.8	96.3
3	30	1	1	30.0	29.2
4	6	6	1	56.4	55.9
5	6	3.5	4	86.0	86.5
6	6	1	1	31.0	29.8
7	18	3.5	4	87.1	86.6
8	18	3.5	4	86.7	86.6
9	18	3.5	7	96.1	95.5
10	30	1	7	94.9	95.3
11	30	3.5	4	87.0	86.7
12	6	6	7	98.9	98.9
13	6	1	7	95.7	96.0
14	18	3.5	4	85.0	86.6
15	18	3.5	1	41.0	40.9
16	30	6	1	57.0	56.9
17	18	1	4	81.2	81.0

An empirical model for FAME conversions, determined from the experimental data using the DoE response method, is shown in Equation 4.1, where X is the methanol molar ratio, Y is the catalyst loading (wt.%), and Z is the reaction time (h).

$$\text{FAME conversion (\%)} = 0.581 - 0.0385 X + 3.694 Y + 28.164 Z + 0.3190 \text{ Cat. } Y \times Y \quad (4.1) \\ - 2.0451 Z \times Z + 0.01292 X \times Y - 0.7750 Y \times Z.$$

The DoE model predicted that the maximum conversion would occur at: 10.3:1 molar ratio of methanol to oil, 6.5 h reaction time and 5.9 wt.% H₂SO₄ catalyst. These conditions were validated experimentally, and the results showed 99 ± 1.1% conversions of the WSLO to FAME.

The interactions of reaction parameters—time, methanol molar ratio and catalyst concentration—on FAME conversion are shown in Figure 4.8. Clearly, FAME conversions increased with the methanol molar ratio, up to a maximum of 18:1. After this maximum was reached, further increase in the methanol molar ratio led to reductions in the FAME conversion. This is in line with findings for the transesterification of Cynara oil using different molar ratios between 3:1 and 15:1, where the yield of biodiesel increased with molar ratio up to a value of 12:1, and decreased up to the maximum molar ratio of 15:1, because a fraction of the glycerol remained in the biodiesel phase (Musa, 2016).

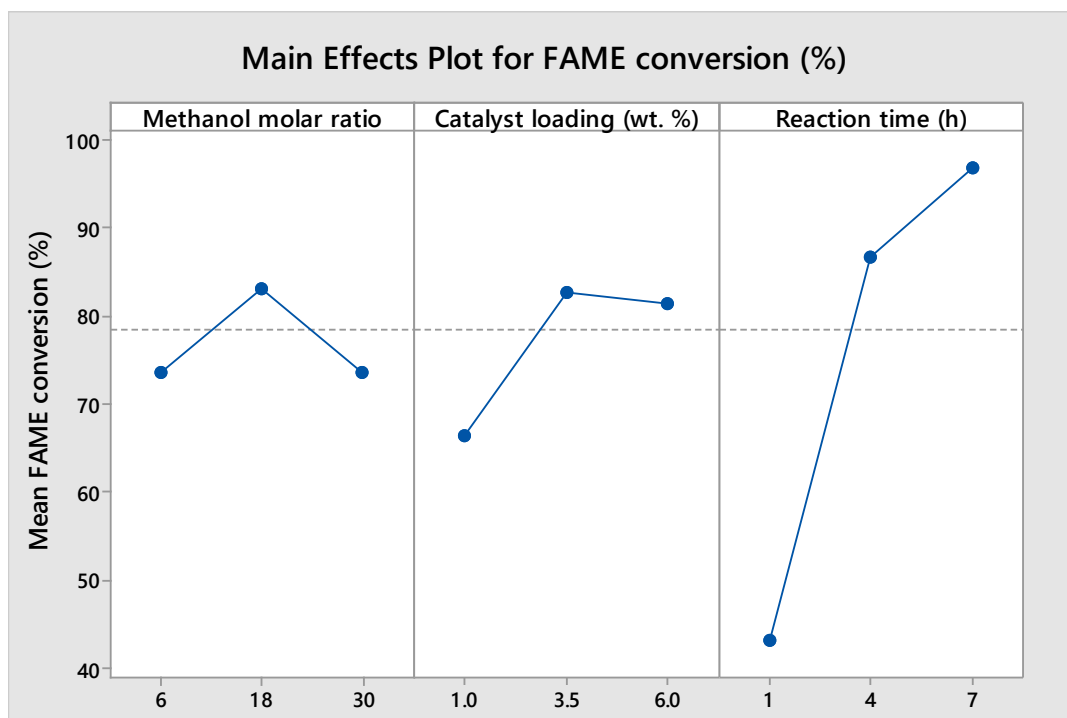


Figure 4.8: effect of the reaction parameters (reaction time (h), methanol molar ratio and catalyst concentration (wt.%)) on conversions of WSLO to FAME.

The p-value obtained from DoE for the molar ratio was 0.039, so it was statistically significant. The increase in catalyst concentration from 1 wt.% to 3.5 wt.% resulted in a sharp rise in FAME conversions. However, further increases in the catalyst concentration, up to 6 wt.%, did not improve the FAME conversions. Reaction time also increased conversion over the selected range, as expected. The p-values obtained from DoE for the catalyst loading and reaction time were 0.00, and that indicates strong evidence for rejecting the null hypothesis which shows that there is no statistically significant variation in the variables. Therefore, the catalyst loading and reaction time are statistically significant.

4.6 Squalene Recovery from Waste Shark Liver Oil

DoE, using a response surface methodology with a central composite design, was employed to obtain the parametric conditions for the highest squalene recovery. The DoE was conducted across the following parameter space: (i) an alcohol to WSLO molar ratio of 20:1 to 100:1, (ii) reaction times of 5 to 60 min and (iii) water contents in the range of 0 to 20 wt.%. Each experiment was carried out using 6 g of WSLO, spiked with 1.2 g of squalene, corresponding to 16.7 wt. % squalene in WSLO. The alkali catalyst concentration was NaOH at 25 wt.% (based on WSLO dissolved in the alcohol-water solutions) at 60°C with a 720 rpm mixing speed. The experimental squalene recovery is shown in Table 4.5, with a margin of error of ± 1.3 %, based on the three repeats around central points which are 60:1 molar ratio of ethanol to WSLO, 10 wt. % water loading to the reaction and 32.5 min reaction time. The GC chromatograms for squalene recovery at different reaction times (5, 30 and 60 min) and after washing are attached in appendices (C1, C2, C3 and C4). An empirical model for squalene extraction determined from the experimental data using the DoE response method is shown in Equation 4.2, where X is the ethanol molar ratio, Y is the water loading (wt.%) and Z is the reaction time (min).

$$\begin{aligned} \text{Squalene recovery(\%)} = & 95.2 + 0.19 X - 2.36 Z + 8.38 Y \\ & - 0.00250 X \times X + 0.0146 Z \times Z - 0.390 Y \times Y + 0.00629 X \times Z - 0.0477 X \times Y + 0.0548 Z \times Y \end{aligned} \quad (4.2)$$

Table 4.5: Squalene recovery at different parameter spaces

Run	Ethanol molar ratio	Reaction time (min)	Water loading (wt. %)	Squalene recovery (%)	Model predicted recover of squalene
1	60	32.5	20	33	38.6
2	100	5	20	2.5	2.6
3	100	32.5	10	44.3	63.3
4	100	5	0	81.2	80.9
5	20	5	20	93.8	85.2
6	60	32.5	0	35.4	48.6
7	60	60	20	36.7	51.3
8	100	60	20	28.1	19.9
9	20	32.5	10	64.4	93.9
10	20	60	20	87.5	74.8
11	20	5	0	84.0	87.2
12	60	60	10	71.3	80.3
13	100	60	0	42.3	37.9
14	60	32.5	10	99.9	82.6
15	60	32.5	10	97.3	82.6
16	20	60	0	26	16.5
17	60	32.5	10	98.5	82.6

The main effects plot of the interactions of the investigated parameters—molar ratio, reaction time and water loading—on mean squalene recovery are shown in Figure 4.9. The middle range for molar ratio, reaction time and water loading achieved high squalene recovery. Further increase, after the middle range, in ethanol molar ratio, reaction time and water loading decreased the squalene recovery.

The p-values obtained from the DoE data for the ethanol molar ratio, reaction time and water loading were 0.00, 0.003 and 0.023, respectively. All values are less than 0.05, which indicates that the null hypothesis can be rejected. Therefore, the ethanol molar ratio, reaction time and water loading are statistically significant regarding squalene recovery.

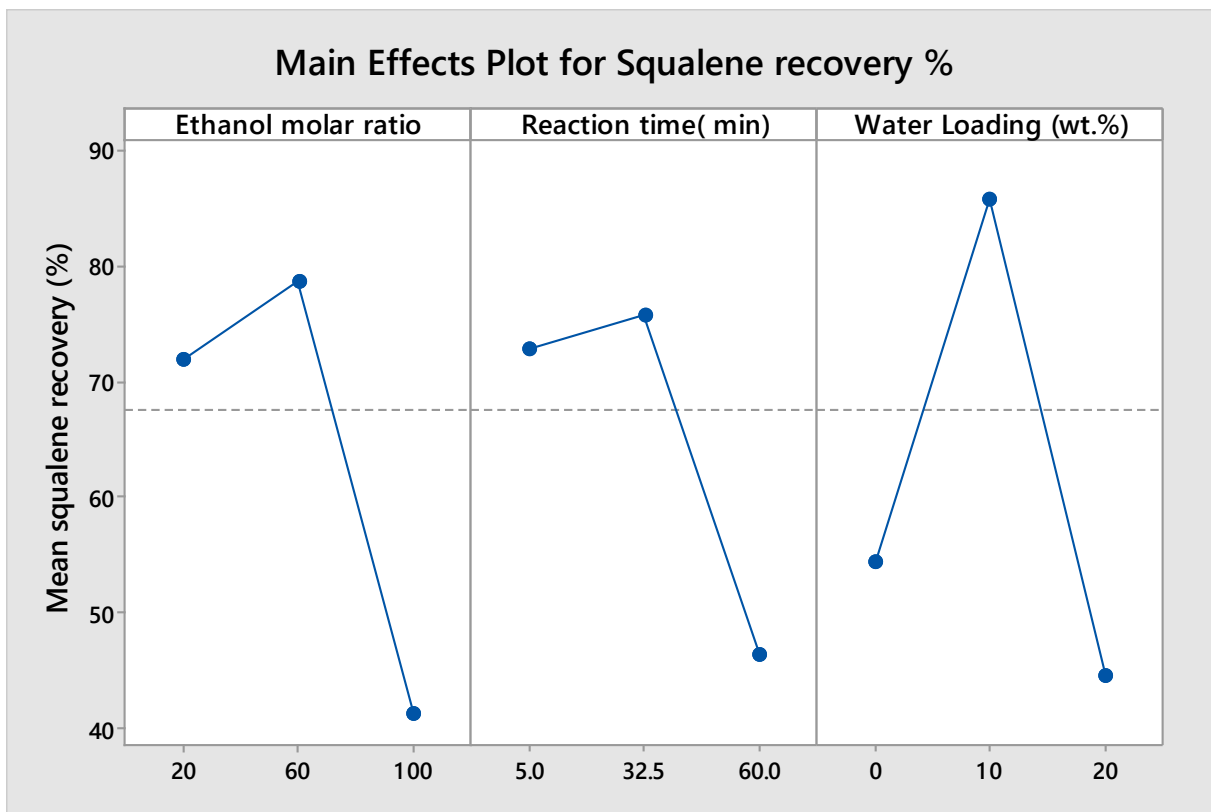


Figure 4.9: Effects plot for squalene recovery

4.6.1 Effect of the Extraction Parameters on Squalene Recovery

The interactions of the ethanol molar ratio and reaction time on mean squalene recovery are shown in Figure 4.10 (a). Clearly, squalene recovery increased with the ethanol molar ratio, up to 72:1, after which, further increase in the ethanol molar ratio led to decreasing squalene recovery.

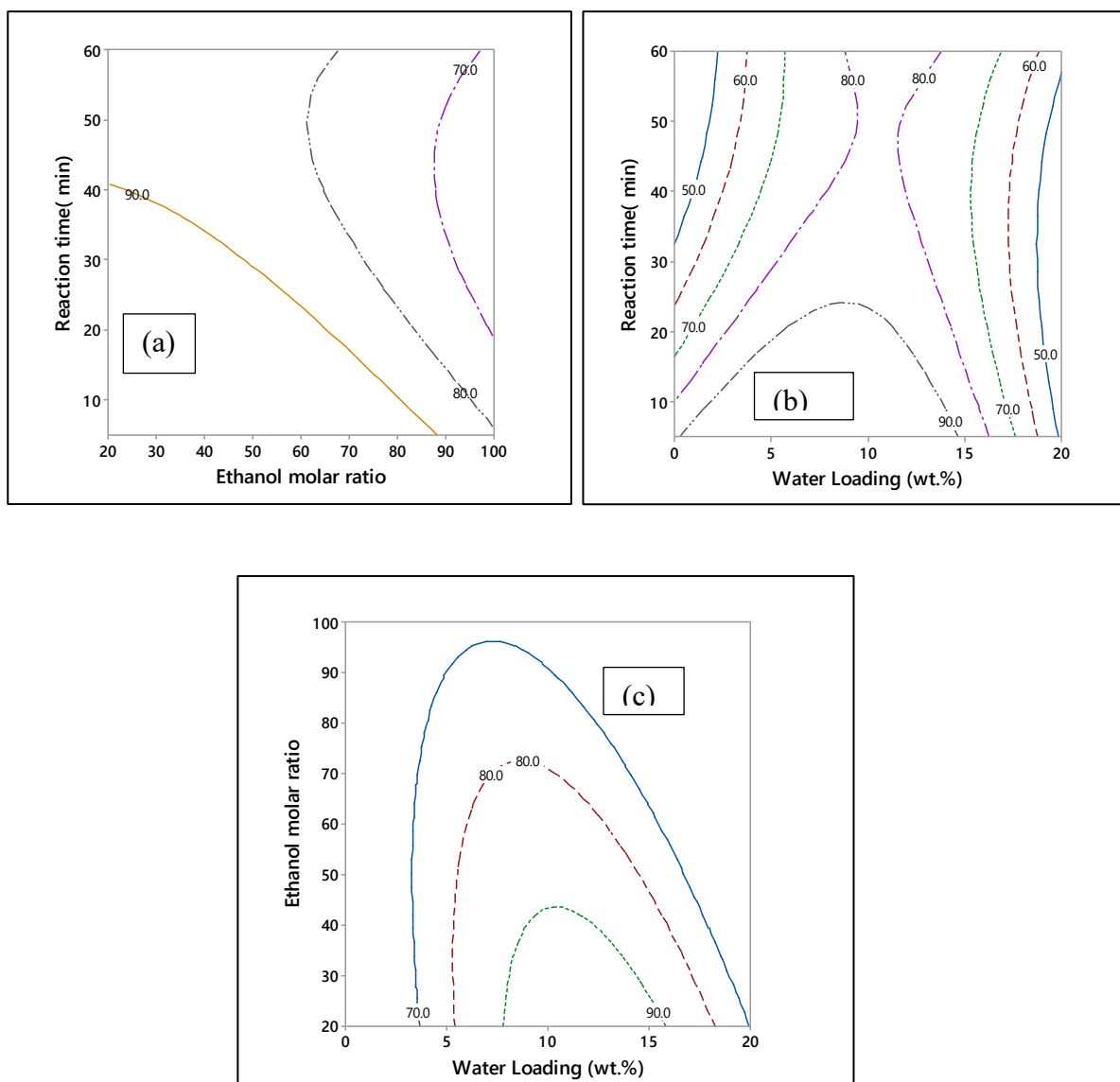


Figure 4.10: Effect of process parameters on squalene recovery; (a) ethanol molar ratio and reaction time; (b) reaction time and water loading; (c) water loading and ethanol molar ratio

This is explained by the fact that, at low ethanol molar ratios, the soap produced was in the form of an emulsion, as shown in Figure 4.11 (a), which makes squalene recovery difficult. However, with a slight increase in the ethanol molar ratio, the soap became particulate/granular in form, as shown in Figure 4.11 (b), allowing for easy squalene recovery. Further increase in the ethanol molar ratio, up to 100:1, led to reductions in squalene recovery, because the higher ethanol molar ratio pushed equilibrium further toward ethoxide formation, and this reduced the mole fraction of hydroxide ions and, consequently, the rates of saponification (Eze *et al.*, 2015).



(a) Soap in form of emulsion



(b) Soap in form of particulate/granular

Figure 4.11: Soap in form of (a) emulsion and (b) particulate/granular

The amount of water introduced in the reaction mixture can affect the level of saponification, and, accordingly, the separation of squalene. Figure 4.11 (b) shows the interaction between reaction time and water loading on squalene recovery. As the water content increased from 0% to 7.5%, the saponification rates increased because of the hydroxide-ethoxide equilibrium reaction, leading to the production of more hydroxide ions, as shown in Equation 4.3. The increase in hydroxide concentration led to higher rates of saponification, as reported elsewhere (Eze *et al.*, 2015). However, with further increases in water loading from 7.5% to 20%, the squalene recovery declined as the type of soap produced was in the form of an emulsion rather than particulates, leading to the loss of some squalene to the soap layer.

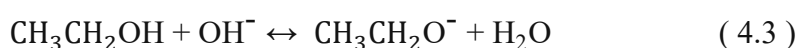


Figure 4.10 (c) shows the interaction of water loading and the ethanol molar ratio on squalene recovery. Both parameters have similar trends. Moderate increase in water content and ethanol molar ratio resulted in enhanced saponification and, consequently, increased the squalene recovery. However, further increase in ethanol molar ratio and water loading reduced squalene recovery because the excess ethanol molar ratio pushed equilibrium further toward ethoxide formation, which reduced the mole fraction of hydroxide ions required for WSLO saponification. Moreover, the soap produced at high ethanol molar ratios and high water loading was in the form of an emulsion, leading to loss of some squalene in the soap layer.

4.6.2 Optimal Conditions for Squalene Recovery

Optimal squalene recovery was predicted by the DoE model at the following operating conditions: 20:1 molar ratio of ethanol to oil, 5 min reaction time and 9.9 wt. % water loading. These conditions were validated experimentally, and the results showed 101.6 ± 1.3 % squalene recovery. The squalene recovery process developed in this study has been compared with the most common techniques applied in the industry for squalene extraction, such as short path distillation and supercritical fluid extraction techniques.

Short path distillation can be used to achieve 97% squalene extraction from shark liver oil (Pietsch and Jaeger, 2007b), whereas the use of supercritical carbon dioxide has been reported to achieve squalene recovery of 95% (Catchpole *et al.*, 1997). However, squalene recovery above 97% using supercritical carbon dioxide can only be achieved using reflux, which increases operational costs (Catchpole *et al.*, 1997).

The main drawback of the supercritical fluid extraction (SFE) is the high cost of equipment and the complexity of the operation (Popa *et al.*, 2015b). In terms of energy utilisation, SFE's requires more energy than short path distillation, and the investment cost of short path distillation is about one-third that of the supercritical process (Pietsch and Jaeger, 2007b). Furthermore, from an operational perspective, the saponification extraction technique does not require high energy to pressurise the oil feedstock or to reach the supercritical conditions, as is the case for the supercritical fluid extraction technique.

4.7 EPA and DHA Extraction

A parametric study was conducted to obtain the optimal process conditions for EPA and DHA recovery from FAEE using aqueous silver nitrate by complexation between the double bonds of PUFA ethyl ester and silver ions. Ethyl ester is used instead of methyl ester because ethyl ester is edible. Methyl ester, when hydrolysed in the stomach, will produce methanol, which is toxic. That methanol will metabolise to form formaldehyde, which is also poisonous—causing blindness and death. However, ethyl ester, when hydrolysed, will produce ethanol, which is not toxic.

The FAEE was produced by converting the residual soap from the WSLO saponification. The saponification was performed at the optimal conditions obtained from the DoE: 20:1 molar ratio of ethanol to oil, 5 min reaction time and 9.9 wt.% water loading. The soap produced was then neutralised with 0.5M HCl and esterified to FAEE using the H₂SO₄ catalyst. The FAEE conversion was 98.6% at the optimum conditions obtained from the DoE results: 10.3 molar ratio of ethanol to WSLO, 6.5 h reaction time, 60°C temperature, and 5.9 wt.% of the H₂SO₄ catalyst. The amounts of EPA and DHA in the FAEE produced from the WSLO were 6.1% and 15 %, respectively. The extraction experiments were carried out using a ratio of 3:1 (v/v) silver nitrate to the FAEE across the following parameter space: (i) reaction time at 0.5, 1, 2 and 4 h and (ii) aqueous silver nitrate concentrations of 15, 30 and 50 wt.% AgNO₃ in water.

Figure 4.12 shows an overview of aqueous silver nitrate extraction of EPA and DHA from WSLO. The reaction temperature was kept constant at 20°C (Lembke, 2013a), and the mixing speed was 300 rpm, based on a previous mixing study (Bura Mohanarangan, 2012). The solvent was hexane, based on the screening conducted by Teramoto *et al* (1994), which achieved the highest EPA and DHA extraction in comparison to heptane, benzene, toluene and other solvents (Teramoto *et al.*, 1994).

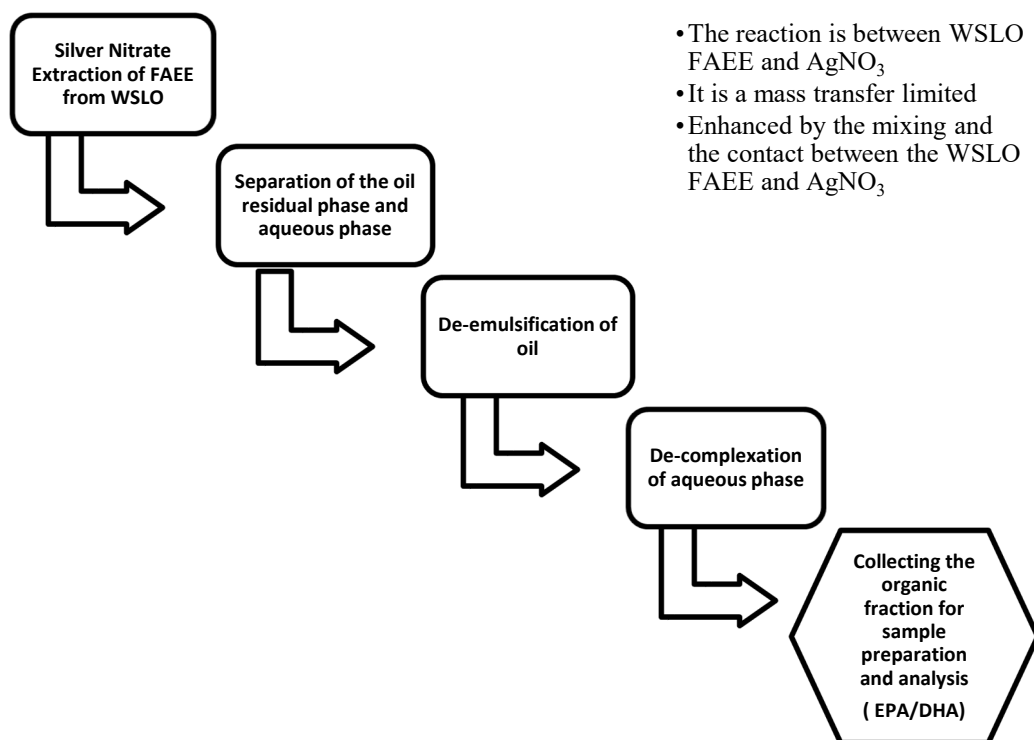


Figure 4.12: Overview of aqueous silver nitrate extraction of EPA and DHA from WSLO

4.7.1 Effect of Process Parameters on EPA and DHA Extraction

Figure 4.13 (a) shows that EPA and DHA recovery increased, from 11.2% to 21.6% for DHA and from 10.9% to 14.1% for the EPA, between the reaction times of 0.5 and 2 h. There was a sharp increase in the EPA and DHA recovery from 0.5 to 1.5 h and a moderate increase in recovery between 1.5 and 2 h. However, for the reaction time after 2 h and up to 4 h, there was no substantial change in the amounts of EPA and DHA extracted, which indicates that equilibrium extraction was reached at 2 h.

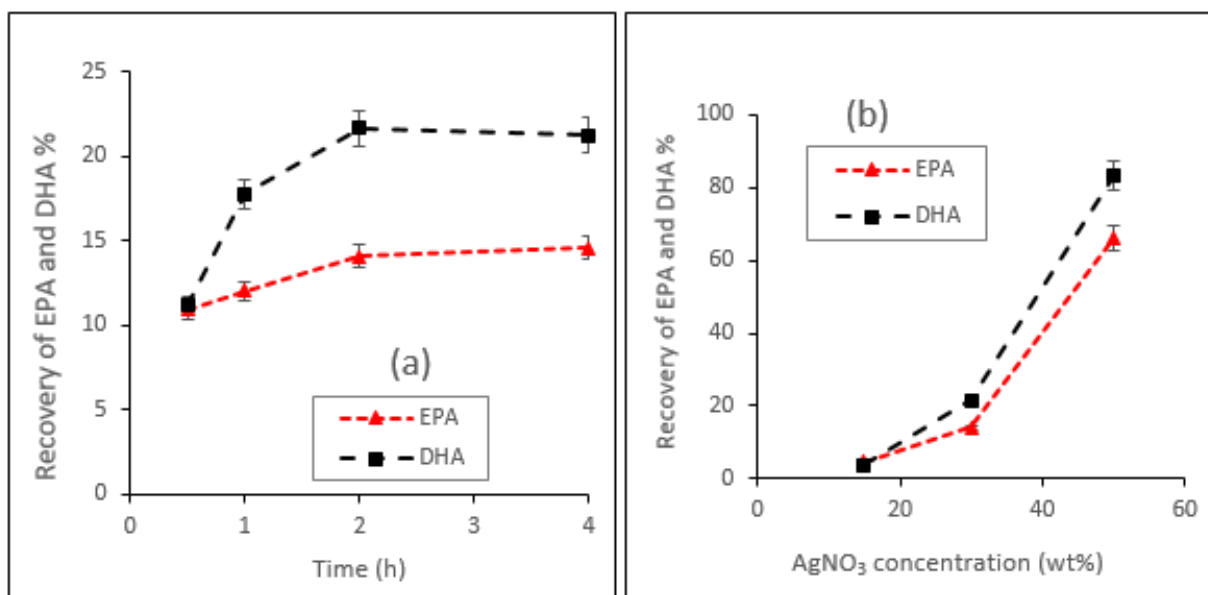


Figure 4.13: Effects of process parameters on EPA and DHA recovery %; (a) at different reaction times and 30 wt.% AgNO₃ concentration; (b) at different AgNO₃ concentrations and 2 h reaction time.

Figure 4.13 (b) illustrates the correlation between silver nitrate concentration and EPA and DHA extraction. The extractions of EPA and DHA mainly depended on the complexation of silver ion Ag⁺ with the polyunsaturated fatty acid double bonds (Teramoto *et al.*, 1994; Li *et al.*, 2009). Clearly, the silver nitrate concentration is an important parameter in EPA and DHA extraction. Silver nitrate concentrations were examined in the range of 15 to 50 wt.% at fixed a reaction time of 2h, based on the time required to achieve maximum equilibrium extraction in Figure 4.13(a).

Clearly, the EPA and DHA extraction increased rapidly with the silver nitrate concentration. It was observed that a sharp increase in EPA and DHA recovery occurred above 30 wt.% silver nitrate concentration, reaching 66.2% EPA and 83.4% DHA extractions at 50 wt.% silver nitrate concentration. Increasing the silver nitrate concentration above 50 wt.% was not possible at the operating conditions, as this exceeded the solubility limit, which is 256 g per 100 mL water at 25 °C and 1 atm (Seidell, 1919).

The observed trends of AgNO₃ concentration on EPA and DHA were dependent on the number of double bond complexations. The complexation of Ag⁺ increased with the degree of unsaturation in the fatty acid chain. The composition of the extracted PUFAs showed that there was substantially higher extraction of DHA. The higher degree of DHA extraction compared to EPA could be explained by the number of double bonds, which is higher in DHA (n = 6) than in EPA (n = 5) (Teramoto *et al.*, 1994; Li *et al.*, 2009b).

The results derived from this study should now be compared with the most common techniques used in the industry for EPA and DHA extraction—including molecular distillation, supercritical extraction technology and supercritical fluid chromatography. The molecular distillation achieved 50-60% recovery of EPA and DHA from (18/12EE) fish oil ethyl ester (Lembke, 2013b). However, this process requires relatively high operating temperatures of 140-170°C (Lembke, 2013b), which can result in degradation of EPA and DHA due to thermal stress (Nakano *et al.*, 1996).

Furthermore, Lemhke (1997) reports that fish oil processed using the molecular distillation method could suffer up to 350% higher thermal stress than fish oil processed using the supercritical fluid extraction method (Lemhke, 1997). However, the main advantage of molecular distillation is the low investment cost in comparison to the supercritical fluid extraction method. The high cost associated with supercritical fluid extraction is mainly due to the cost of pressurising both the fish oil and the CO₂ to achieve supercritical conditions—73 bar (~1070 psig) and temperatures of ~32°C (Shahidi and Wanasundara, 1998).

Supercritical fluid extraction using CO₂ achieved 96.4% recovery of omega-3 rich oil obtained from the by-products of the fish industry in 3h and under the following extraction conditions: 25 MPa, 40°C and around 13.75 kg CO₂/h (Rubio-Rodríguez *et al.*, 2008). Omega-3 PUFA from fish oil can be separated at the bench scale from an ester mixture, with 90% purity of EPA, using silica gel as a stationary phase and supercritical chromatography with SC-CO₂ as a mobile phase (Pettinello *et al.*, 2000).

The advantage of the supercritical fluid chromatography technique is the moderate working temperatures in the range of 40-50°C. These low temperatures prevent thermal stress on EPA and DHA, which makes supercritical fluid chromatography one of the most appropriate technologies for the concentration of polyunsaturated fatty acids. However, it has the same disadvantage as supercritical fluid extraction—high pressure requirements, which necessitate high investment costs (Nakano *et al.*, 1996).

Clearly, the aqueous silver nitrate method for extracting EPA and DHA offers advantages over molecular distillation due to the mild operating temperatures and the suitability of large scale production (Lembke, 2013b). Moreover, the investment cost of silver nitrate extraction is much lower than either supercritical extraction technology or supercritical fluid chromatography because of the process's simplicity and moderate operating temperature and pressure (up to 30°C and 1 bar) (Lembke, 2013b).

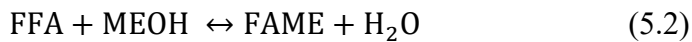
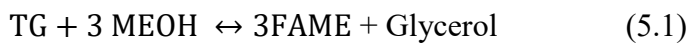
However, the major challenge in commercial applications of this process for EPA and DHA extraction is the cost of AgNO_3 and the requirement to recycle the silver nitrate from the aqueous solutions after the de-complexation process in order to reduce the cost of materials. There are several methods for silver nitrate recovery, including multi-effect evaporation, electrochemical oxidation using copper electrode, and the chemical reaction method using sodium hydroxide and nitric acid (Shanmugam *et al.*, 2015).

Chapter 5 Techno-economic Analysis

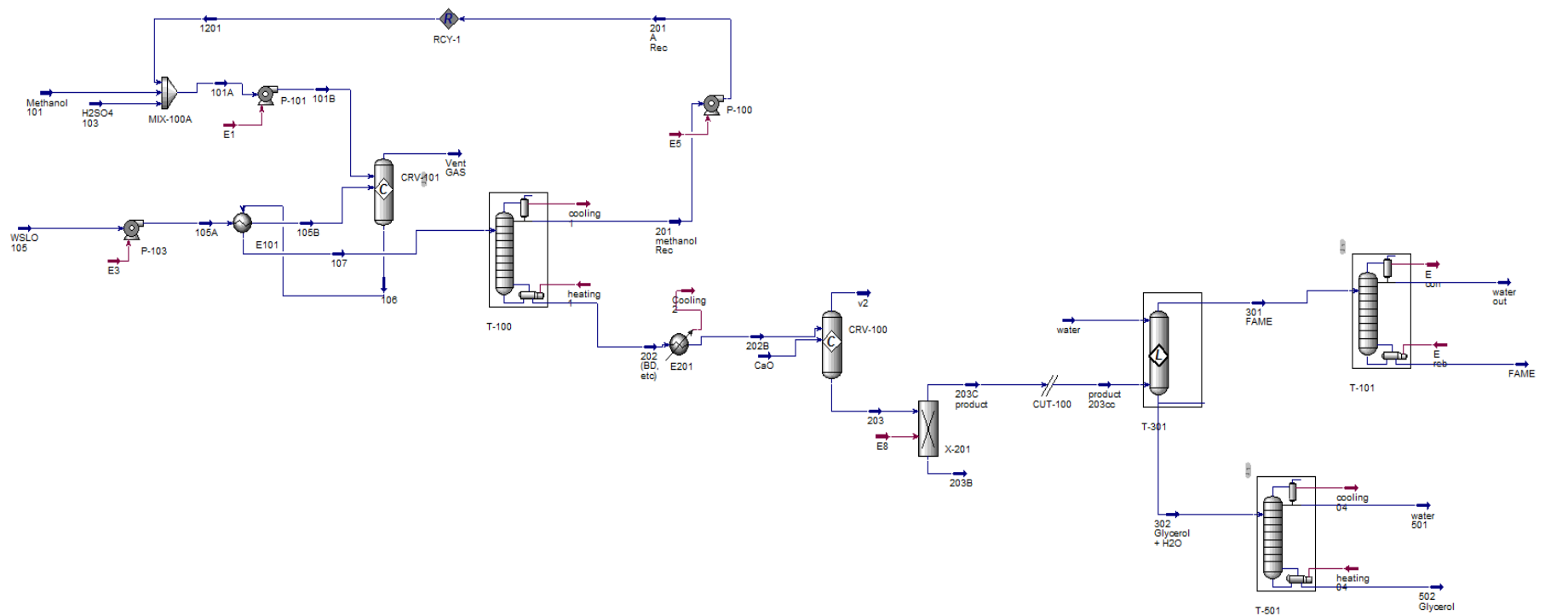
Techno-economic analysis (TEA) is a vital tool for assessing the economic feasibilities of a project or an investment. In this study, TEA was used to assess the commercial feasibility of the proposed process for biodiesel production from WSLO, compared with conventional biodiesel production from refined vegetable oil (rapeseed oil). Aspen HYSYS-V9 was used to simulate both plants. The process simulations for both plants were based on the plant' biodiesel production capacity of 12,000 te/y. Non-random two liquid (NRTL) is the fluid package selected in this case due to the presence of polar components such as methanol and glycerol (Gess *et al.*, 1991).

5.1 Process Description

Process simulation steps primarily involve defining chemical components, choosing a thermodynamic model, defining the plant capacity, selecting the operating units, and setting up the charge conditions such as flowrate, temperature, and pressure. The simulated process flow sheet of acid-catalysed transesterification of WSLO for the production of biodiesel with the stream composition is illustrated in . The reactions involved in this process are shown in Equations 5.1 and 5.2. The reaction was performed with a methanol-to-oil molar ratio of 10.3:1, 6.5 h reaction time, 60 °C reaction temperature, and 5.9 wt% H₂SO₄ catalyst concentration. The glycerides (TG, DG and MG), free fatty acid, biodiesel, glycerol, water and H₂SO₄ were as defined in the components list in Aspen HYSYS-V9 as triolein, oleic acid, m-oleate, glycerol, H₂O, and H₂SO₄, respectively.



Where, TG=Triglycerides, FAME=Fatty acid methyl ester, MEOH=Methanol, FFA=Free Fatty acid.

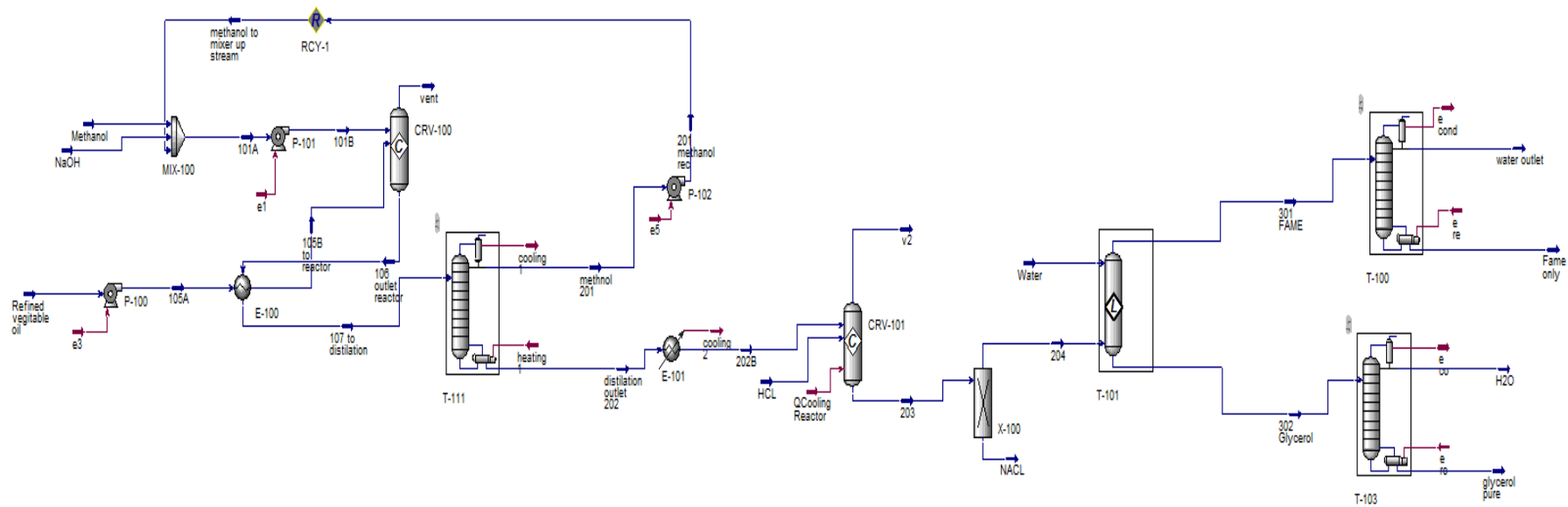


Stream Name	101	105	103	105B	106	101B	201	202	202B	203C	301 FAME	501	502	Water out	FAME pure	Oil	
Temperature [C]	0.00	0.00	0.00	0.00	0.00	0.00	0.00	0.00	0.00	0.00	0.00	0.00	0.00	1.00	0.00	0.00	
Pressure [kPa]	25.00	25.00	25.00	60.00	100.11	43.59	64.73	240.50	60.00	60.00	55.17	99.99	239.68	286.56	286.56	331.71	
Molar Flow [kgmole/h]	101.32	101.32	101.32	400.00	400.00	400.00	101.32	101.32	101.30	130.00	101.30	101.30	101.30	101.30	101.30	70.00	
Mass Flow [kg/h]	4.66	1.81	6.90	1.81	24.01	22.20	10.64	13.37	13.37	10.95	3.90	76.53	0.30	0.17	3.72	0.01	
Components mole fraction																	
(Triolein)	0.00	0.80	0.00	0.80	0.00	0.00	0.00	0.00	0.00	0.00	0.00	0.00	0.00	0.00	0.00	0.00	0.08
(Methanol)	1.00	0.00	0.00	0.00	0.44	0.68	0.98	0.00	0.00	0.00	0.00	0.00	0.00	0.00	0.00	0.00	0.00
(M-Oleate)	0.00	0.00	0.00	0.00	0.19	0.00	0.00	0.35	0.35	0.34	0.96	0.00	0.00	0.24	0.99	0.92	
(Glycerol)	0.00	0.00	0.00	0.00	0.06	0.00	0.00	0.11	0.11	0.03	0.00	0.00	0.95	0.00	0.00	0.00	
(H ₂ SO ₄)	0.00	0.00	1.00	0.00	0.29	0.31	0.00	0.52	0.52	0.00	0.00	0.00	0.00	0.00	0.00	0.00	
(H ₂ O)	0.00	0.00	0.00	0.00	0.02	0.01	0.02	0.03	0.03	0.63	0.04	1.00	0.05	0.76	0.01	0.00	
(OleicAcid)	0.00	0.20	0.00	0.20	0.00	0.00	0.00	0.00	0.00	0.00	0.00	0.00	0.00	0.00	0.00	0.00	

Figure 5.1: Process flow sheet for acid-catalysed transesterification of WSLO for the production of biodiesel

The simulated process flow sheet for conventional biodiesel production using alkali-catalysed transesterification of refined vegetable oil with the stream composition is shown in . The reaction was conducted with a methanol-to-oil molar ratio of 6:1, 1 h reaction time, 60 °C reaction temperature and 1.5 wt.% NaOH catalyst concentration. The triglycerides, biodiesel, glycerol, water, NaOH, HCl, and NaCl was as defined in the components list in Aspen HYSYS-V9 as triolein, m-oleate, glycerol and H₂O, NaOH, HCl, and NaCl, respectively. The reaction conversion for both plants was assumed to be 99%.

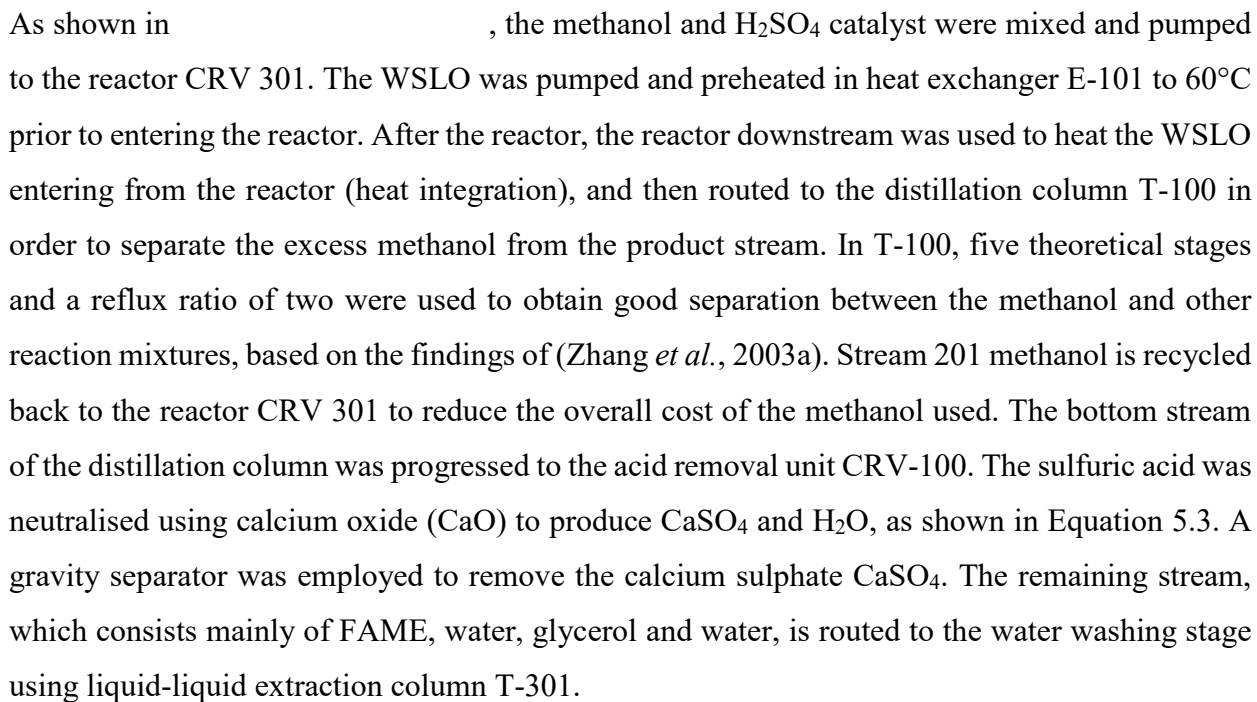
The determination of plant capacity for the biodiesel production from WSLO was based on the reported availability of shark liver oil in Oman. Total shark landings by species for all governorates in Oman during 2016 was 7,507 tonnes (Ministry of Agriculture and Fisheries, 2014). Since, as noted, a shark's liver comprises 25-30% of its body weight (Popa *et al.*, 2015c), around 2,000 te/y is the amount of shark liver oil in Oman. Assuming this statistic is applicable to the neighbouring six Gulf countries, around 12,000 te/y is the proposed plant capacity. For the sake of comparison, the same capacity was used for the conventional biodiesel process using refined vegetable oil.

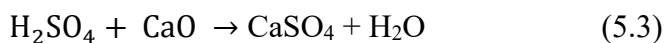


Stream Name	RS Oil	Methanol	NaOH	105B	101B	107	201	202	202B	203	204	301	302	Glycerol pure	H2O	water outlet	Fame only
Temperature [C]	0.00	0.00	0.00	0.00	0.00	0.00	0.00	0.00	0.00	0.00	0.00	0.00	0.00	0.00	0.00	0.00	0.00
Pressure [kPa]	25.00	25.00	25.00	60.00	62.77	72.78	64.73	323.25	25.00	30.00	30.00	40.92	1.97	239.68	99.99	164.11	346.11
Molar Flow [kgmole/h]	101.30	101.30	101.30	400.00	400.00	350.00	101.30	101.30	101.30	101.30	101.30	101.30	102.00	101.30	101.30	101.30	105.00
Mass Flow [kg/h]	1.55	6.24	0.52	1.55	124.86	126.40	119.76	6.65	6.65	7.17	6.65	4.83	12.81	1.59	11.22	1.50	3.33
components mole fraction																	
(Triolein)	1.00	0.00	0.00	1.00	0.00	0.00	0.00	0.00	0.00	0.00	0.00	0.00	0.00	0.00	0.00	0.00	0.00
(Methanol)	0.00	1.00	0.00	0.00	0.99	0.94	0.99	0.00	0.00	0.00	0.00	0.00	0.00	0.00	0.00	0.00	0.00
(M-Oleate)	0.00	0.00	0.00	0.00	0.00	0.04	0.00	0.69	0.69	0.64	0.69	0.95	0.00	0.00	0.00	0.85	1.00
(Glycerol)	0.00	0.00	0.00	0.00	0.01	0.02	0.01	0.23	0.23	0.21	0.23	0.00	0.12	0.95	0.00	0.00	0.00
(H2SO4)	0.00	0.00	0.00	0.00	0.00	0.00	0.00	0.00	0.00	0.00	0.00	0.00	0.00	0.00	0.00	0.00	0.00
(NaOH)	0.00	0.00	1.00	0.00	0.00	0.00	0.00	0.08	0.08	0.00	0.00	0.00	0.00	0.00	0.00	0.00	0.00
(H2O)	0.00	0.00	0.00	0.00	0.00	0.00	0.00	0.00	0.00	0.07	0.08	0.05	0.88	0.05	1.00	0.15	0.00

Figure 5.2: Process flow sheet for conventional biodiesel production (alkali-catalysed process) from refined vegetable oil

5.1.1 Acid-Catalysed Transesterification of WSLO to Biodiesel

As shown in , the methanol and H₂SO₄ catalyst were mixed and pumped to the reactor CRV 301. The WSLO was pumped and preheated in heat exchanger E-101 to 60°C prior to entering the reactor. After the reactor, the reactor downstream was used to heat the WSLO entering from the reactor (heat integration), and then routed to the distillation column T-100 in order to separate the excess methanol from the product stream. In T-100, five theoretical stages and a reflux ratio of two were used to obtain good separation between the methanol and other reaction mixtures, based on the findings of (Zhang *et al.*, 2003a). Stream 201 methanol is recycled back to the reactor CRV 301 to reduce the overall cost of the methanol used. The bottom stream of the distillation column was progressed to the acid removal unit CRV-100. The sulfuric acid was neutralised using calcium oxide (CaO) to produce CaSO₄ and H₂O, as shown in Equation 5.3. A gravity separator was employed to remove the calcium sulphate CaSO₄. The remaining stream, which consists mainly of FAME, water, glycerol and water, is routed to the water washing stage using liquid-liquid extraction column T-301.



The main purpose of the water washing stage is to separate the FAME from glycerol and water. Water was added as a solvent to wash the FAME in four theoretical stages in the liquid-liquid extraction column. The same stages were used to separate FAME from glycerol and water, based on the findings of (Connemann and Fischer, 1998).

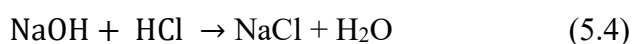
In order to obtain a final biodiesel product adhering to ASTM specifications (more than 96.5% purity), a FAME distillation column with five theoretical stages and a reflux ratio of two were employed. The distillation column was operated under vacuum to reduce thermal stress and avoid FAME degradation. Water was removed from the FAME and the final FAME purity was 99.93%.

The bottom stream of the water washing unit, which consists of glycerol and water, is forwarded to the glycerol purification distillations column T-501. The distillation column consists of five theoretical stages and a reflux ratio of two. The glycerol was separated from water with 99.0% purity.

5.1.2 Alkali-Catalysed Transesterification of Refined Vegetable Oil

The simulated process flow sheet for the conventional biodiesel production using alkali-catalysed transesterification of refined vegetable oil is shown in . The reaction was conducted with a methanol-to-oil molar ratio of 6:1, 1 h reaction time, 60°C reaction temperature and 1.5 wt.% NaOH catalyst concentration; these are the conventional conditions used for transesterification of soybean oil (Freedman *et al.*, 1986). The triglycerides, biodiesel, glycerol, water, NaOH, HCl, and NaCl were as defined from the components list in Aspen HYSYS-V9 as triolein, m-oleate, glycerol, H₂O, NaOH, HCl and NaCl, respectively.

As shown in the methanol and NaOH catalyst were mixed and pumped to the reactor CRV 100. The refined vegetable oil was pumped and preheated in heat exchanger E-100 to 60°C prior to entering the reactor. After the reactor, the reactor downstream was utilised to heat the incoming refined vegetable oil from the reactor and then routed to the distillation column to separate the excess methanol from the product stream. Five theoretical stages and a reflux ratio of 2 were used to separate the methanol and other reaction mixtures in the distillation column. The methanol was then recycled back to the reactor CRV 100 in order to reduce the overall cost, as indicated previously. The bottom stream of the distillation column was then transferred to the alkali neutralisation reactor. The NaOH was neutralised using HCl to produce NaCl and H₂O, as shown in Equation 5.4. Next, a gravity separator removed the sodium chloride NaCl, and the remaining stream consisting mainly of FAME, water, glycerol and water, was then routed to the water washing stage using the liquid-liquid extraction column.



The main purpose of the water washing stage is to separate the FAME from glycerol and water. Water was added as a solvent to wash the FAME in four theoretical stages in a liquid-liquid extraction column. The FAME purity achieved after this stage was 99.6%. However, because the content of water was at this point more than the maximum allowable water content for biodiesel, as per the ASTM standards ($\leq 0.05\%$), further purification of the FAME was required. To obtain a final biodiesel product which adhered to ASTM specifications, a FAME distillation column with five theoretical stages and a reflux ratio of two were employed. The distillation column was operated under vacuum to reduce thermal stress and avoid FAME degradation. Water was removed from the FAME and the final FAME purity was 99.87%. The bottom stream of the water washing unit consisting of glycerol and water is forwarded to the glycerol purification distillations column. The distillation column consists of five theoretical stages and a reflux ratio of two. The glycerol was separated from water with 99.0% purity.

5.2 Economic Analysis

The purpose of this economic analysis is to assess the profitability of the acid-catalysed biodiesel plant using WSLO and compare it with the conventional biodiesel production using refined vegetable oil (rapeseed oil) with an alkali catalyst. The economic analysis was based on the following assumptions:

- (i) A biodiesel plant production capacity of 12,000 te/y;
- (ii) A plant life time of 20 years;
- (iii) An operation of 100% of the plant capacity all the time;
- (iv) A discount rate of 15%;
- (v) Raw material/feedstock (waste shark liver oil) costs mainly associated with the logistic cost.

The plant life time, discount rate and plant operation are assumed based on a similar biodiesel production plant using palm oil (Zhang *et al.*, 2003a).

Table 5.1 presents a summary of the materials and chemicals used to produce the biodiesel, and utilities such as heating energy and cooling water. The cost of the utilities is based on the cost of heating and cooling.

Table 5.1: A summary of the raw materials used to produce biodiesel, and utilities including heating energy and cooling water

Materials/Chemicals	Price US \$/tonne	Reference
Methanol	428	(Methanex, 2018)
Biodiesel	1250	(NESTE, November 2018)
Waste shark liver oil (WSLO transport and collection)	400	Based on local survey and fishermen in OMAN Alalawi, K. (2019)
Refined vegetable oil (Rapeseed oil)	840	(NESTE, November 2018)
Glycerol	125	AliBaba.com (1)
Sulfuric acid H ₂ SO ₄	200	AliBaba.com (2)
CaO Calcium oxide	100	AliBaba.com (3)
Sodium hydroxide NOH (99% purity)	400	AliBaba.com (4)
Hydrochloric acid HCl	200	AliBaba.com (5)
Utilities	Acid-catalysed process	Alkali-catalysed process
Heating	10.3 US \$/h	9.87 US \$/h
Cooling water	16.2 US \$/h	8.96 US \$/h

Table 5.2 compares the results obtained from the simulation of the acid and alkali processes. The conversion used in both cases is 99%, and the same amounts of biodiesel were produced from both processes, since the same quantity of feedstock was used. Clearly, the quantity of glycerol produced in the alkali process is higher than the glycerol produced from the acid catalyst. This is because the feedstock (rapeseed oil) for the alkali process contains 99% TG, and therefore with an alkali catalyst and alcohol it predominantly produces FAME and glycerol. However, since WSLO contains less TG (~44%), it produces less glycerol. Furthermore, as WSLO contains more FFA (~20%), this gives FAME and water. The simulation results are shown in Table 5.2.

Table 5.2: Material balance and process conditions

Item	Conditions	
	Acid process plant (WSLO)	Alkali process plant (vegetable oil)
Process condition		
Temperature (°C)	60	60
Pressure (kPa)	101.3	101.3
Molar ratio	10.3:1	6:1
Conversion (%)	99	99
Material flow input		
Waste shark liver oil/rapeseed oil	1370	1370
Make up methanol (kg/h)	232.31	200.8
Recycling methanol (kg/h)	365.89	100.8
Catalyst (kg/h)	81.6	13.84
Catalyst neutralising agent (kg/h)	46.6	12.6
Washing water (kg/h)	230.0	198
Product		
Biodiesel (kmol/h)	4.6	4.6
Glycerol (kmol/h)	0.3	1.55

Total capital investment (TCI) in biodiesel production consists of the total equipment cost, installation costs, and other indirect costs (such as engineering, construction, contractors, and contingency costs). The production costs include those of total raw materials added to the total operation and maintenance costs. Overall utilities costs and the revenue generated from biodiesel and glycerol were calculated based on the quantity of product and the selling price. Table 5.3 shows the total capital investment, and costs of utilities and production, as obtained from Aspen HYSYS-V9. Net present value (NPV) is a useful tool to determine the profitability of a project or investment. A positive NPV shows a profit, while a negative NPV indicates a loss. It is calculated based on the difference in the present value of cash inflow and outflow over a period of time. Table 5.3 shows a positive NPV of US \$34.8 and US \$4.9 million for the acid-catalysed process and alkali-catalysed process, respectively.

Internal rate of return (IRR) is a discount rate that makes the NPV of all cash flow equal to zero. IRR is used to evaluate the profitability of potential investments. The IRR in this project was calculated to be 260% for the acid-catalysed WSLO process and 56% for the alkali-catalysed vegetable oil process. It is clear that the acid-catalysed process is more attractive than the alkali-catalysed process due to the higher IRR% of the acid-catalysed process. The break-even price is the minimum selling price required to have a positive NPV for the process. The break-even price for the biodiesel obtained from the acid-catalysed WSLO process is 600.3 US \$ /te. In other words, the minimum price for selling biodiesel and making a profit is 600.3 US \$/te. If the selling price is lower than this, the project is not profitable. The break-even price for the biodiesel obtained from the alkali-catalysed process is US \$1,100 which is US \$150 lower than the current market price of biodiesel (Neste, November 2018).

Considering all the results obtained from the economic analysis, it is clear that producing biodiesel from WSLO using an acid catalyst and with a plant capacity of 12,000 te/y is more profitable and attractive than the alkali-catalysed process. The main factor in the economic analysis in both processes is the fact that WSLO is a waste. These results are in line with the literature, which shows that the use of cheap, non-edible feedstocks such as waste oils improves the production costs and makes the process economically viable (Banković-Ilić *et al.*, 2012). The other advantage of this acid-catalysed process is the lower methanol-to-oil ratio of 10.3:1 in comparison to the typical acid-catalysed transesterification alcohol-to-oil molar ratio of 30:1. The lower molar ratio contributes effectively to the economics in comparison to the high molar ratio of methanol, which requires a larger reactor and consequently consumes more heat duties for the complete conversion.

Table 5.3: Economic analysis for the biodiesel production capacity of 12000 te/y

Item	Cost in US \$ millions	
	Acid-catalysed plant (WSLO)	Alkali-catalysed plant (vegetable oil)
Total capital investment	2.07	1.98
Utilities cost	0.22	0.17
Revenue from biodiesel	12.01	12.01
Revenue from glycerol	0.05	0.27
Production costs	6.06	11.1
Net annual profit	6.0	1.18
NPV (20 y)	34.8	4.9
IRR (% , 20 y)	260	56

The techno-economic analysis results obtained from alkali catalysed transesterification of vegetable oil and acid catalysed transesterification of WSLO for biodiesel production plant are compared with a techno-economic analysis study conducted by Sakdarsi *et al* (2018), for biodiesel production from palm oil with supercritical methanol (SCM) at low molar ratio and plant capacity of 40,000 te/y (Sakdasri *et al.*, 2018). The process was simulated under a continues flow process to meet the requirement of an industrial production plant. The SCM process has been successfully investigated for a good quality biodiesel production that meet both the ASTM (D6751) and EN (14214) biodiesel standards (Sakdasri *et al.*, 2016). The study were conducted in both a batch and continuous reactor. Biodiesel was produced at the optimal condition of 400 °C reaction

temperature, 15 MPa reaction pressure and a methanol: oil molar ratio of 12:1 (Sawangkeaw *et al.*, 2011). The process flow sheet of the biodiesel production plant from palm oil with supercritical methanol at low molar ratio is shown in Figure 5.3.

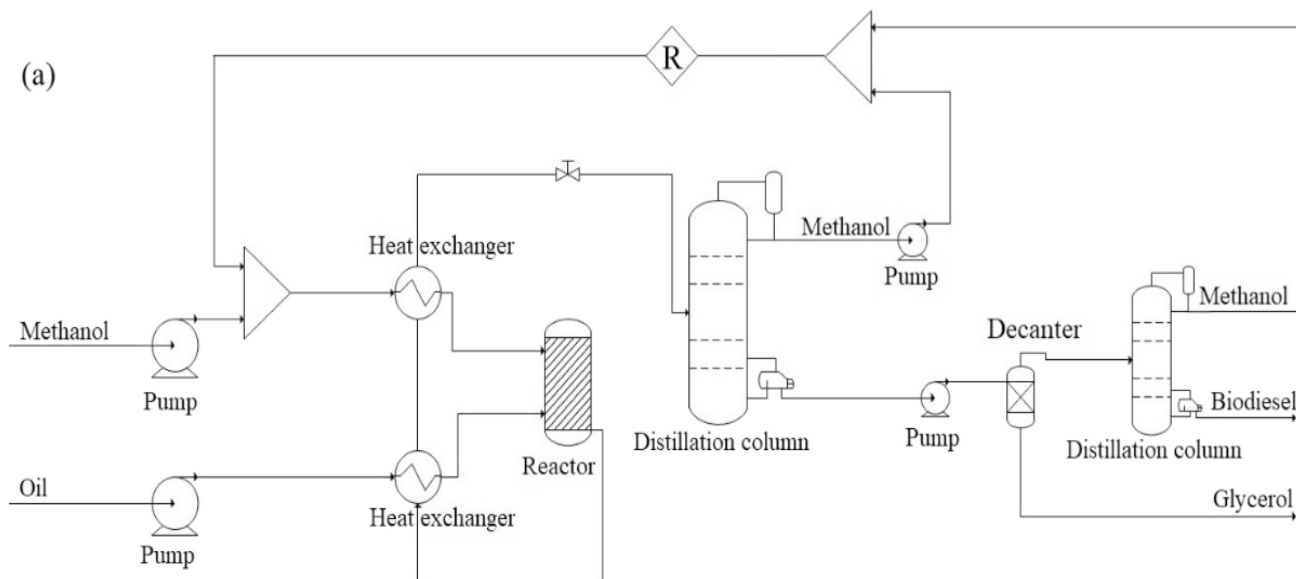


Figure 5.3 Process flow sheet of biodiesel production plant from palm oil with supercritical methanol at low molar ratio (Sakdasri *et al.*, 2018).

The reaction conditions for the SCM process were obtained from literature based on a similar studies. The SCM process reaction temperature was 300 °C and reaction pressure of 20 MPa and a methanol : oil molar ratio of 42:1(Saka and Kusdiana, 2001). The palm oil and methanol were separately fed into the supercritical reactor by two high-pressure pumps at 25°C and 1 bar (Sakdasri *et al.*, 2018). Both streams were heated by heat exchangers and pressurised to the required pressure of 20 MPa before entering the reactor. Palm oil and methanol streams were mixed and converted to their respective products in the reactor at reaction temperature of 300°C. After that, the liquid product stream was routed to the heat exchangers in order to preheat the feeds (Sakdasri *et al.*, 2018). The excess methanol from the product stream was separated using a distillation column, which was recycled to the process in order to reduce the overall cost of methanol. A decanter was employed to separate the glycerol as a by-product. Finally, the product stream was introduced to a distillation column to remove the trace amounts of residual methanol (Sakdasri *et al.*, 2018). The economic analysis of biodiesel production from palm oil using SCM was investigated for a three different plant capacities (10,000 te/y, 40,000 te/y and 100,000 te/y) as shown in Table 5.4

Table 5.4: The economic analysis results for biodiesel production from palm oil using SCM process with different plant capacities in US\$ millions (Sakdasri *et al.*, 2018).

Item	Capacity (te/y)		
	10,000	40,000	100,000
Total capital investment cost (TCI)	\$3.66	\$7.19	\$11.41
Total manufacturing cost	\$8.95	\$37.28	\$91.24
Net annual profit	\$0.43	\$9.57	\$25.43
Payback period (y)	–	2.39	2.26
NPV (20 y)	-\$1.36	\$45.48	\$127.18
IRR (% , 20 y)	–6.86%	31.61%	45.74%
Break-even prices (\$/tonne)	\$1047.08	\$840.68	\$816.45

Comparing the economic analysis results for the acid catalysed transesterification of WSLO shown in Table 5.3 with the economic analysis results of the biodiesel production from palm oil using SCM in Table 5.4. It is clear that, acid catalysed transesterification of WSLO for plant capacity of 12,000 te/y was profitable with NPV of 34.8 US\$ millions while the SCM process for a relatively similar plant capacity (10,000 te/y) was not profitable with NPV of -1.36 US\$ millions (Sakdasri *et al.*, 2018). However, for a higher plant capacity of 40,000 te/y and 100,000 te/y, it appeared to be feasible from the economic point of view with NPV of 45.48 and 127.18 US\$ millions respectively as shown in Table 5.4 (Sakdasri *et al.*, 2018).

The TCI for the small plant (10,000 te/y) was higher than the medium and large plants as the TCI is directly correlated to the equipment cost. The TCI were 40.89%, 19.29%, and 12.51% of the total production cost for the capacity of 10,000, 40,000, and 100,000 te/y, respectively. In addition to the TCI, it leads to a rise in the maintenance cost, operating cost, depreciation and plant overhead cost, thus, the small plant consequently ran into a deficit. This conclusion is in line with a similar results reported elsewhere (Van Kasteren and Nisworo, 2007) where the operating labour, maintenance, and overhead were major cost contribution to the biodiesel production from waste cooking oil in supercritical transesterification (Van Kasteren and Nisworo, 2007).

5.3 Sensitivity Analysis

A sensitivity analysis was conducted to show the effect of the variables on the NPV of the biodiesel production plant from WSLO using an acid catalyst, and a biodiesel production plant from rapeseed oil using an alkali catalyst. The variables tested in this study are the price of methanol, WSLO, and rapeseed oil, and the selling price of biodiesel and glycerol based on a plant life of 20 years. The degree of variation of all these variables was between -50% and 50% of the original values which is the NPV at zero year and same as the investment cost. The 0% price variation is meant to be the investment cost or the NPV at zero year. Figure 5.4 (a) and (b) show the change in the NPV as a function of the WSLO, rapeseed oil, and methanol purchase prices. Clearly, the variation in rapeseed oil is more sensitive than the variation in WSLO prices, due to the low price of the WSLO, which is mainly associated with the logistics cost. The NPV for the alkali process using rapeseed oil decreased by US \$6.2 million with every 10% increase in the rapeseed oil price. However, the NPV for the WSLO process was less sensitive and decreased US \$2.9 million with every 10% increase in the WSLO price.

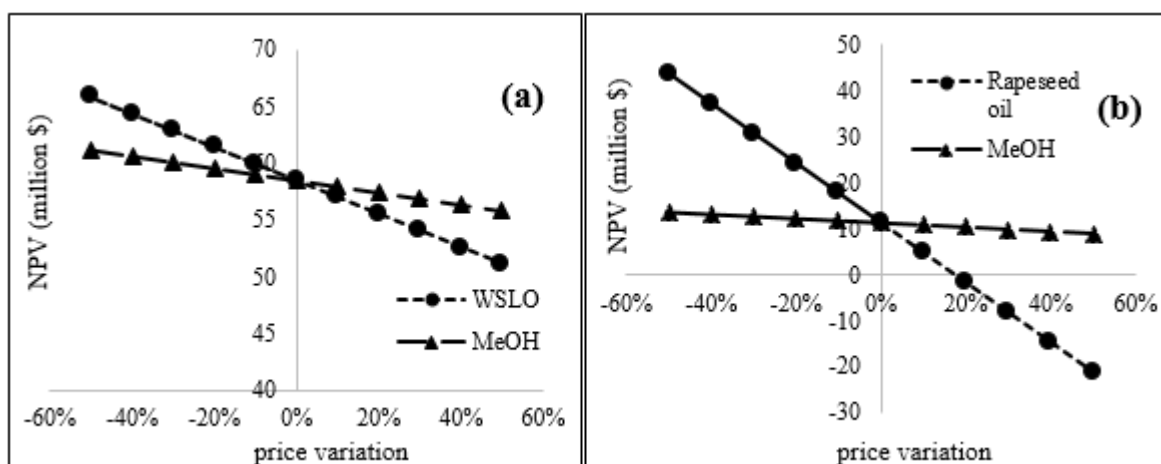


Figure 5.4: The change in the NPV as functions of the purchase prices of (a) WSLO and methanol (b) rapeseed oil and methanol

Furthermore, a 10% increase in the methanol price resulted in a reduction in NPV, as the price increased by US \$0.54 million for the acid-catalysed process and US \$0.46 million for the alkali-catalysed process. Thus, rapeseed oil price has the most significant effect on NPV in comparison to the variation in methanol price. As shown in Figure 5.4(b), an increase in rapeseed oil price of 20% or more will cause the process to run at a deficit, but a 50% variation in WSLO price will not result in a loss.

Clearly, Figure 5.5 shows the change in the NPV as functions of the biodiesel and glycerol selling prices for the acid- and alkali-catalysed process. The NPV was sensitive to the biodiesel selling price, since biodiesel is the main product in the process and plays a significant role in its economics. The NPV increased US \$7.4 million with every 10% increase in the biodiesel selling price. In addition, the effect of a 10% glycerol variation was US \$0.03 million for the acid-catalysed process and US \$ 0.17 for the alkali-catalysed. The effect of a glycerol price variation on NPV is more significant for the alkali process than the acid due to the higher amount of glycerol produced from the alkali process using rapeseed oil, which is mainly triglycerides.

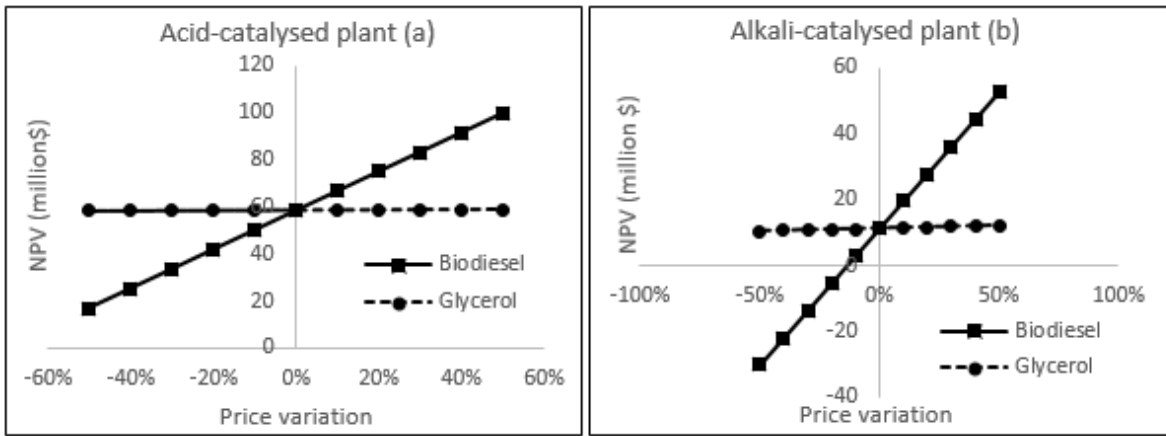


Figure 5.5: The change in the NPV as functions of the biodiesel and glycerol selling prices for (a) the acid-catalysed plant using WSLO, and (b) the alkali-catalysed plant using vegetable oil (rapeseed oil)

It can be clearly noticed that the biodiesel selling price has more influence on the NPV in comparison to the glycerol variation prices. Moreover, the sensitivity analysis as shown in Figure 5.4 and Figure 5.5 gives an idea of the minimum selling price required to have a positive NPV for the process, which is known as the break-even price. The break-even price for producing biodiesel from the acid-catalysed WSLO process was 600.3 US \$/te, and 1,100 US \$/te for the alkali-catalysed rapeseed oil process.

5.4 Summary

The feedstock purchase price has the largest influence on the economics of the two processes. These results are in line with the literature, which shows that the cost of feedstock accounts for 70–95% of total biodiesel production costs (Banković-Ilić *et al.*, 2012). This has caused increasing research interest in the use of cheap, non-edible feedstocks, such as waste oils, to improve production costs and make the process economically viable. Taken together, the economic analysis suggests that producing biodiesel from WSLO using an acid catalyst at a plant capacity of 12,000 t/y is more profitable and attractive than an alkali-catalysed process. However, the limited supply of WSLO in one location is the main downside of this process.

Chapter 6 Conclusions and Further Work

6.1 Conclusions

The main goal of this project was to identify an efficient and cost-effective technique for converting WSLO to biodiesel, whilst producing high added value co-products of squalene, eicosapentaenoic acid (EPA), and docosahexaenoic acid (DHA). The high price of biodiesel compared to the petroleum-based diesel is the main challenge for biodiesel production. Currently, the biodiesel market is based on subsidies, and the cost of biodiesel is predominantly a function of the feedstock cost rather than the processing costs. Therefore, the use of cheap, non-edible feedstock such as WSLO should reduce the cost and make biodiesel production economically viable.

This research has shown that the conventional method of biodiesel production, homogeneous alkali-catalysed (NaOH) transesterification, was ineffective at converting WSLO to FAME due to the high FFA content. Instead, it has been demonstrated here that acid-catalysed (H_2SO_4) transesterification of the WSLO is technically feasible. Furthermore, the FAME conversions increased with the methanol-to-oil molar ratio, reaction time and catalyst concentration, reaching a maximum of $99.0 \pm 1.1\%$, achieved at 10.3 molar ratio, 6.5 h and 5.9 wt. % of H_2SO_4 acid catalyst. It was also demonstrated that WSLO can be converted to biodiesel using existing biodiesel processing technologies, and that squalene, EPA and DHA can be extracted.

Squalene is a value-added product obtainable from WSLO, and is used in various cosmetic applications as well as being an adjuvant in vaccines, including the pandemic H_1N_1 vaccine. Saponification extraction can achieve $101.6 \pm 1.3\%$ squalene recovery (at 20:1 alcohol to oil, 5 min reaction time and 9.9 wt. % water loading).

Aqueous silver nitrate (AgNO_3) was employed for extractions of EPA and DHA from fatty acid ethyl esters produced from the WSLO. The extractions of the EPA and DHA depended on the complexation of silver ion Ag^+ with the poly-unsaturated fatty acid double bonds. Extraction was carried out by mixing aqueous silver nitrate with the FAEE produced from the WSLO in a ratio of 3:1 silver nitrate to FAEE. The results of this investigation for EPA and DHA extraction showed that the highest EPA and DHA recoveries occurred at 50 wt.% silver nitrate concentration, reaching 66.2 % EPA and 83.4% DHA extractions.

Techno-economic analysis was used to compare the commercial feasibilities of the acid-catalysed biodiesel production from the WSLO, with the conventional, commercial alkali-catalysed biodiesel process using refined vegetable oil (rapeseed oil). Aspen HYSYS-V9 was used to

simulate both plants. The simulation process of acid-catalysed transesterification of WSLO for the production of biodiesel was performed with a methanol-to-oil molar ratio of 10.3:1, 6.5 h reaction time, 60 °C reaction temperature and 5.9 wt.% H₂SO₄ catalyst concentration. However, the simulated process for conventional biodiesel production using alkali-catalysed transesterification of refined vegetable oil (rapeseed oil) was conducted with a methanol-to-oil molar ratio of 6:1, 1 h reaction time, 60 °C reaction temperature and 1.5 wt.% NaOH catalyst concentration.

The NPVs were US \$34.8 and US \$4.9 million for the acid-catalysed biodiesel process from the WSLO and alkali-catalysed processes, respectively. The IRR% in this project was calculated to be 260% for the acid-catalysed process and 56% for the alkali-catalysed process. Clearly, the acid-catalysed process is more economically attractive than the alkali-catalysed due to the higher IRR% for the acid-catalysed process than the alkali-catalysed process. The break-even prices for producing biodiesel from the WSLO process was 600.3 US \$ /te, and 1,100 US \$ /te for the alkali-catalysed rapeseed oil process. The main reason the WSLO-biodiesel, by all these metrics, is so much more profitable is that the WSLO is waste, whereas rapeseed oil typically costs 840 US \$/te. The other economic advantage of this acid-catalysed process is the lower methanol-to-oil ratio of 10.3:1, in comparison to the typical acid-catalysed transesterification alcohol-to-oil molar ratio of 30:1. This reduces the operating costs by reducing the methanol recycling, capital costs, and energy duties of the larger unit's operation, including the reactor and distillation column.

Sensitivity analysis showed that the rapeseed oil process was substantially more sensitive to all of the variables than the WSLO-based process. For instance, the NPV for the alkali process using rapeseed oil decreased by US \$6.2 million with every 10% increase in the rapeseed oil price. However, the NPV for the WSLO process was less sensitive and decreased US \$2.9 million with every 10% increase in the WSLO price. A variation in the methanol price of 10% resulted in a change in the NPV of US \$0.54 million for the acid-catalysed process and US \$0.46 million for the alkali-catalysed process. Overall, the rapeseed oil price had the most significant effect on NPV. Another observation was that the biodiesel selling price had significantly more influence on the NPV than the glycerol price. This is because biodiesel is the main product and is produced at approximately five times the volume of the glycerol. Furthermore, the price of glycerol is historically low due to oversupply from the biodiesel industry worldwide. Taken together, the economic analysis suggests that producing biodiesel from WSLO using an acid catalyst at a plant capacity of 12,000 te/year is more profitable and attractive than producing biodiesel from vegetable oil using an alkali-catalysed process. Furthermore, this will become significantly more profitable if the various co-products (EPA, DHA, and squalene) are also considered.

6.2 Further Work

It is recommended that further research be undertaken in the following areas:

- I. The current research was not specifically designed to evaluate factors related to biodiesel quality. Therefore, further experimental investigations are needed to carry out biodiesel tests to meet ASTM and European biodiesel standards. These tests include but not limited to calorific value test, emission test, high cold filter plugging point (CFPP), cloud point and pour point.
- II. Systematically investigate the recovery of silver nitrate used for the extraction of the EPA and DHA from WSLO ethyl ester. Since the cost of silver nitrate is high, it is imperative to recover the silver nitrate from aqueous phase after de-complexation to reduce the cost of raw materials. There are several recovery techniques for silver nitrate from waste solution including multi-effect evaporation, electrochemical oxidation using a copper electrode, and a chemical reaction method using sodium hydroxide and nitric acid (Murphy, 1991 and Rawat, 1986).
- III. Investigate the possibility of recycling the solid “particles” and ashes obtained after the filtration of WSLO. These solid particles contains phospholipid (Debouzy *et al.*, 2008) which can be utilised as a fertiliser to improve the plant growth (Kopp *et al.*, 1996). There are several studies on valorising fish waste as fertiliser due to the high content of nutrients in the fish waste, such as N, P, and Ca (Radziemska *et al.*, 2018).
- IV. Model the biorefinery as a complete process using Aspen HYSYS and scale-up the biorefinery from laboratory to pilot plant to enable more accurate techno-economic analysis and life cycle assessment of the process. Data from such scale up could then more reliably be compared to industrial-scale and commercial processes.

References

- Abdullah, A.Z., Razali, N. and Lee, K.T. (2009) 'Optimization of mesoporous K/SBA-15 catalyzed transesterification of palm oil using response surface methodology', *Fuel Processing Technology*, 90(7), pp. 958-964.
- Al Hatrooshi, A.S., Eze, V.C. and Harvey, A.P. (2020) 'Production of biodiesel from waste shark liver oil for biofuel applications', *Renewable Energy*, 145, pp. 99-105.
- Ali, Y., Hanna, M.A. and Cuppett, S.L. (1995) 'Fuel properties of tallow and soybean oil esters', *Journal of the American Oil Chemists' Society*, 72(12), pp. 1557-1564.
- AliBaba.com 2018, *China Popular Manufacturer High Quality Glycerol For Sale - Buy Glycerol, Glycerol Manufacture, Glycerol For Sale Product on Alibaba.com.* [online] www.alibaba.com. Available at: <https://www.alibaba.com/product-detail/China-Popular-Manufacturer-High-Quality-Glycerol> [Accessed 12 Nov. 2018].
- AliBaba.com 2018, *High Purity 98% Industrial Grade Sulphuric Acid H₂SO₄ For Sale - Buy Price For High Purity 98% Industrial Grade Sulphuric Acid H₂SO₄, High Purity 98% Industrial Grade Sulphuric Acid H₂SO₄, 98% Industrial Grade Sulphuric Acid H₂SO₄ For Sale Product on Alibaba.com.* [online] www.alibaba.com. Available at: <https://www.alibaba.com/product-detail/High-Purity-98-Industrial-Grade-Sulphuric> [Accessed 12 Nov. 2018].
- AliBaba.com 2018, *High Quality Calcium Oxide With Good Price/cas No.:1305-78-8 - Buy Calcium Oxide, High Quality Calcium Oxide, Calcium Oxide With Good Price Product on Alibaba.com.* [online] www.alibaba.com. Available at: <https://www.alibaba.com/product-detail/High-Quality-Calcium-Oxide> [Accessed 12 Nov. 2018].
- AliBaba.com 2018, *Best Price Soap Paper Making Pearls Sodium Hydroxide Caustic Soda - Buy Caustic Soda For Paper Making, Caustic Soda Pearls 99%, Cheap Caustic Soda*

Pearls Product on Alibaba.com. [online] www.alibaba.com. Available at: <https://www.alibaba.com/product-detail/best-price-soap-paper-making> [Accessed 12 Nov. 2018].

AliBaba.com 2018, *Hydrochloric Acid - 33% Min - Buy Hydrochloric Acid Industry Grade & Food Grade, Hydrochloric Acid 31% To 37% Industrial Grade, Hydrochloric Acid Industry Grade & Food Grade Product on Alibaba.com*. [online] www.alibaba.com. Available at: <https://www.alibaba.com/product-detail/HYDROCHLORIC-ACID> [Accessed 12 Nov. 2018].

Amorim, H.V., Lopes, M.L., de Castro Oliveira, J.V., Buckeridge, M.S. and Goldman, G.H. (2011) 'Scientific challenges of bioethanol production in Brazil', *Applied Microbiology and Biotechnology*, 91(5), p. 1267.

Ardi, M.S., Aroua, M.K. and Hashim, N.A. (2015) 'Progress, prospect and challenges in glycerol purification process: A review', *Renewable & Sustainable Energy Reviews*, 42, pp. 1164-1173.

Atadashi, I.M., Aroua, M.K., Abdul Aziz, A.R. and Sulaiman, N.M.N. (2012a) 'The effects of water on biodiesel production and refining technologies: A review', *Renewable and Sustainable Energy Reviews*, 16(5), pp. 3456-3470.

Atadashi, I.M., Aroua, M.K., Aziz, A.R.A. and Sulaiman, N.M.N. (2012b) 'The effects of water on biodiesel production and refining technologies: A review', *Renewable and Sustainable Energy Reviews*, 16(5), pp. 3456-3470.

Atadashi, I.M., Aroua, M.K., Aziz, A.R.A. and Sulaiman, N.M.N. (2013) 'The effects of catalysts in biodiesel production: A review', *Journal of industrial and engineering chemistry*, 19(1), pp. 14-26.

Balat, M. and Balat, H. (2008) 'A critical review of bio-diesel as a vehicular fuel', *Energy Conversion and Management*, 49(10), pp. 2727-2741.

- Balat, M. and Balat, H. (2010) 'Progress in biodiesel processing', *Applied Energy*, 87(6), pp. 1815-1835.
- Banković-Ilić, I.B., Stamenković, O.S. and Veljković, V.B. (2012) 'Biodiesel production from non-edible plant oils', *Renewable and Sustainable Energy Reviews*, 16(6), pp. 3621-3647.
- Barabás, I. and Todoruț, I.-A. (2011) 'Biodiesel quality, standards and properties', in *Biodiesel-quality, emissions and by-products*. Intechopen.
- Berthod, A., Ruiz-Ángel, M.J. and Carda-Broch, S. (2009) 'Countercurrent chromatography: People and applications', *Journal of Chromatography A*, 1216(19), pp. 4206-4217.
- Bin-Mahfouz, A., Mahmoud, K. and Mourad, M. (2018) 'Influence of Biodiesel Inlet Temperature on the Performance of a Small DI Diesel Engine', *American Journal of Science and Technology*, 5(3), pp. 42-48.
- Breivik, H., Haraldsson, G.G. and Kristinsson, B. (1997) 'Preparation of highly purified concentrates of eicosapentaenoic acid and docosahexaenoic acid', *Journal of the American Oil Chemists' Society*, 74(11), pp. 1425-1429.
- Breivik, H., Thorstad, O. and Libnau, F.O. (2015) 'Process for concentrating omega-3 fatty acids'. Google Patents.
- Bura Mohanarangan, A. (2012) 'EXTRACTION OF OMEGA-3 FATTY ACIDS FROM ATLANTIC HERRING (*Clupea harengus*)'.
- Burton, R. and Biofuels, P. (2008) 'An overview of ASTM D6751: biodiesel standards and testing methods', *Alternative fuels consortium*.

- Calder, P.C. (2013) 'Omega - 3 polyunsaturated fatty acids and inflammatory processes: nutrition or pharmacology?', *British Journal of Clinical Pharmacology*, 75(3), pp. 645-662.
- Canas, B.J. and Yurawecz, M.P. (1999) 'Ethyl carbamate formation during urea complexation for fractionation of fatty acids', *Journal of the American Oil Chemists' Society*, 76(4), pp. 537-537.
- Catchpole, O.J., von Kamp, J.-C. and Grey, J.B. (1997) 'Extraction of Squalene from Shark Liver Oil in a Packed Column Using Supercritical Carbon Dioxide', *Industrial & Engineering Chemistry Research*, 36(10), pp. 4318-4324.
- Celante, D., Schenkel, J.V.D. and de Castilhos, F. (2018) 'Biodiesel production from soybean oil and dimethyl carbonate catalyzed by potassium methoxide', *Fuel*, 212, pp. 101-107.
- Chaddad, F.R. (2010) 'UNICA: Challenges to Deliver Sustainability in the Brazilian Sugarcane Industry1', *International Food and Agribusiness Management Review*, 13(4).
- Chaintreau, A. (2007) '6.2 - Analytical Methods to Determine Potentially Allergenic Fragrance-Related Substances in Cosmetics', in Salvador, A. and Chisvert, A. (eds.) *Analysis of Cosmetic Products*. Amsterdam: Elsevier, pp. 257-275.
- Chen, T.-C. and Ju, Y.-H. (2000) 'Enrichment of eicosapentaenoic acid and docosahexaenoic acid in saponified menhaden oil', *Journal of the American Oil Chemists' Society*, 77(4), pp. 425-428.
- Connemann, J. and Fischer, J. (1998) *Int. Liquid Biofuels Congress, Curitiba, Brasil*.
- Cuenot, F., Fulton, L. and Staub, J. (2012) 'The prospect for modal shifts in passenger transport worldwide and impacts on energy use and CO₂', *Energy Policy*, 41, pp. 98-106.

- Davenport, S.R.D., P. P. (1989) *Market opportunities for shark liver oil* (Accessed: 21 August).
- de Caprariis, B., Di Rita, M., Stoller, M., Verdone, N. and Chianese, A. (2012) 'Reaction-precipitation by a spinning disc reactor: Influence of hydrodynamics on nanoparticles production', *Chemical Engineering Science*, 76, pp. 73-80.
- de Lima, A.L. and Mota, C.J.A. (2019) 'Biodiesel: A Survey on Production Methods and Catalysts', in Mulpuri, S., Carels, N. and Bahadur, B. (eds.) *Jatropha, Challenges for a New Energy Crop: Volume 3: A Sustainable Multipurpose Crop*. Singapore: Springer Singapore, pp. 475-491.
- De Oliveira, F.C. and Coelho, S.T. (2017) 'History, evolution, and environmental impact of biodiesel in Brazil: A review', *Renewable and Sustainable Energy Reviews*, 75, pp. 168-179.
- Debouzy, J.-C., Crouzier, D., Lefebvre, B. and Dabouis, V. (2008) 'Study of Alkylglycerol Containing Shark Liver Oil: A Physico Chemical Support for Biological Effect?', *Drug Target Insights*, 3, p. DTI.S671.
- Deshmane, V.G. and Adewuyi, Y.G. (2013) 'Synthesis and kinetics of biodiesel formation via calcium methoxide base catalyzed transesterification reaction in the absence and presence of ultrasound', *Fuel*, 107, pp. 474-482.
- Dessimoz, A.-L., Cavin, L., Renken, A. and Kiwi-Minsker, L. (2008) 'Liquid-liquid two-phase flow patterns and mass transfer characteristics in rectangular glass microreactors', *Chemical Engineering Science*, 63(16), pp. 4035-4044.
- Diomedede, L., Colotta, F., Piovani, B., Re, F., Modest, E.J. and Salmona, M. (1993) 'Induction of apoptosis in human leukemic cells by the ether lipid 1-octadecyl-2-methyl-rac-glycero-3-phosphocholine. A possible basis for its selective action', *International Journal of Cancer*, 53(1), pp. 124-130.

- Dorado, M.P., Ballesteros, E., De Almeida, J.A., Schellert, C., Löhrlein, H.P. and Krause, R. (2002) 'An alkalai-catalyzed transesterification process for high free fatty acid waste oils', *Transactions of the American Society of Agricultural Engineers*, 45(3), pp. 525-529.
- Drake, P.L. and Hazelwood, K.J. (2005) 'Exposure-Related Health Effects of Silver and Silver Compounds: A Review', *Annals of Work Exposures and Health*, 49(7), pp. 575-585.
- Eevera, T., Rajendran, K. and Saradha, S. (2009) 'Biodiesel production process optimization and characterization to assess the suitability of the product for varied environmental conditions', *Renewable Energy*, 34(3), pp. 762-765.
- Enweremadu, C.C. and Mbarawa, M.M. (2009) 'Technical aspects of production and analysis of biodiesel from used cooking oil—A review', *Renewable and Sustainable Energy Reviews*, 13(9), pp. 2205-2224.
- Escobar, J.C., Lora, E.S., Venturini, O.J., Yáñez, E.E., Castillo, E.F. and Almazan, O. (2009) 'Biofuels: Environment, technology and food security', *Renewable and Sustainable Energy Reviews*, 13(6–7), pp. 1275-1287.
- Eze, V.C., Harvey, A.P. and Phan, A.N. (2015) 'Determination of the kinetics of biodiesel saponification in alcoholic hydroxide solutions', *Fuel*, 140, pp. 724-730.
- Eze, V.C., Phan, A.N. and Harvey, A.P. (2014) 'A more robust model of the biodiesel reaction, allowing identification of process conditions for significantly enhanced rate and water tolerance', *Bioresource Technology*, 156, pp. 222-231.
- Eze, V.C., Phan, A.N. and Harvey, A.P. (2018) 'Intensified one-step biodiesel production from high water and free fatty acid waste cooking oils', *Fuel*, 220, pp. 567-574.

- Fernández, Ó., Vázquez, L., Reglero, G. and Torres, C.F. (2013) 'Discrimination against diacylglycerol ethers in lipase-catalysed ethanolysis of shark liver oil', *Food Chemistry*, 136(2), pp. 464-471.
- Fifield, F.W. and Kealey, D. (1995) *Principles and practice of analytical chemistry*. Blackie academic & professional.
- Fiori, L., Manfrini, M. and Castello, D. (2014) 'Supercritical CO₂ fractionation of omega-3 lipids from fish by-products: Plant and process design, modeling, economic feasibility', *Food and Bioproducts Processing*, 92(2), pp. 120-132.
- Flavourtech (2009) *Omega-3 Concentrate Process Line*. Available at: http://www.flavourtech.com/Technologies/System_Process_Lines/omega-concentrate.html.
- FluidsScience (2015) *supercritical fluid extraction*. Available at: <http://eng.ege.edu.tr/~otles/SupercriticalFluidsScienceAndTechnology/bolumb/Wc34c920327cd9.htm>.
- Foutch, G. (2003) *Reactors in Process Engineering*.
- Fowler, S.L., International Union for Conservation of, N. and Natural, R. (2005) *Sharks, Rays and Chimaeras: The Status of the Chondrichthyan Fishes : Status Survey*. IUCN.
- Fox, C. (2009) 'Squalene Emulsions for Parenteral Vaccine and Drug Delivery', *Molecules*, 14(9), p. 3286.
- Freedman, B., Butterfield, R.O. and Pryde, E.H. (1986) 'Transesterification kinetics of soybean oil 1', *Journal of the American Oil Chemists' Society*, 63(10), pp. 1375-1380.

- Georgogianni, K.G., Katsoulidis, A.K., Pomonis, P.J., Manos, G. and Kontominas, M.G. (2009) 'Transesterification of rapeseed oil for the production of biodiesel using homogeneous and heterogeneous catalysis', *Fuel Processing Technology*, 90(7–8), pp. 1016-1022.
- Gerpen, J.V. (2005) 'Biodiesel processing and production', *Fuel Processing Technology*, 86(10), pp. 1097-1107.
- Gess, M.A., Danner, R.P. and Nagvekar, M. (1991) *Thermodynamic analysis of Vapor-liquid equilibria: Recommended models and a standard data base*. Design Institute for Physical Property Data, American Institute of Chemical Engineers.
- Gog, A., Roman, M., Toşa, M., Paizs, C. and Irimie, F.D. (2012) 'Biodiesel production using enzymatic transesterification – Current state and perspectives', *Renewable Energy*, 39(1), pp. 10-16.
- Gole, V.L. and Gogate, P.R. (2012) 'A review on intensification of synthesis of biodiesel from sustainable feed stock using sonochemical reactors', *Chemical Engineering and Processing: Process Intensification*, 53, pp. 1-9.
- Graham, A.S., McConvey, I.F. and Shering, P. (2001) 'An evaluation of the performance of a preparative CCC machine for the separation of an active pharmaceutical ingredient', *Journal of liquid chromatography & related technologies*, 24(11-12), pp. 1811-1825.
- Halder, P., Azad, K., Shah, S. and Sarker, E. (2019) '8 - Prospects and technological advancement of cellulosic bioethanol ecofuel production', in Azad, K. (ed.) *Advances in Eco-Fuels for a Sustainable Environment*. Woodhead Publishing, pp. 211-236.
- Hall, D.W., Marshall, S.N., Gordon, K.C. and Killeen, D.P. (2016) 'Rapid Quantitative Determination of Squalene in Shark Liver Oils by Raman and IR Spectroscopy', *Lipids*, 51(1), pp. 139-147.

- Harvey, A.P. and Lee, J.G.M. (2012) '5.12 - Intensification of Biofuel Production', in Sayigh, A. (ed.) *Comprehensive Renewable Energy*. Oxford: Elsevier, pp. 205-215.
- Helwani, Z., Othman, M.R., Aziz, N., Kim, J. and Fernando, W.J.N. (2009) 'Solid heterogeneous catalysts for transesterification of triglycerides with methanol: A review', *Applied Catalysis A: General*, 363(1–2), pp. 1-10.
- Holub, D.J. and Holub, B.J. (2004) 'Omega-3 fatty acids from fish oils and cardiovascular disease', *Molecular and Cellular Biochemistry*, 263(1), pp. 217-225.
- Hoydonckx, H.E., De Vos, D.E., Chavan, S.A. and Jacobs, P.A. (2004) 'Esterification and Transesterification of Renewable Chemicals', *Topics in Catalysis*, 27(1), pp. 83-96.
- Huong, L.M. (2007) 'Polyunsaturated fatty acid enrichment by complexation with silver ion', *Vietnam Journal of Chemistry*, 45(6), p. 757.
- Iagher, F., de Brito Belo, S.R., Souza, W.M., Nunes, J.R., Naliwaiko, K., Sasaki, G.L., Bonatto, S.J.R., de Oliveira, H.H.P., Brito, G.A.P., de Lima, C., Kryczyk, M., de Souza, C.F., Steffani, J.A., Nunes, E.A. and Fernandes, L.C. (2013) 'Antitumor and anti-cachectic effects of shark liver oil and fish oil: comparison between independent or associative chronic supplementation in Walker 256 tumor-bearing rats', *Lipids in health and disease*, 12, pp. 146-146.
- IEA (2017) 'World Energy Outlook', *world Energy Outlook* Available at: <http://www.worldenergyoutlook.org>
- Issariyakul, T., Kulkarni, M.G., Dalai, A.K. and Bakhshi, N.N. (2007) 'Production of biodiesel from waste fryer grease using mixed methanol/ethanol system', *Fuel Processing Technology*, 88(5), pp. 429-436.

- Jabado, R.W., Al Ghais, S.M., Hamza, W., Henderson, A.C., Spaet, J.L.Y., Shivji, M.S. and Hanner, R.H. (2015) 'The trade in sharks and their products in the United Arab Emirates', *Biological Conservation*, 181, pp. 190-198.
- Jähnisch, K., Hessel, V., Löwe, H. and Baerns, M. (2004) 'Chemistry in Microstructured Reactors', *Angewandte Chemie International Edition*, 43(4), pp. 406-446.
- Kim, S.-K. and Karadeniz, F. (2012) 'Chapter 14 - Biological Importance and Applications of Squalene and Squalane', in Se-Kwon, K. (ed.) *Advances in Food and Nutrition Research*. Academic Press, pp. 223-233.
- Knothe, G. (2006) 'Analyzing biodiesel: standards and other methods', *Journal of the American Oil Chemists' Society*, 83(10), pp. 823-833.
- Kole, C., Joshi, C.P. and Shonnard, D.R. (2012) *Handbook of bioenergy crop plants*. CRC Press.
- Kopp, H., Weiss, A. and Schlue, R. (1996) 'Use of phospholipids to improve plant growth', *World patent WO012685*.
- Kromann, N. and Green, A. (1980) 'Epidemiological Studies in the Upernavik District, Greenland', *Acta Medica Scandinavica*, 208(1 - 6), pp. 401-406.
- Kumar, D., Kumar, G., Poonam and Singh, C.P. (2010) 'Fast, easy ethanolsis of coconut oil for biodiesel production assisted by ultrasonication', *Ultrasonics Sonochemistry*, 17(3), pp. 555-559.
- Lam, M.K., Lee, K.T. and Mohamed, A.R. (2010) 'Homogeneous, heterogeneous and enzymatic catalysis for transesterification of high free fatty acid oil (waste cooking oil) to biodiesel: a review', *Biotechnology advances*, 28(4), pp. 500-518.

- Lee, J.-S. and Saka, S. (2010) 'Biodiesel production by heterogeneous catalysts and supercritical technologies', *Bioresource technology*, 101(19), pp. 7191-7200.
- Lembke, P. (2013a) 'Production Techniques for Omega-3 Concentrates', in De Meester, F., Watson, R.R. and Zibadi, S. (eds.) *Omega-6/3 Fatty Acids*. Humana Press, pp. 353-364.
- Lembke, P. (2013b) 'Production Techniques for Omega-3 Concentrates', in De Meester, F., Watson, R.R. and Zibadi, S. (eds.) *Omega-6/3 Fatty Acids: Functions, Sustainability Strategies and Perspectives*. Totowa, NJ: Humana Press, pp. 353-364.
- Lembke, P. (1997) 'Production of High Purity n-3 Fatty Acid-Ethyl Esters by Process Scale Supercritical Fluid Chromatography', *Supercritical Fluid Chromatography with Packed Columns: Techniques and Applications*, 75, p. 429.
- Leung, D.Y.C. and Guo, Y. (2006) 'Transesterification of neat and used frying oil: Optimization for biodiesel production', *Fuel Processing Technology*, 87(10), pp. 883-890.
- Leung, D.Y.C., Wu, X. and Leung, M.K.H. (2010) 'A review on biodiesel production using catalyzed transesterification', *Applied Energy*, 87(4), pp. 1083-1095.
- Li, M. and Li, T. (2008) 'Enrichment of Omega-3 Polyunsaturated Fatty Acid Methyl Esters by Ionic Liquids Containing Silver Salts', *Separation Science and Technology*, 43(8), pp. 2072-2089.
- Li, M., Pittman, C.U. and Li, T. (2009a) 'Extraction of polyunsaturated fatty acid methyl esters by imidazolium-based ionic liquids containing silver tetrafluoroborate—Extraction equilibrium studies', *Talanta*, 78(4), pp. 1364-1370.

- Li, M., Pittman Jr, C.U. and Li, T. (2009b) 'Extraction of polyunsaturated fatty acid methyl esters by imidazolium-based ionic liquids containing silver tetrafluoroborate—Extraction equilibrium studies', *Talanta*, 78(4-5), pp. 1364-1370.
- Lodha, H., Jachuck, R. and Suppiah Singaram, S. (2012) 'Intensified Biodiesel Production Using a Rotating Tube Reactor', *Energy & Fuels*, 26(11), pp. 7037-7040.
- Lu, H.-T., Jiang, Y. and Chen, F. (2003) 'Preparative separation and purification of squalene from the microalga *Thraustochytrium* ATCC 26185 by high-speed counter-current chromatography', *Journal of Chromatography A*, 994(1), pp. 37-43.
- Ma, F. and Hanna, M.A. (1999a) 'Biodiesel production: A review', *Bioresource Technology*, 70(1), pp. 1-15.
- Ma, F. and Hanna, M.A. (1999b) 'Biodiesel production: a review1', *Bioresource Technology*, 70(1), pp. 1-15.
- Mathimani, T., Uma, L. and Prabakaran, D. (2015) 'Homogeneous acid catalysed transesterification of marine microalga *Chlorella* sp. BDUG 91771 lipid – An efficient biodiesel yield and its characterization', *Renewable Energy*, 81, pp. 523-533.
- Mazubert, A., Poux, M. and Aubin, J. (2013) 'Intensified processes for FAME production from waste cooking oil: A technological review', *Chemical Engineering Journal*, 233, pp. 201-223.
- Mbatia, B., Adlercreutz, D., Adlercreutz, P., Mahadhy, A., Mulaa, F. and Mattiasson, B. (2010) 'Enzymatic oil extraction and positional analysis of ω -3 fatty acids in Nile perch and salmon heads', *Process Biochemistry*, 45(5), pp. 815-819.

- Meher, L.C., Vidya Sagar, D. and Naik, S.N. (2006) 'Technical aspects of biodiesel production by transesterification—a review', *Renewable and Sustainable Energy Reviews*, 10(3), pp. 248-268.
- Ministry of Agriculture and Fisheries (2014) 'Fisheries Statistics Book '. 13/12/2015. Muscat: Ministry of Agriculture and Fisheries, Department of Fisheries Statistics, p.252. Available:<http://omanagriculture.net/Pages/BulletinDetails.aspx?Id=596&lang=EN&I=0&DI=0&CI=0&CMSId=800183#726>
- Moser, B.R. (2009) 'Biodiesel production, properties, and feedstocks', *In Vitro Cellular & Developmental Biology - Plant*, 45(3), pp. 229-266.
- Musa, I.A. (2016) 'The effects of alcohol to oil molar ratios and the type of alcohol on biodiesel production using transesterification process', *Egyptian Journal of Petroleum*, 25(1), pp. 21-31.
- Nakano, K., Kato, S., Noritomi, H. and Nagahama, K. (1996) 'Extraction of polyunsaturated fatty acid ethyl esters from sardine oil using Ag⁺-containing o/w/o emulsion liquid membranes', *Journal of Membrane Science*, 110(2), pp. 219-227.
- Nakazawa, A., Matsuura, H., Kose, R., Kato, S., Honda, D., Inouye, I., Kaya, K. and Watanabe, M.M. (2012) 'Optimization of culture conditions of the thraustochytrid *Aurantiochytrium* sp. strain 18W-13a for squalene production', *Bioresource Technology*, 109, pp. 287-291.
- Navarro-García, G., Pacheco-Aguilar, R., Bringas-Alvarado, L. and Ortega-García, J. (2004) 'Characterization of the lipid composition and natural antioxidants in the liver oil of *Dasyatis brevis* and *Gymnura marmorata* rays', *Food Chemistry*, 87(1), pp. 89-96.
- Navarro-Garcia, G., Pacheco-Aguilar, R., Vallejo-Cordova, B., Ramirez-Suarez, J.C. and Bolaños, A. (2000) 'Lipid Composition of the Liver Oil of Shark Species from the

Caribbean and Gulf of California Waters', *Journal of Food Composition and Analysis*, 13(5), pp. 791-798.

Navarro-García, G., Ramírez-Suárez, J.C., Cota-Quiñones, E., Márquez-Farías, F. and Bringas-Alvarado, L. (2010) 'Storage stability of liver oil from two ray (*Rhinoptera bonasus* and *Aetobatus narinari*) species from the Gulf of Mexico', *Food Chemistry*, 119(4), pp. 1578-1583.

Neto, A.C., Guimarães, M.J.O.C. and Freire, E. (2018) 'Business models for commercial scale second-generation bioethanol production', *Journal of Cleaner Production*, 184, pp. 168-178.

Okada, T. and Morrissey, M.T. (2007) 'Production of n-3 polyunsaturated fatty acid concentrate from sardine oil by lipase-catalyzed hydrolysis', *Food chemistry*, 103(4), pp. 1411-1419.

Pask, S.D., Nuyken, O. and Cai, Z. (2012) 'The spinning disk reactor: an example of a process intensification technology for polymers and particles', *Polymer Chemistry*, 3(10), pp. 2698-2707.

Patil, P.D. and Deng, S. (2009) 'Optimization of biodiesel production from edible and non-edible vegetable oils', *Fuel*, 88(7), pp. 1302-1306.

Patil, R.A., Kausley, S.B., Balkunde, P.L. and Malhotra, C.P. (2013) 'Comparative study of disinfectants for use in low-cost gravity driven household water purifiers', *Journal of Water and Health*, 11(3), pp. 443-456.

Pavia, D., Lampman, G., Kriz, G. and Vyvyan, J. (2008) *Introduction to spectroscopy*. Cengage Learning.

- Peters, J. and Thielmann, S. (2008) 'Promoting biofuels: Implications for developing countries', *Energy Policy*, 36(4), pp. 1538-1544.
- Pettinello, G., Bertucco, A., Pallado, P. and Stassi, A. (2000) 'Production of EPA enriched mixtures by supercritical fluid chromatography: From the laboratory scale to the pilot plant', *Journal of Supercritical Fluids*, 19(1), pp. 51-60.
- Phan, A.N., Harvey, A.P. and Eze, V. (2012) 'Rapid Production of Biodiesel in Mesoscale Oscillatory Baffled Reactors', *Chemical Engineering & Technology*, 35(7), pp. 1214-1220.
- Pietsch, A. and Jaeger, P. (2007a) 'Concentration of squalene from shark liver oil by short-path distillation', *European Journal of Lipid Science and Technology*, 109(11), pp. 1077-1082.
- Pietsch, A. and Jaeger, P. (2007b) 'Concentration of squalene from shark liver oil by short - path distillation', *European journal of lipid science and technology*, 109(11), pp. 1077-1082.
- PikeResearch (2012) 'Biofuels Markets and Technologies', p. 3.
- Popa, O., Băbeanu, N.E., Popa, I., Niță, S. and Dinu-Pârvu, C.E. (2015a) 'Methods for obtaining and determination of squalene from natural sources', *BioMed research international*, 2015.
- Popa, O., Băbeanu, N.E., Popa, I., Niță, S. and Dinu-Pârvu, C.E. (2015b) 'Methods for obtaining and determination of squalene from natural sources', *BioMed research international*, 2015, pp. 367202-367202.

- Popa, O., x, beanu, N.E., Popa, I., Ni, x21b, x, Sultana, Dinu, P., xe and rvu, C.E. (2015c) 'Methods for Obtaining and Determination of Squalene from Natural Sources', *BioMed Research International*, 2015, p. 16.
- Pullen, J. and Saeed, K. (2015) 'Investigation of the factors affecting the progress of base-catalyzed transesterification of rapeseed oil to biodiesel FAME', *Fuel Processing Technology*, 130, pp. 127-135.
- Qiu, Z., Petera, J. and Weatherley, L.R. (2012) 'Biodiesel synthesis in an intensified spinning disk reactor', *Chemical Engineering Journal*, 210, pp. 597-609.
- Qiu, Z., Zhao, L. and Weatherley, L. (2010) 'Process intensification technologies in continuous biodiesel production', *Chemical Engineering and Processing: Process Intensification*, 49(4), pp. 323-330.
- Radich, A. (1998) 'Biodiesel performance, costs, and use', *Combustion*, 24(2), pp. 131-132.
- Radziemska, M., Vaverková, M.D., Adamcová, D., Brtnický, M. and Mazur, Z. (2018) 'Valorization of Fish Waste Compost as a Fertilizer for Agricultural Use', *Waste and Biomass Valorization*, pp. 1-9.
- Rahimi, M., Aghel, B., Alitabar, M., Sepahvand, A. and Ghasempour, H.R. (2014) 'Optimization of biodiesel production from soybean oil in a microreactor', *Energy Conversion and Management*, 79, pp. 599-605.
- Rasal, A., Saxena, S., Nair, N., Vikal, M., Yadav, K. and Dwivedi, G. (2019) Singapore. Springer Singapore.
- Regalado-Méndez, A., Romero, R.R., Rangel, R.N. and Skogestad, S. (2015) 'Biodiesel production in stirred tank chemical reactors: a numerical simulation', in *New Trends*

in Networking, Computing, E-learning, Systems Sciences, and Engineering. Springer, pp. 109-116.

Rubio-Rodríguez, N., Beltrán, S., Jaime, I., de Diego, S.M., Sanz, M.T. and Carballido, J.R. (2010) 'Production of omega-3 polyunsaturated fatty acid concentrates: A review', *Innovative Food Science & Emerging Technologies*, 11(1), pp. 1-12.

Rubio-Rodríguez, N., de Diego, S.M., Beltrán, S., Jaime, I., Sanz, M.T. and Rovira, J. (2008) 'Supercritical fluid extraction of the omega-3 rich oil contained in hake (*Merluccius capensis*–*Merluccius paradoxus*) by-products: Study of the influence of process parameters on the extraction yield and oil quality', *The Journal of Supercritical Fluids*, 47(2), pp. 215-226.

Saka, S. and Kusdiana, D. (2001) 'Biodiesel fuel from rapeseed oil as prepared in supercritical methanol', *Fuel*, 80(2), pp. 225-231.

Sakdasri, W., Sawangkeaw, R. and Ngamprasertsith, S. (2016) 'Response surface methodology for the optimization of biofuel production at a low molar ratio of supercritical methanol to used palm olein oil', *Asia - Pacific Journal of Chemical Engineering*, 11(4), pp. 539-548.

Sakdasri, W., Sawangkeaw, R. and Ngamprasertsith, S. (2018) 'Techno-economic analysis of biodiesel production from palm oil with supercritical methanol at a low molar ratio', *Energy*, 152, pp. 144-153.

Sawangkeaw, R., Teeravitud, S., Bunyakiat, K. and Ngamprasertsith, S. (2011) 'Biofuel production from palm oil with supercritical alcohols: Effects of the alcohol to oil molar ratios on the biofuel chemical composition and properties', *Bioresource technology*, 102(22), pp. 10704-10710.

Seidell, A. (1919) *Solubilities of inorganic and organic compounds c. 2*. D. Van Nostrand Company.

- Shahidi, F. and Wanasundara, U.N. (1998) 'Omega-3 fatty acid concentrates: nutritional aspects and production technologies', *Trends in Food Science & Technology*, 9(6), pp. 230-240.
- Shanmugam, K. and Donaldson, A.A. (2015) 'Extraction of EPA/DHA from 18/12EE Fish Oil Using AgNO₃(aq): Composition, Yield, and Effects of Solvent Addition on Interfacial Tension and Flow Pattern in Mini-Fluidic Systems', *Industrial & Engineering Chemistry Research*, 54(33), pp. 8295-8301.
- Shanmugam, K., Neima, A. and Donaldson, A.A. (2015) 'Design and Feasibility Analysis of Commercial Silver-Based Solvent Extraction of Omega-3 PUFA', *Global Journal of Research In Engineering*.
- Sherma, J. and Fried, B. (2002) 'Handbook of thin layer chromatography', *Anal. Chem*, 72, pp. 9R-25R.
- Singh, D.P. and Dwevedi, A. (2019) 'Chapter 2 - Production of clean energy by green ways', in Dwevedi, A. (ed.) *Solutions to Environmental Problems Involving Nanotechnology and Enzyme Technology*. Academic Press, pp. 49-90.
- Singh, S.P. and Singh, D. (2010) 'Biodiesel production through the use of different sources and characterization of oils and their esters as the substitute of diesel: a review', *Renewable and sustainable energy reviews*, 14(1), pp. 200-216.
- Skalicka-Woźniak, K. and Garrard, I. (2014) 'Counter-current chromatography for the separation of terpenoids: a comprehensive review with respect to the solvent systems employed', *Phytochemistry reviews : proceedings of the Phytochemical Society of Europe*, 13(2), pp. 547-572.
- Smith, T.J., Yang, G.Y., Seril, D.N., Liao, J. and Kim, S. (1998) 'Inhibition of 4-(methylnitrosamino)-1-(3-pyridyl)-1-butanone-induced lung tumorigenesis by dietary olive oil and squalene', *Carcinogenesis*, 19(4), pp. 703-706.

- Sootchiewcharn, N., Attanatho, L. and Reubroycharoen, P. (2015) 'Biodiesel Production from Refined Palm Oil using Supercritical Ethyl Acetate in A Microreactor', *Energy Procedia*, 79, pp. 697-703.
- Sun, T., Pigott, G.M. and Herwig, R.P. (2002) 'Lipase - assisted concentration of n - 3 polyunsaturated fatty acids from viscera of farmed Atlantic salmon (*Salmo salar* L.)', *Journal of Food Science*, 67(1), pp. 130-136.
- Teramoto, M., Matsuyama, H., Ohnishi, N., Uwagawa, S. and Nakai, K. (1994) 'Extraction of ethyl and methyl esters of polyunsaturated fatty acids with aqueous silver nitrate solutions', *Industrial & engineering chemistry research*, 33(2), pp. 341-345.
- Thanh, L.T., Okitsu, K., Sadanaga, Y., Takenaka, N., Maeda, Y. and Bandow, H. (2010) 'Ultrasound-assisted production of biodiesel fuel from vegetable oils in a small scale circulation process', *Bioresource Technology*, 101(2), pp. 639-645.
- Thompson, J.C. and He, B.B. (2006) 'Characterization of crude glycerol from biodiesel production from multiple feedstocks', *Applied engineering in agriculture*, 22(2), pp. 261-265.
- Thompson, J.C. and He, B.B. (2007) 'Biodiesel production using static mixers', *Transactions of the ASABE*, 50(1), pp. 161-165.
- Tsujimoto, M. (1916) 'A highly unsaturated hydrocarbon in shark liver oil', *Industrial & Engineering Chemistry*, 8(10), pp. 889-896.
- Urban, T. (2015) 'worldwide energy consumption', *worldwide energy consumption 2013*. Available at: <http://waitbutwhy.com/2015/06/how-tesla-will-change-your-life.html>.

- Van Kasteren, J.M.N. and Nisworo, A.P. (2007) 'A process model to estimate the cost of industrial scale biodiesel production from waste cooking oil by supercritical transesterification', *Resources, Conservation and Recycling*, 50(4), pp. 442-458.
- Vannuccini, S. (1999) 'Shark utilization, marketing and trade', *FAO Fisheries and Technical paper*, p. 470.
- Vázquez, L., Torres, C.F., Fornari, T., Señoráns, F.J. and Reglero, G. (2007) 'Recovery of squalene from vegetable oil sources using countercurrent supercritical carbon dioxide extraction', *The Journal of Supercritical Fluids*, 40(1), pp. 59-66.
- Wanasundara, U.N. (2001) 'Marine oils: Stabilization, structural characterization and omega-3 fatty acid concentration'.
- Wanasundara, U.N. and Shahidi, F. (1999) 'Concentration of omega 3-polyunsaturated fatty acids of seal blubber oil by urea complexation: optimization of reaction conditions', *Food Chemistry*, 65(1), pp. 41-49.
- Wang, C.-X. and McCurry, J. (2006) 'Determining the Ester and Linolenic Acid Methyl Ester Content to Comply with EN14103', *Agilent Technologies*.
- Wen, Z., Yu, X., Tu, S.-T., Yan, J. and Dahlquist, E. (2009) 'Intensification of biodiesel synthesis using zigzag micro-channel reactors', *Bioresource Technology*, 100(12), pp. 3054-3060.
- Wetherbee, B.M. and Nichols, P.D. (2000) 'Lipid composition of the liver oil of deep-sea sharks from the Chatham Rise, New Zealand', *Comparative Biochemistry and Physiology Part B: Biochemistry and Molecular Biology*, 125(4), pp. 511-521.

- Yang, L., Takase, M., Zhang, M., Zhao, T. and Wu, X. (2014) 'Potential non-edible oil feedstock for biodiesel production in Africa: A survey', *Renewable and Sustainable Energy Reviews*, 38, pp. 461-477.
- Yokochi, T., Usita, M.T., Kamisaka, Y., Nakahara, T. and Suzuki, O. (1990) 'Increase in the γ -linolenic acid content by solvent winterization of fungal oil extracted from *Mortierella* genus', *Journal of the American Oil Chemists' Society*, 67(11), pp. 846-851.
- Zabeti, M., Wan Daud, W.M.A. and Aroua, M.K. (2009) 'Activity of solid catalysts for biodiesel production: A review', *Fuel Processing Technology*, 90(6), pp. 770-777.
- Zhang, Y., Dube, M.A., McLean, D.D.L. and Kates, M. (2003a) 'Biodiesel production from waste cooking oil: 1. Process design and technological assessment', *Bioresource technology*, 89(1), pp. 1-16.
- Zhang, Y.A., Dubé, M.A., McLean, D. and Kates, M. (2003b) *Biodiesel production from waste cooking oil: 1. Process design and technological assessment.*

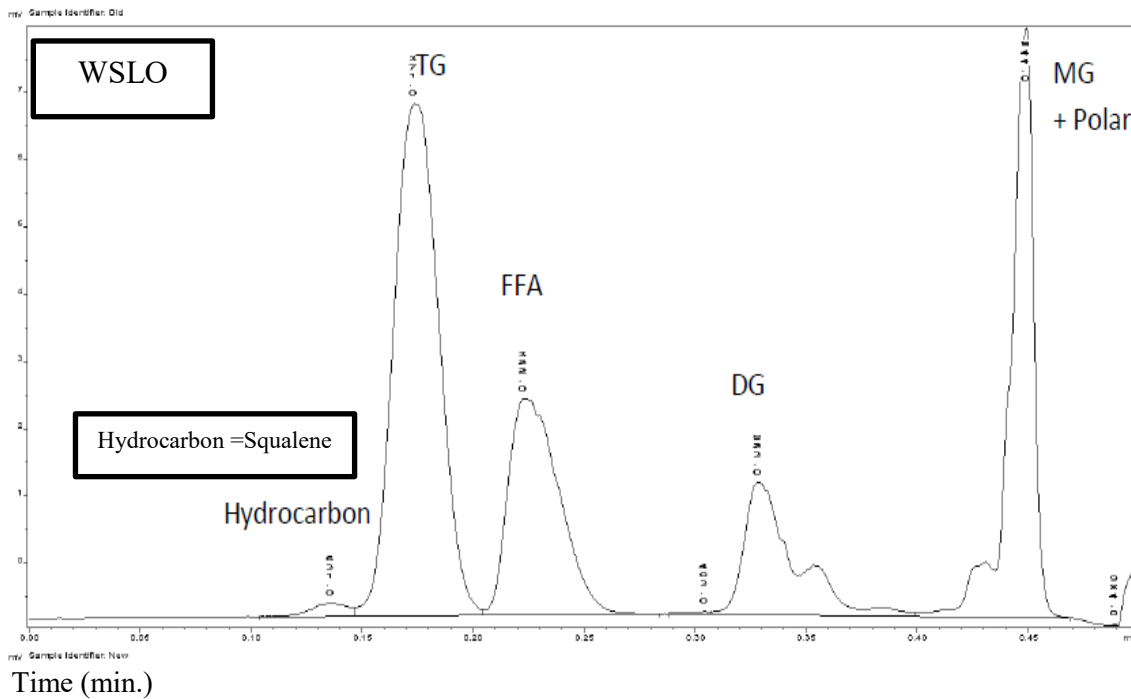
Appendices

Appendix A: WSLO Fatty Acid Profile

<i>GC ID</i>	<i>AM020715-16</i>	
	<i>ECL</i>	<i>%</i>
14:0	14.01	5.0
15:0	15.00	0.6
16:0	16.00	19.5
16:1n-9	16.25	0.7
16:1n-7	16.30	6.0
16:1n-5	16.42	0.1
16:2n-4	16.92	1.0
17:0	16.99	0.8
16:3n-4	17.27	0.6
16:4n-1	17.86	0.3
18:0	18.00	6.3
18:1n-9	18.23	11.4
18:1n-7	18.30	4.0
18:2n-6	18.71	1.1
18:2n-4	18.91	0.2
18:3n-6	19.03	0.2
18:3n-4	19.24	0.2
18:3n-3	19.37	0.4
18:4n-3	19.70	0.8
20:0	20.00	0.3
20:1n-11	20.18	0.6
20:1n-9	20.21	1.9
20:1n-7	20.29	0.4
20:2n-6	20.70	0.3
20:3n-6	20.97	0.4
20:4n-6	21.20	2.2
20:4n-3	21.63	0.7
20:5n-3 (EPA)	21.87	6.1
22:0	22.00	0.2
22:1n-11	22.12	1.8
22:1n-9	22.19	0.5
21:5n-3	22.90	0.3
22:4n-6	23.18	1.0
22:5n-6	23.46	1.8
22:5n-3	23.83	3.7
24:0	24.00	0.2
22:6n-3 (DHA)	24.12	15.0
24:1n-9	24.16	0.5
Others		2.8
Total fatty acid (g/100g sample)		94.6

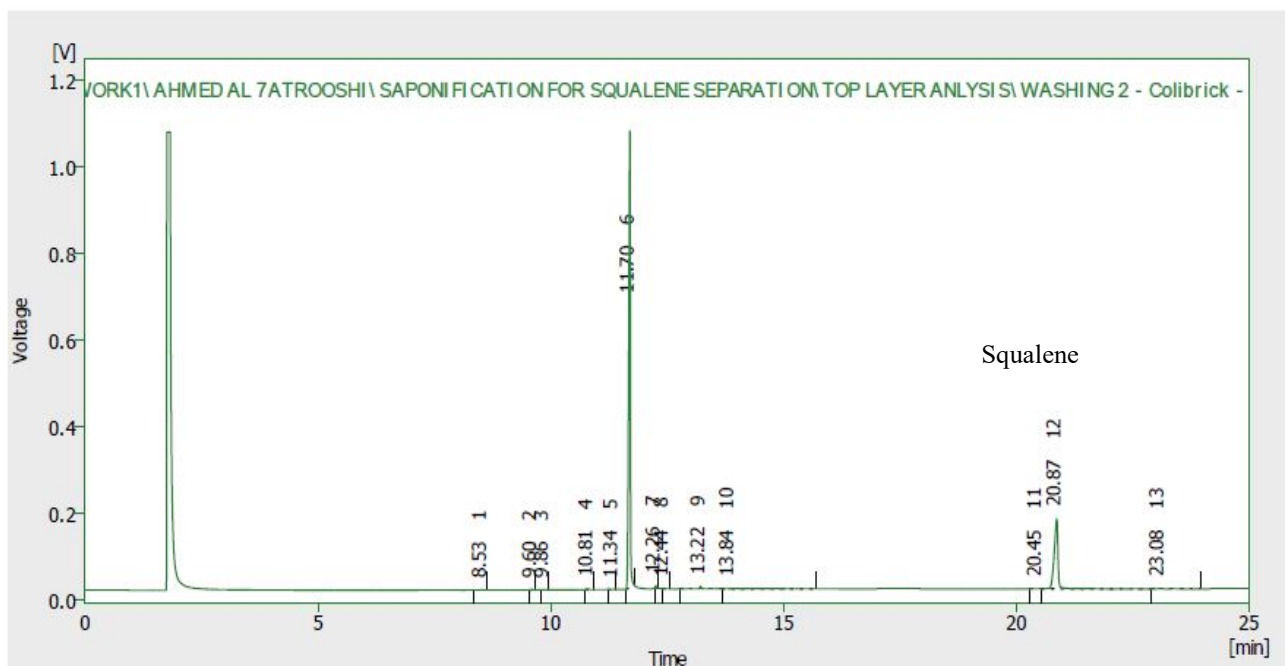
Appendix B: Analysis of Waste Shark Liver Oil by Iatroscan MK-6

Voltage (v)



The Figure above is an Iatroscan Traces for Waste Shark Liver Oils. The Iatroscan thin-layer chromatography (TLC)–flame-ionization detection is a widely used technique for determination of lipid-classes and FFA contents. The glycerides (TG, DG and MG), and FFA contents of the WSLO was determined by the Iatroscan MK-6 were 44.0 wt.% for TG, 14.3 wt.% for DG, 21.1 wt.% for MG, and 19.9 wt.% for FFA as shown in Figure above. The WSLO was also found to contain 0.7 wt. % of squalene. The amounts of squalene in the WSLO sample was low (0.7%) as the squalene content is strongly dependent on the shark species. It is reported that shallow sharks has very low amount of squalene (Wetherbee and Nichols, 2000) and the samples tested are from shallow sharks in Oman.

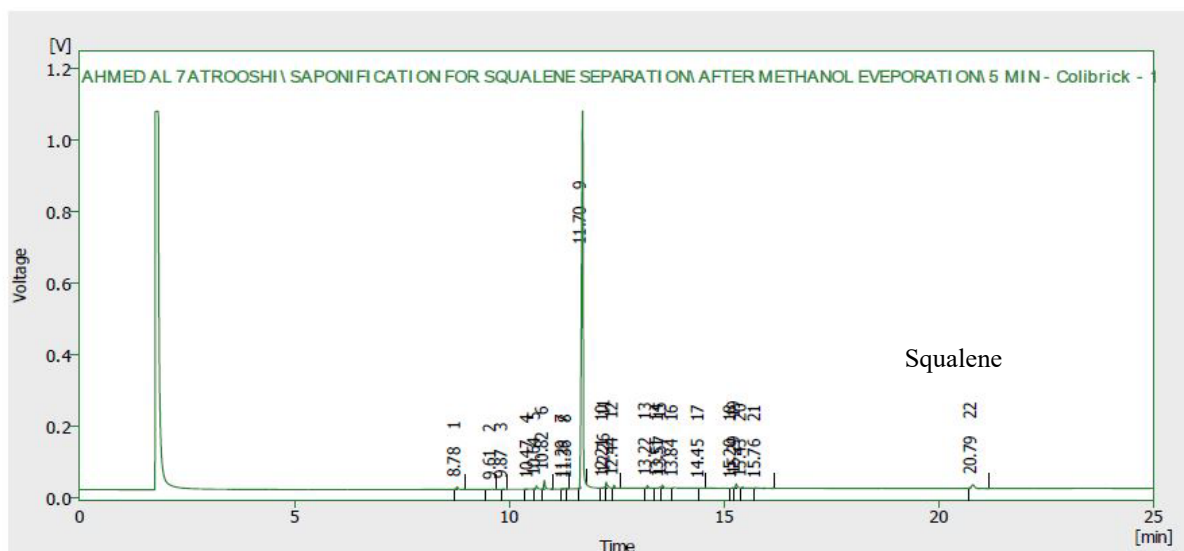
Appendix C: GC Chromatogram showing squalene in the WSLO FAME Sample



Result Table (Uncal - C:|CLARITY|WORK1|AHMED AL 7ATROOSHI\SAPONIFICATION FOR SQUALENE SEPARATION|TOP LAYER ANALYSIS|WASHING 2 - Colibrick - 1)

	Reten. Time [min]	Area [mV.s]	Height [mV]	Area [%]	Height [%]	W05 [min]	Compound Name
1	8.529	1.909	0.686	0.1	0.1	0.04	
2	9.603	1.286	0.579	0.0	0.0	0.03	
3	9.857	1.169	0.455	0.0	0.0	0.04	
4	10.813	4.067	1.543	0.1	0.1	0.04	
5	11.344	0.376	0.125	0.0	0.0	0.04	
6	11.699	2508.980	1054.601	71.0	85.5	0.04	Squalene
7	12.259	9.760	5.326	0.3	0.4	0.03	
8	12.440	2.988	1.375	0.1	0.1	0.03	
9	13.217	20.762	5.644	0.6	0.5	0.03	
10	13.839	24.186	0.432	0.7	0.0	1.25	
11	20.452	2.265	0.238	0.1	0.0	0.18	
12	20.868	944.789	161.931	26.7	13.1	0.09	
13	23.079	12.155	0.494	0.3	0.0	0.15	
	Total	3534.692	1233.428	100.0	100.0		

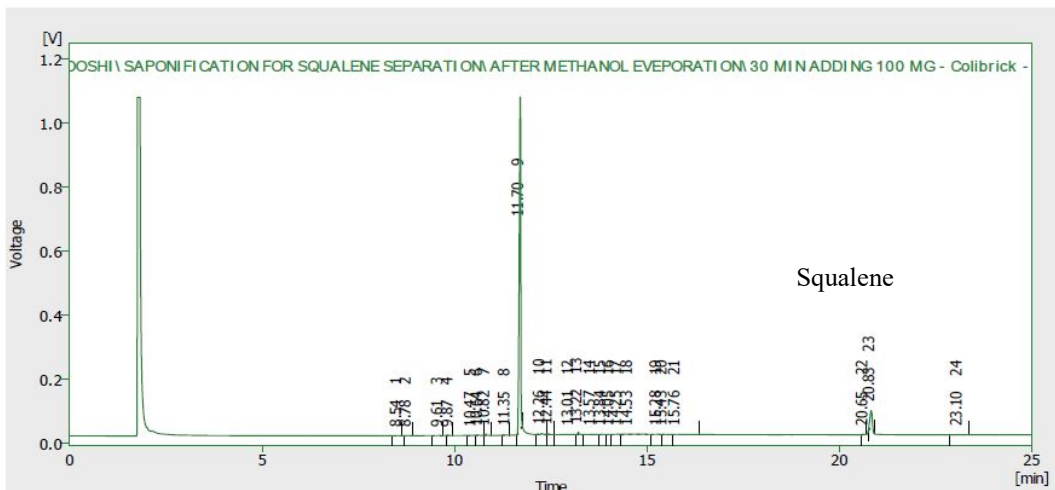
Appendix C 1: Squalene peak after 5 min reaction time of WSLO saponification



Result Table (Uncal - C: |CLARITY|WORK1|AHMED AL 7ATROOSHI|SAPONIFICATION FOR SQUALENE SEPARATION|AFTER METHANOL EVEPORATION|5 MIN - Colibrick - 1)

	Reten. Time [min]	Area [mV.s]	Height [mV]	Area [%]	Height [%]	W05 [min]	Compound Name
1	8.784	18.695	6.849	0.6	0.6	0.04	
2	9.605	2.120	0.617	0.1	0.1	0.03	
3	9.867	2.927	1.253	0.1	0.1	0.04	
4	10.465	3.876	0.876	0.1	0.1	0.09	
5	10.636	24.698	8.938	0.8	0.8	0.04	
6	10.819	55.317	24.344	1.7	2.1	0.03	
7	11.287	2.085	0.960	0.1	0.1	0.03	
8	11.361	1.282	0.530	0.0	0.0	0.04	
9	11.703	2901.405	1048.633	89.1	89.9	0.04	
10	12.213	5.952	1.763	0.2	0.2	0.03	
11	12.259	48.374	16.680	1.5	1.4	0.03	
12	12.443	15.551	7.539	0.5	0.6	0.03	
13	13.219	15.527	6.822	0.5	0.6	0.03	
14	13.507	6.408	2.834	0.2	0.2	0.04	
15	13.565	26.982	8.474	0.8	0.7	0.04	
16	13.837	12.057	1.940	0.4	0.2	0.05	
17	14.452	0.999	0.357	0.0	0.0	0.04	
18	15.201	3.910	1.463	0.1	0.1	0.05	
19	15.287	37.344	11.469	1.1	1.0	0.05	
20	15.433	13.511	3.109	0.4	0.3	0.05	
21	15.764	5.906	1.026	0.2	0.1	0.06	
22	20.793	50.052	9.977	1.5	0.9	0.08	Squalene
	Total	3254.979	1166.454	100.0	100.0		

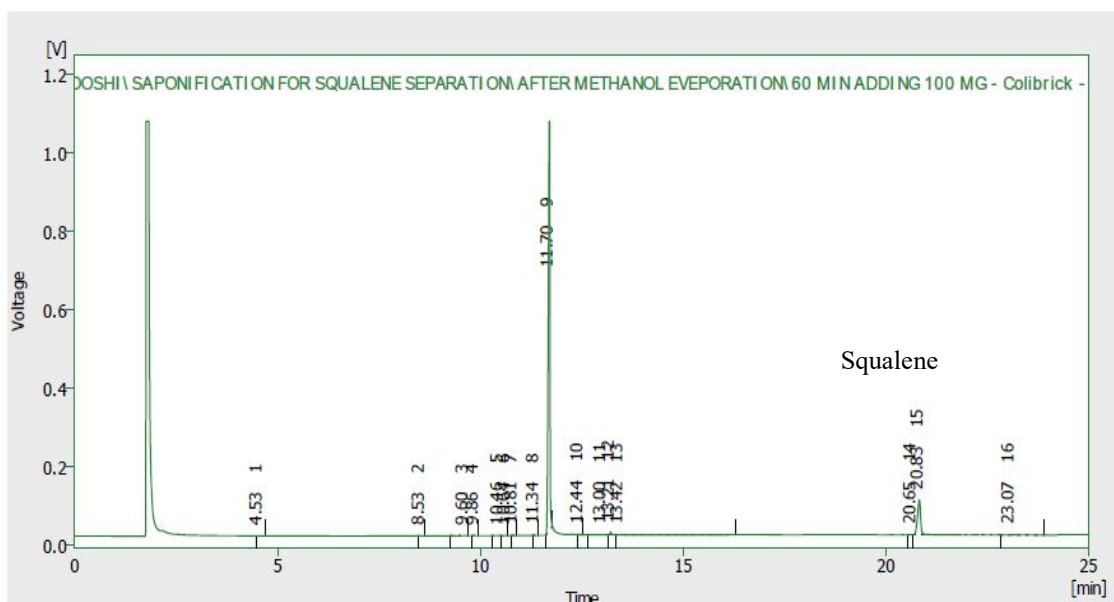
Appendix C 2: Squalene peak after 30 min reaction time of WSLO saponification



Result Table (Uncal - C: [CLARITY]WORK1\AHMED AL 7ATROOSHI\SAPONIFICATION FOR SQUALENE SEPARATION\AFTER METHANOL EVAPORATION\30 MIN ADDING 100 MG - Colibrick - 1)

	Reten. Time [min]	Area [mV.s]	Height [mV]	Area [%]	Height [%]	W05 [min]	Compound Name
1	8.536	1.108	0.354	0.0	0.0	0.04	
2	8.781	1.599	0.534	0.0	0.0	0.04	
3	9.611	1.652	0.611	0.0	0.1	0.04	
4	9.867	1.507	0.558	0.0	0.0	0.04	
5	10.468	0.749	0.215	0.0	0.0	0.04	
6	10.636	2.595	0.875	0.1	0.1	0.04	
7	10.819	8.996	3.902	0.3	0.3	0.03	
8	11.349	1.697	0.565	0.1	0.0	0.04	
9	11.704	2855.907	1040.075	86.0	91.8	0.04	Squalene
10	12.260	14.181	3.446	0.4	0.3	0.03	
11	12.443	5.897	2.849	0.2	0.3	0.03	
12	13.005	11.264	0.707	0.3	0.1	0.23	
13	13.219	19.344	7.106	0.6	0.6	0.03	
14	13.565	15.266	1.095	0.5	0.1	0.08	
15	13.837	7.278	1.135	0.2	0.1	0.13	
16	14.051	5.606	0.816	0.2	0.1	0.15	
17	14.247	14.687	1.068	0.4	0.1	0.26	
18	14.529	52.994	1.535	1.6	0.1	0.78	
19	15.284	15.697	1.264	0.5	0.1	0.29	
20	15.432	9.544	1.085	0.3	0.1	0.13	
21	15.764	10.976	0.924	0.3	0.1	0.09	
22	20.652	1.495	0.397	0.0	0.0	0.06	
23	20.827	258.705	62.046	7.8	5.5	0.07	
24	23.099	3.800	0.388	0.1	0.0	0.13	
	Total	3322.543	1133.556	100.0	100.0		

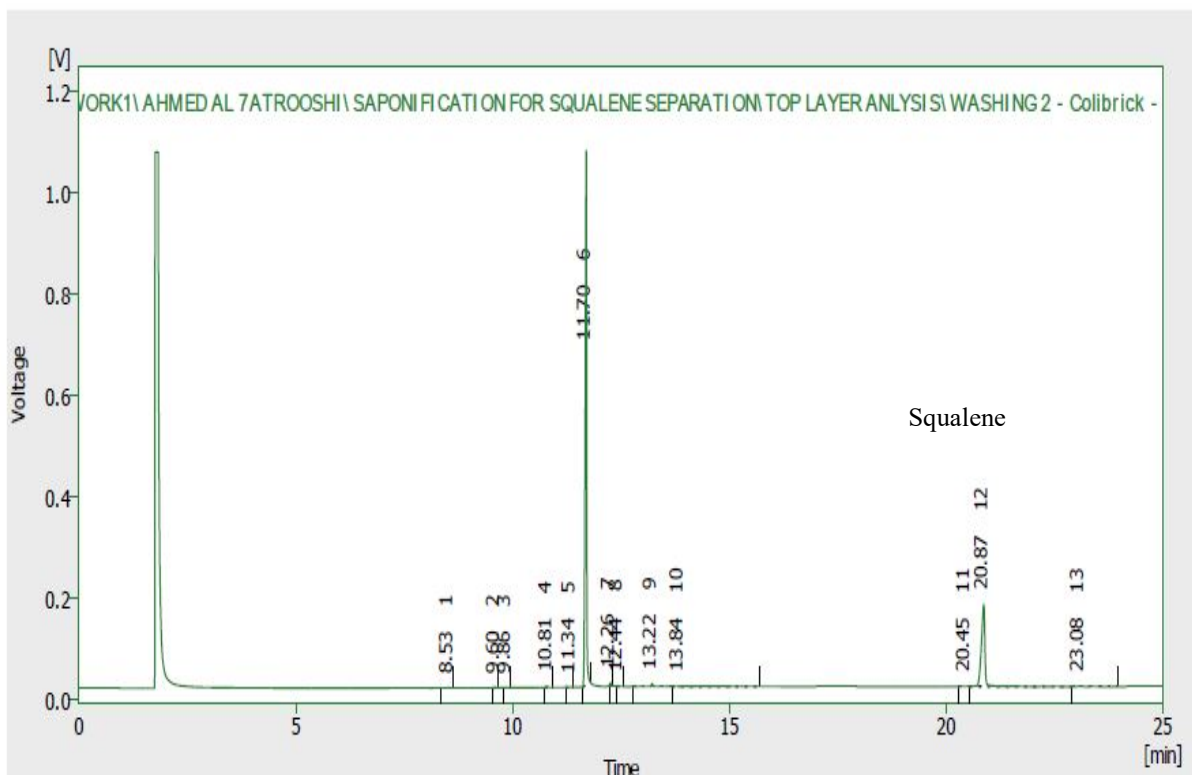
Appendix C 3 :Squalene peak after 60 min reaction time of WSLO saponification



Result Table (Uncal - C:\CLARITY\WORK1\AHMED AL 7ATROOSHI\SAPONIFICATION FOR SQUALENE SEPARATION\AFTER METHANOL EVEPORATION\60 MIN ADDING 100 MG - Colibrick - 1)

	Reten. Time [min]	Area [mV.s]	Height [mV]	Area [%]	Height [%]	W05 [min]	Compound Name
1	4.531	1.157	0.273	0.0	0.0	0.05	
2	8.531	1.165	0.412	0.0	0.0	0.04	
3	9.604	1.928	0.632	0.1	0.1	0.04	
4	9.861	1.434	0.538	0.0	0.0	0.04	
5	10.463	0.698	0.208	0.0	0.0	0.04	
6	10.636	0.624	0.179	0.0	0.0	0.04	
7	10.812	2.898	1.324	0.1	0.1	0.03	
8	11.344	0.939	0.357	0.0	0.0	0.04	
9	11.699	3041.517	1044.037	83.7	90.9	0.05	
10	12.439	3.209	1.496	0.1	0.1	0.03	
11	13.003	5.374	0.420	0.1	0.0	0.18	
12	13.213	17.558	7.308	0.5	0.6	0.03	
13	13.424	32.687	0.515	0.9	0.0	0.08	
14	20.651	4.596	1.023	0.1	0.1	0.07	
15	20.827	509.713	89.207	14.0	7.8	0.08	Squalene
16	23.072	8.766	0.666	0.2	0.1	0.13	
	Total	3634.263	1148.597	100.0	100.0		

Appendix C 4 : Squalene peak after washing



Result Table (Uncal - C:\CLARITY\WORK1\AHMED AL 7ATROOSHI\SAPONIFICATION FOR SQUALENE SEPARATION\TOP LAYER ANALYSIS\WASHING 2 - Colibrick - 1)

	Reten. Time [min]	Area [mV.s]	Height [mV]	Area [%]	Height [%]	W05 [min]	Compound Name
1	8.529	1.909	0.686	0.1	0.1	0.04	
2	9.603	1.286	0.579	0.0	0.0	0.03	
3	9.857	1.169	0.455	0.0	0.0	0.04	
4	10.813	4.067	1.543	0.1	0.1	0.04	
5	11.344	0.376	0.125	0.0	0.0	0.04	
6	11.699	2508.980	1054.601	71.0	85.5	0.04	Squalene
7	12.259	9.760	5.326	0.3	0.4	0.03	
8	12.440	2.988	1.375	0.1	0.1	0.03	
9	13.217	20.762	5.644	0.6	0.5	0.03	
10	13.839	24.186	0.432	0.7	0.0	1.25	
11	20.452	2.265	0.238	0.1	0.0	0.18	
12	20.868	944.789	161.931	26.7	13.1	0.09	
13	23.079	12.155	0.494	0.3	0.0	0.15	
	Total	3534.692	1233.428	100.0	100.0		

Appendix D: European Biodiesel Specification EN 14214

Property	Test method	Limits		Unit
		min	max	
Ester content	EN 14103	96.5	-	% (m/m)
Density at 15°C	EN ISO 3675, EN ISO 12185	860	900	kg/m ³
Viscosity at 40°C	EN ISO 3104, ISO 3105	3.5	5.0	mm ² /s
Flash point	EN ISO 3679	120	-	°C
Sulfur content	EN ISO 20846, EN ISO 20884	-	10.0	mg/kg
Carbon residue (in 10% dist. residue)	EN ISO 10370	-	0.30	% (m/m)
Cetane number	EN ISO 5165	51	-	-
Sulfated ash	ISO 3987	-	0.02	% (m/m)
Water content	EN ISO 12937	-	500	mg/kg
Total contamination	EN 12662	-	24	mg/kg
Copper strip corrosion (3 hours, 50°C)	EN ISO 2160	-	1	class
Oxidative stability, 110°C	EN 14112	6.0	-	hours
Acid value	EN 14104	-	0.50	mg KOH/g
Iodine value	EN 14111	-	120	g I/100 g
Linolenic acid content	EN 14103	-	12	% (m/m)
Content of FAME with ≥ 4 double bonds		-	1	% (m/m)
Methanol content	EN 14110	-	0.20	% (m/m)
Monoglyceride content	EN 14105	-	0.80	% (m/m)
Diglyceride content	EN 14105	-	0.20	% (m/m)
Triglyceride content	EN 14105	-	0.20	% (m/m)
Free glycerine	EN 14105; EN 14106	-	0.02	% (m/m)
Total glycerine	EN 14105	-	0.25	% (m/m)
Alkali metals (Na + K)	EN 14108; EN 14109	-	5.0	mg/kg
Earth alkali metals (Ca + Mg)	EN 14538	-	5.0	mg/kg
Phosphorus content	EN 14107	-	10.0	mg/kg

European Biodiesel Specification EN 14214 (Barabás and Todoruț, 2011)

Appendix E: ASTM Biodiesel Standard D 6751

ASTM Biodiesel Standard D 6751^a

Property	Test method	Limits	Units
Flash point (closed cup)	D 93	130.0 min	°C
Water and sediment	D 2709	0.050 max	% volume
Kinematic viscosity, 40°C	D 445	1.9–6.0	mm ² /s
Sulfated ash	D 874	0.020 max	% mass
Sulfur	D 5453	0.0015 max (S15) 0.05 max (S500)	% mass
(ppm)			
Copper strip corrosion	D 130	No. 3 max	
Cetane number	D 613	47 min	
Cloud point	D 2500	Report	°C
Carbon residue	D 4530	0.050 max	% mass
Acid number	D 664	0.50 max	mg KOH/g
Free glycerin	D 6584	0.020	% mass
Total glycerin	D 6584	0.240	% mass
Phosphorus content	D 4951	0.001 max	% mass
Sodium/potassium	UOP 391	5 max. combined	ppm
Distillation temperature, atmospheric equivalent temperature, 90% recovered	D 1160	360 max	°C

^aThe limits are for Grade S15 and Grade S500 biodiesel, with S15 and S500 referring to maximum sulfur specifications (in ppm).

(Knothe, 2006) ASTM Biodiesel Standard D 6751

